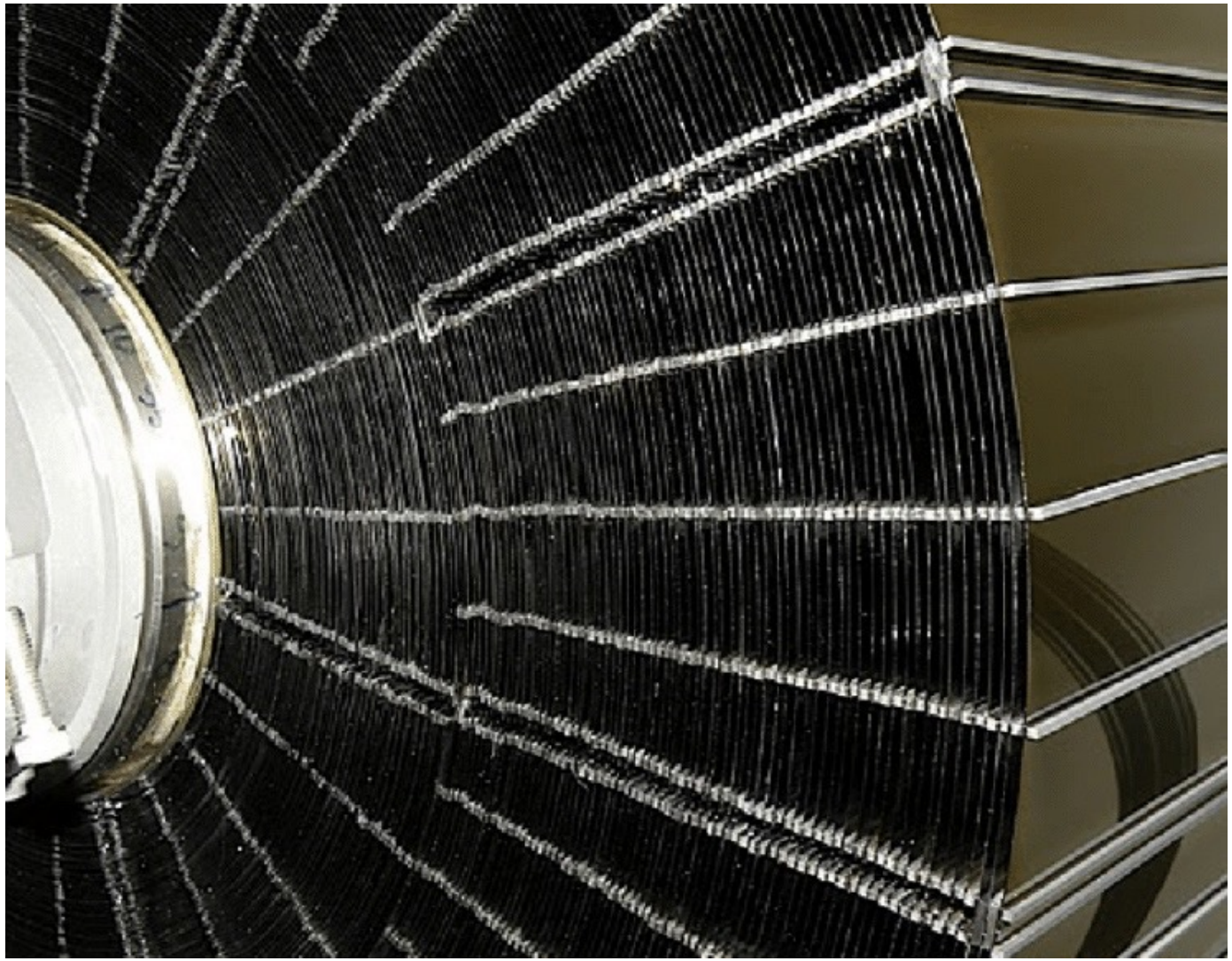
Focusing in on the High Energy Universe

III: High-energy Astrophysics Instrumentation

Dr. Oliver J. Roberts
USRA/NASA Marshall Space Flight Center
National Space Science and Tech. Center
Huntsville, AL, USA.
oroberts@usra.edu

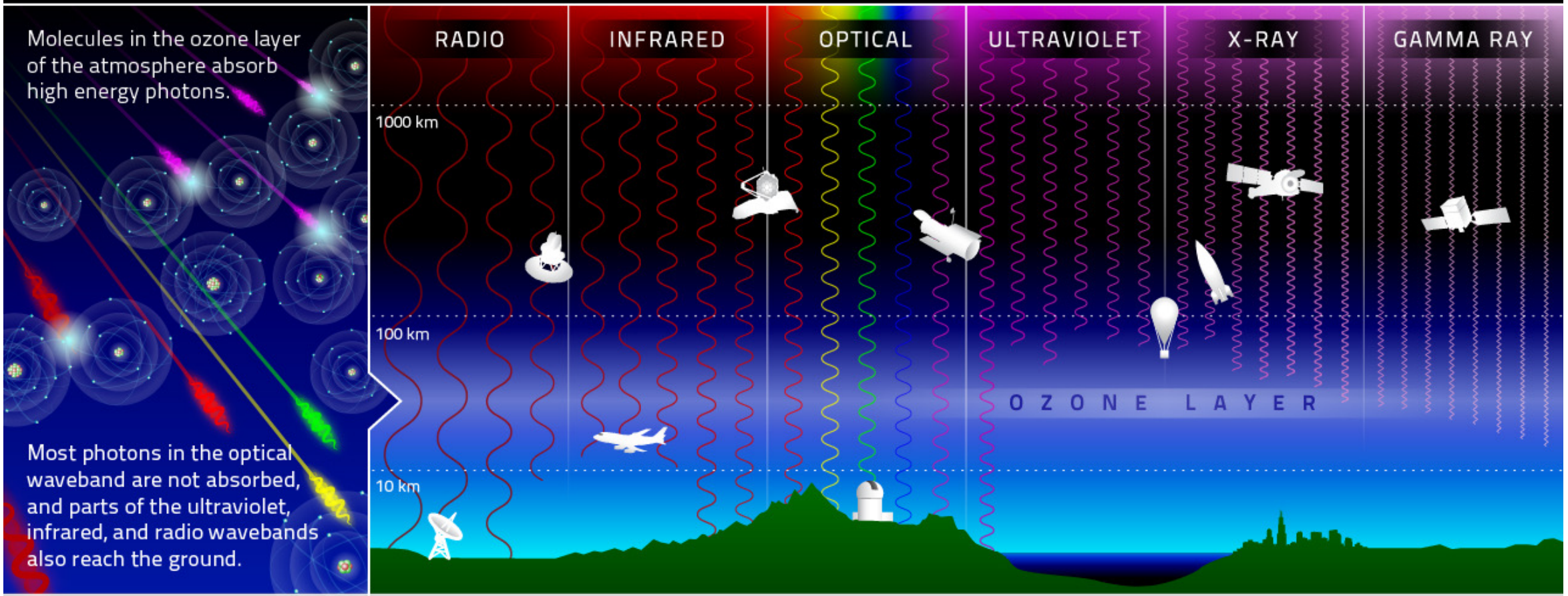


W. Craig, et al. (2011). Fabrication of the NuSTAR flight optics. Proc SPIE. 8147. 10.1117/12.895278.

USRA Universities Space Research Association

NASA

MULTIWAVELENGTH LAND & SPACE BASED OBSERVATORIES



The atomspheric effects on incoming light in each waveband determines the placement of telescopes.

Most of the Radio waveband is detectable using large dish antenae on the ground.

The infrared waveband can be detected from airplanes.

Ground telescopes observe most optical light, and some infrared and ultraviolet.

Balloons and rockets are used to test out new telescope technologies.

Space telescopes avoid atmospheric distortions and access high energy radiation.

Credit: NASA/University of Chicago

History of X-ray Astronomy

- **1895** – Discovery of X-rays by Röntgen
- **1912** – X-ray diffraction from crystals by Laue
- **1940s** – V2 and Aerobee Sounding Rockets used to first study X-rays from upper atmosphere.
- **1962** – Giacconi detects Sco X-1 (X-ray binary) using Aerobee rocket
- **1963** – Boyer detects Crab Nebula using a rocket
- **1965** – First extragalactic X-ray source (M87) discovered by Byram *et al.* using a rocket
- **1966** – OAO-1 launched. Power failure.
- **1967** – First detection of a GRB by Vela 3 and 4.
- **1970** – Uhuru (SAS-1) creates first sky map at 2-20 keV.

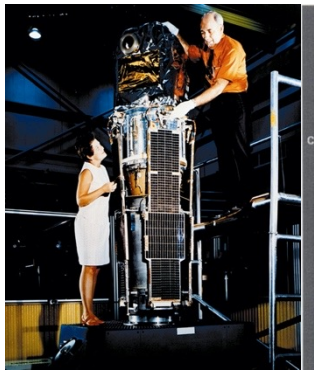


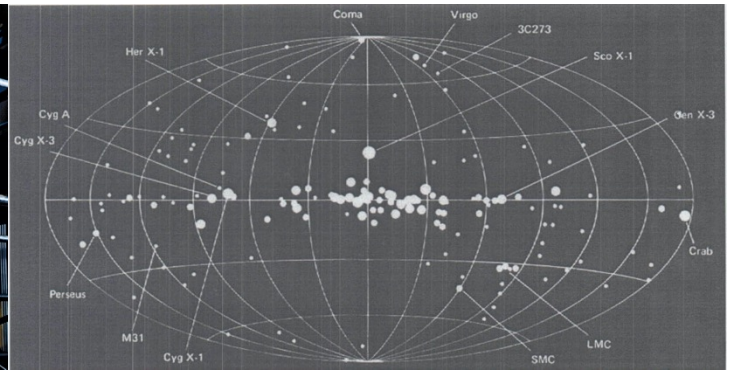




Aerobee rocket launch in 1965.

Credit: NASA https://history.nasa.gov/SP-4402/ch5.htm





Left: Uhuru model. Right: First comprehensive and uniform X-ray sky map by Uhuru ("Freedom") in 1970 (*Credit: NASA*)

History of X-ray Astronomy – 50 years on…



1970 — 1980 — 1990 — 2000 — 2010 — 2020 — 2030+

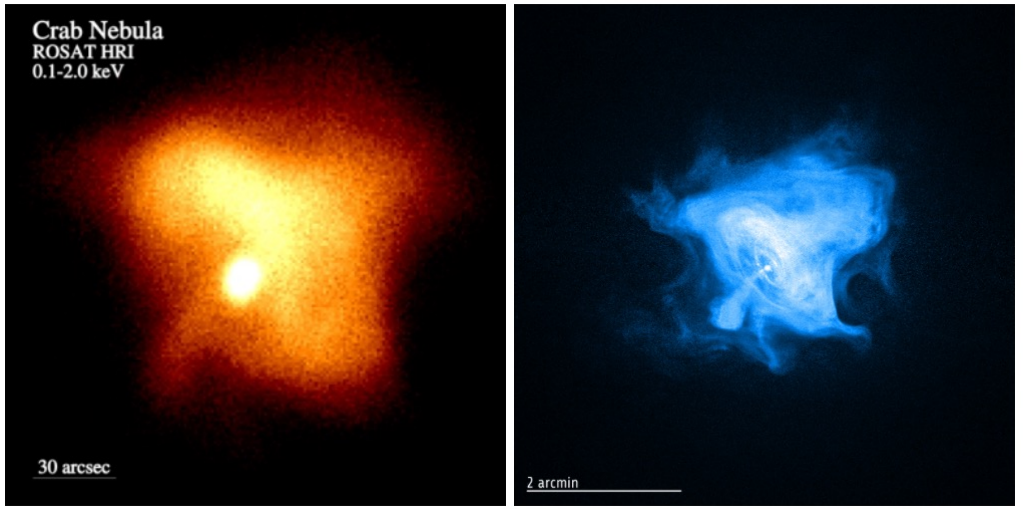
Uhuru **Einstein** OSO-7
Ariel 5 Ariel 6 SAS-3 OSO-8
Skylab HEAO-1 Copernicus
HEAO-3
EXOSAT Astro-A
Ginga Granat
CGRO **ROSAT**
BeppoSAX **RXTE**
ASCA **Chandra** **XMM-Newton**
INTEGRAL RHESSI *Swift*
Suzaku Hinode
Fermi
AGILE MAXI
NuSTAR
Astrosat Astro-H/Hitomi
eROSITA NICER HXMT
ART-XC/Spektr-RG
IXPE ***XRISM***
SVOM (P)
Gamow (P) ***Hi-Z-Gundam (P)***
~~THESEUS (P)~~
Athena (P) ***Lynx (P)***

- **Skylab (Apollo Telescope Mount)**
  - 1st large focusing X-ray telescope. X-ray images of the Sun, predecessor to Einstein X-ray Observatory.
- **Einstein (HEAO-B/2)**
  - First large X-ray telescope with mirrors. First X-ray images of shock waves from exploded stars, galaxy images. Accurately mapped 7000 X-ray sources accurately.
- **ROSAT**
  - **Röntgensatellite**. Larger telescope. Expanded number of X-ray sources to 60,000.
- **ASCA**
  - **Advanced Satellite for Cosmology and Astrophysics**. Important discoveries about elements that make up hot X-ray emitting gas.
- **RXTE**
  - **Rossi X-ray Timing Explorer**. No focusing mirrors, but high time resolution to look at X-ray source variability over a wide energy band (i.e. neutron stars and black holes).
- **BeppoSAX**
  - X-ray imaging of Gamma-ray Burst afterglows. High position accuracy
- **XMM-Newton**
  - High throughput X-ray Spectroscopy mission. Good angular resolution. Excels spectroscopy.
- **Chandra**
  - The premier X-ray observatory. Highest spatial resolution and amongst the most sensitive. Four nested mirrors.

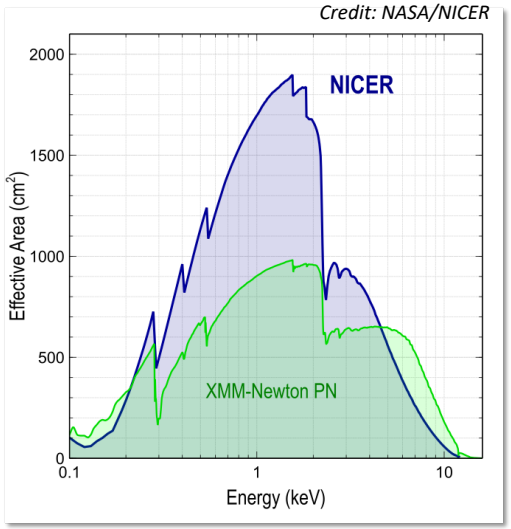
X-ray Instrumentation

- Several fundamental properties of interest that will address the primary science objective. For example:
  - Angular resolution
  - Field of view (FoV)
  - Spectral and temporal resolution
  - Sensitivity
    - Effective Area / Collection Area (min. detectable flux)
    - Energy (Wavelength) range
    - Temporal range

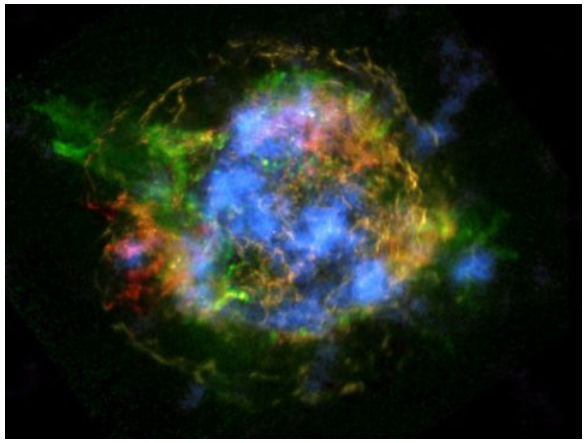
ROSAT Credit: S.L. Snowden, NASA/GSFC. Chandra Credit: NASA/CXC/SAO



Credit: NASA/NICER

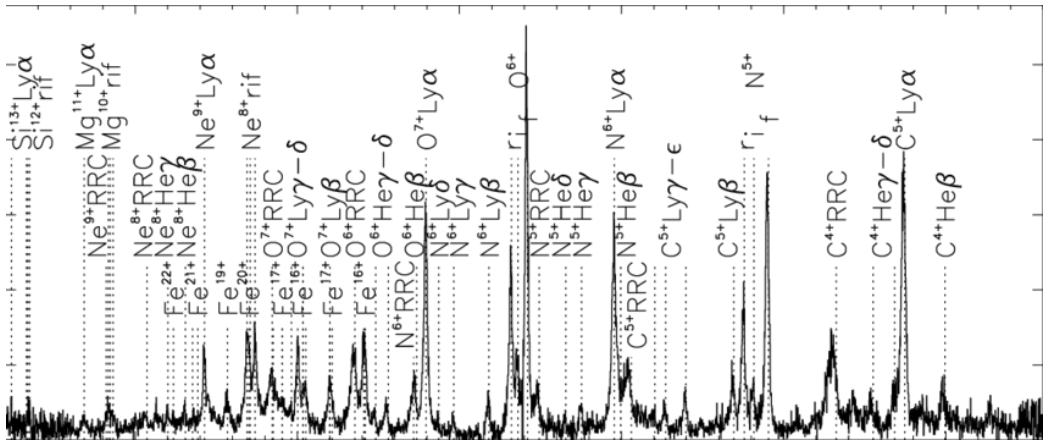


Credit: NASA/JPL-Caltech/CXC/SAO



Cass. A. NuSTAR blue, CXC rest.

XMM RGS of NGC 1068

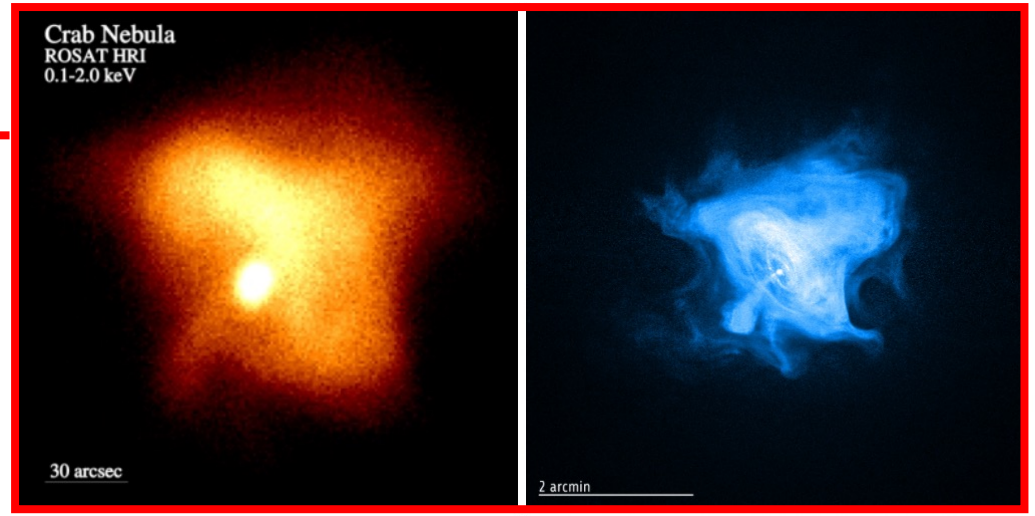


Kahn et al. (2001). https://arxiv.org/abs/astro-ph/0107225

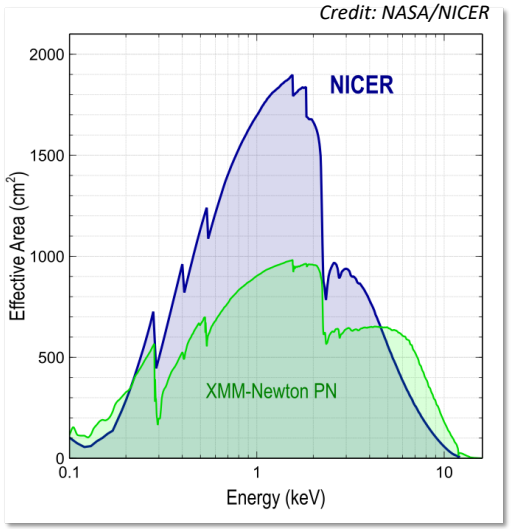
X-ray Instrumentation

- Several fundamental properties of interest that will address the primary science objective. For example:
  - Angular resolution
  - Field of view (FoV)
  - Spectral and temporal resolution
  - Sensitivity
    - Effective Area / Collection Area (min. detectable flux)
    - Energy (Wavelength) range
    - Temporal range

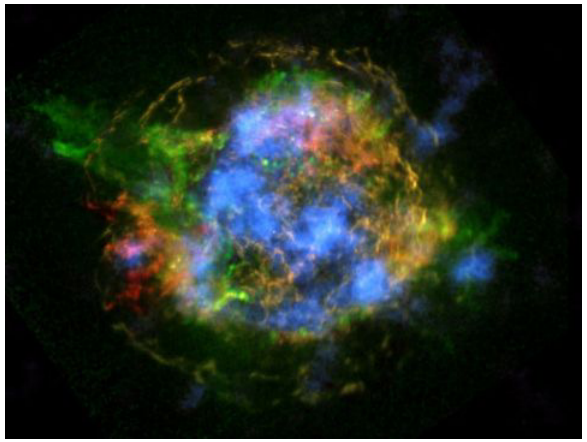
ROSAT Credit: S.L. Snowden, NASA/GSFC. Chandra Credit: NASA/CXC/SAO



Credit: NASA/NICER

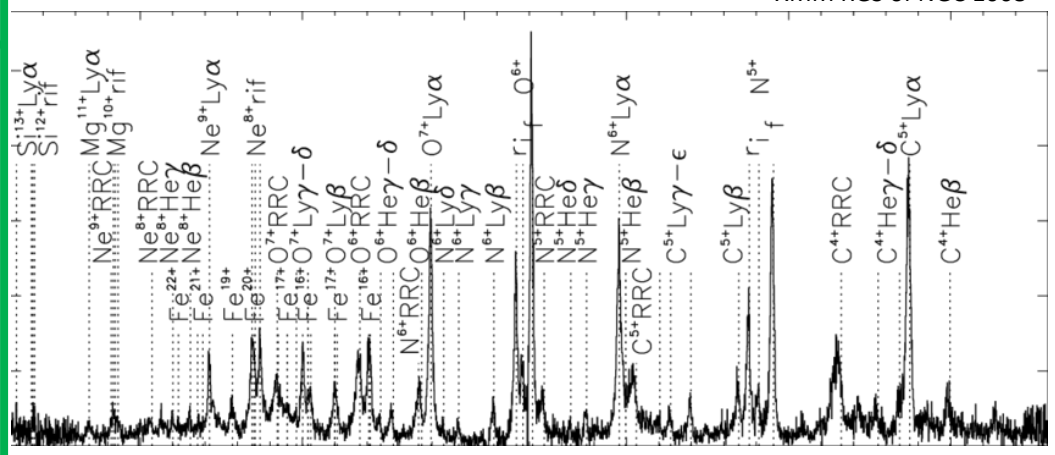


Credit: NASA/JPL-Caltech/CXC/SAO

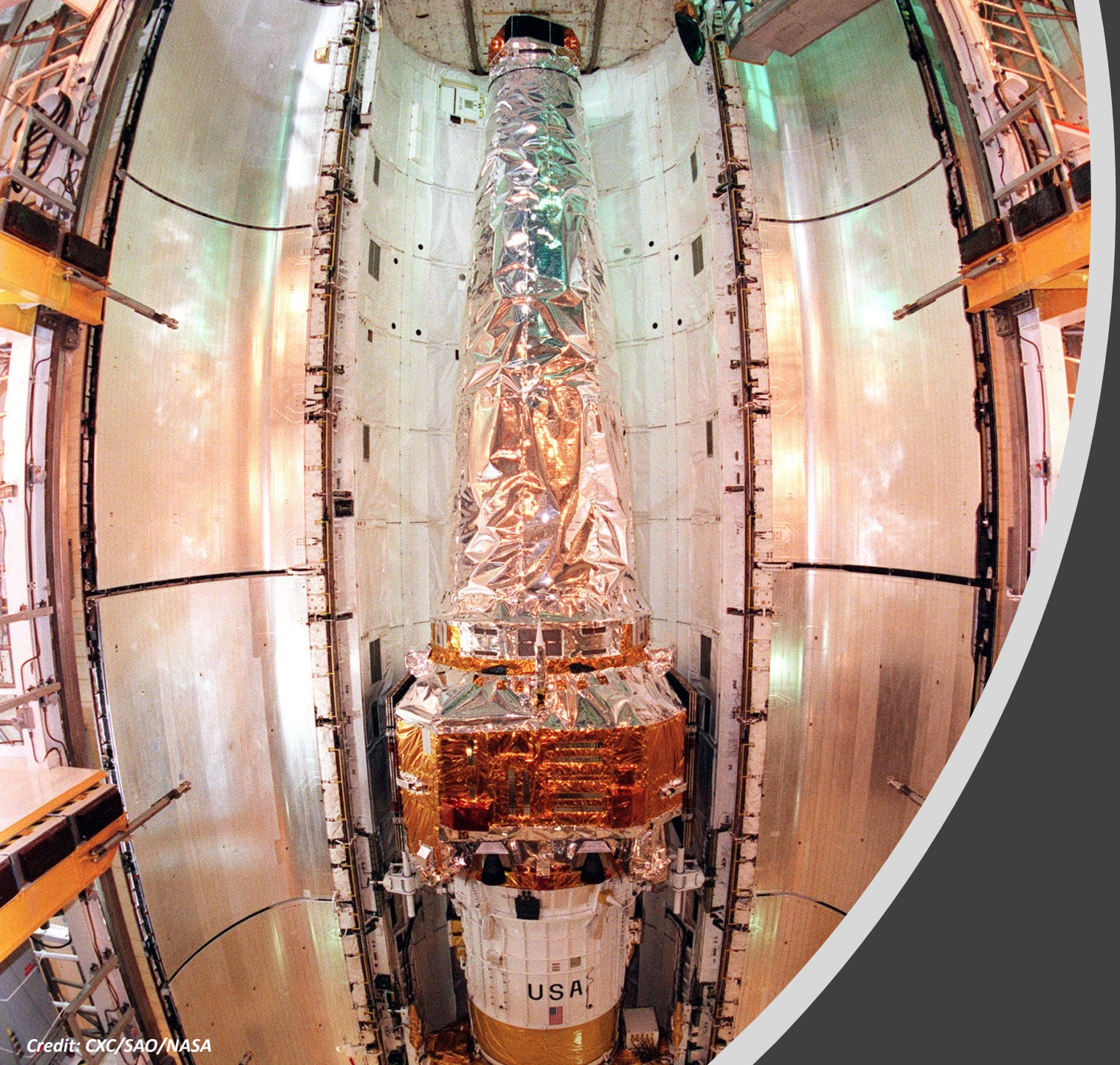


Cass. A. NuSTAR blue, CXC rest.

XMM RGS of NGC 1068



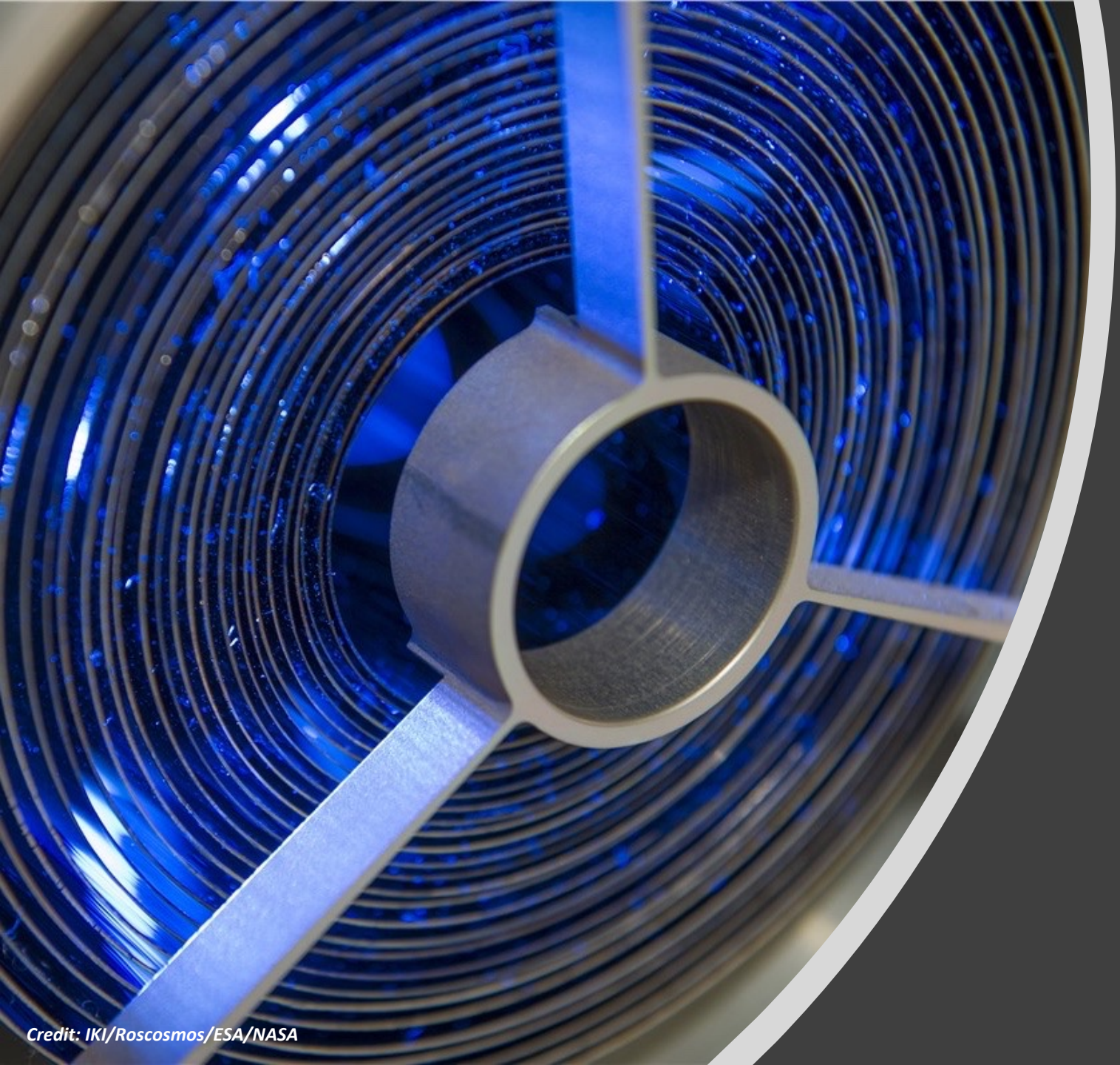
Kahn et al. (2001). https://arxiv.org/abs/astro-ph/0107225



Credit: CXC/SAO/NASA

How to Build an X-ray Telescope

Left: Chandra in Space Shuttle Columbia



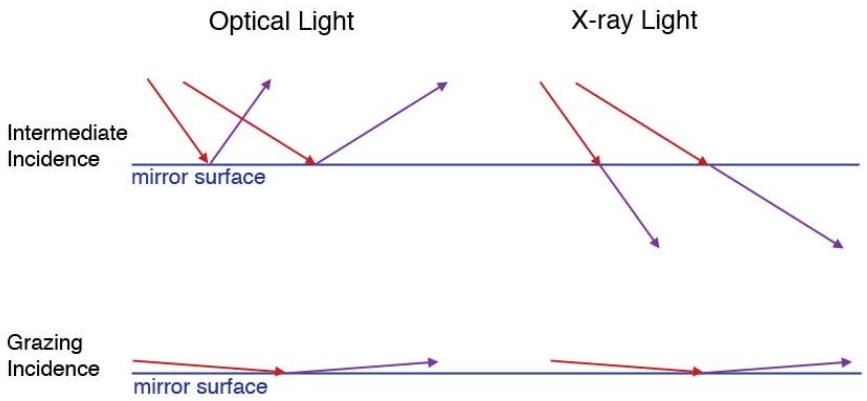
Credit: IKI/Roscosmos/ESA/NASA

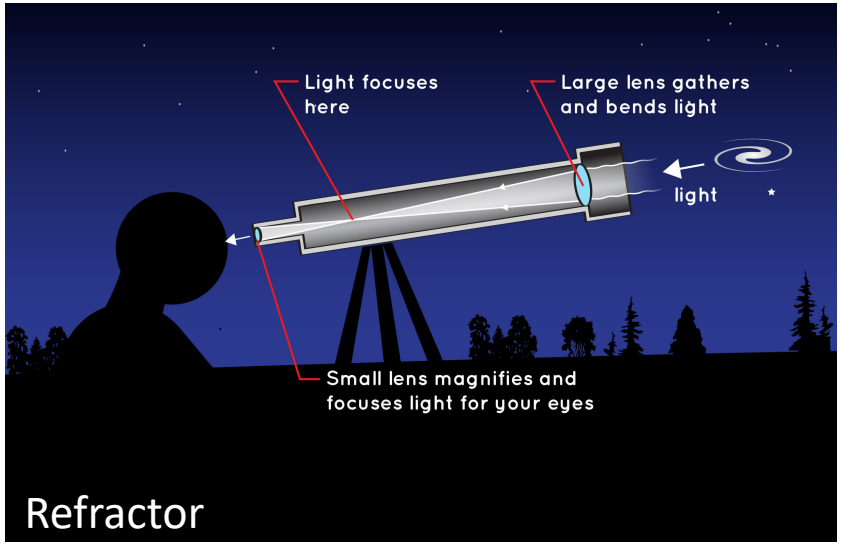
1. Telescope

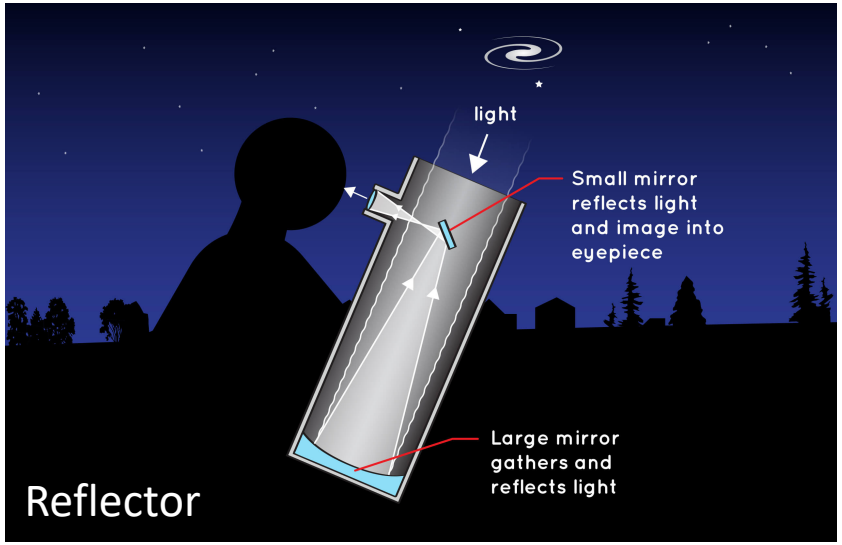
Left: ART-XC X-ray telescope/module

Mirrors and Telescopes

- Conventional telescopes use **reflection** or **refraction** at normal/intermediate incidence (i.e. visible light).
- *Not* applicable for X-rays as rays travelling perpendicular to mirror are absorbed or transmitted (no reflection).
- X-ray telescope work use grazing incidence optics (mirror reflection at shallow angles) for total external reflection.
- Scattering of any wave by electrons is coherent only if the ***angle of incidence equals the angle of reflection***; $\boldsymbol{\phi_i = \phi_o}$





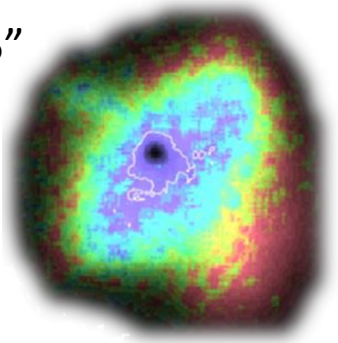


All Image Credit: NASA

Telescopes

- *Some* X-ray mirror Requirements:
  - Field of view (FoV)
    - i.e. Short focal length, larger FoV.
  - High spatial resolution (HPD/HEW<arcsecond)
    - Focusing ability (minimize PSF wings - polishing)
    - 1 arcmin human eye resolution.
  - Thin, robust, cheap
    - Mission costs, nesting (effective area/sensitivity)
  - Broad energy range
    - Longer focal lengths and multi-layers.
  - High spectral and temporal resolution
    - i.e. Sub-keV and Sub-μs, respectively.

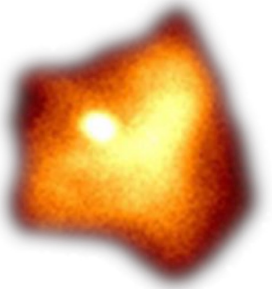
XMM 15”



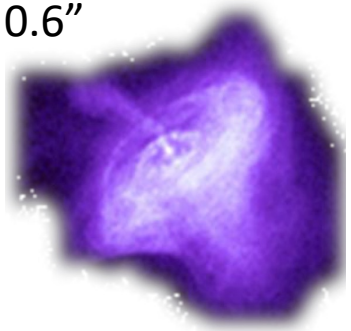
Einstein 10”



ROSAT 5”



Chandra 0.6”



Credit: O’Dell, ArXiv (https://arxiv.org/pdf/1010.4892.pdf)

Telescopes

- A Simple parabolic mirror was conceived in 1960 by Riccardo Giacconi and Bruno Rossi.
- Grazing incidence implies far zone of paraboloid must be used as reflecting surface.
- Not possible to satisfy Abbé sine condition for any single reflection grazing incidence optic.
- Off-axis images severely blurred (Severe comatic aberration or Coma).

Abbé sine condition:

$$sin\,\alpha_o \propto sin\,\alpha_i$$

Where α_o and α_i are the object- and image-space angles, respectively.

Fulfilled by a lens or other optical configuration in order for images to be sharp off-axis as well as on-axis.

Magnification:

$$|M| = \frac{\sin\alpha_o}{\sin\alpha_i} = \frac{\sin\beta_o}{\sin\beta_i}$$

Entrance (α) and exit (β) angles of each ray through an imaging system satisfy the Abbé sine condition when the ratio of these angles equal the magnification of the system

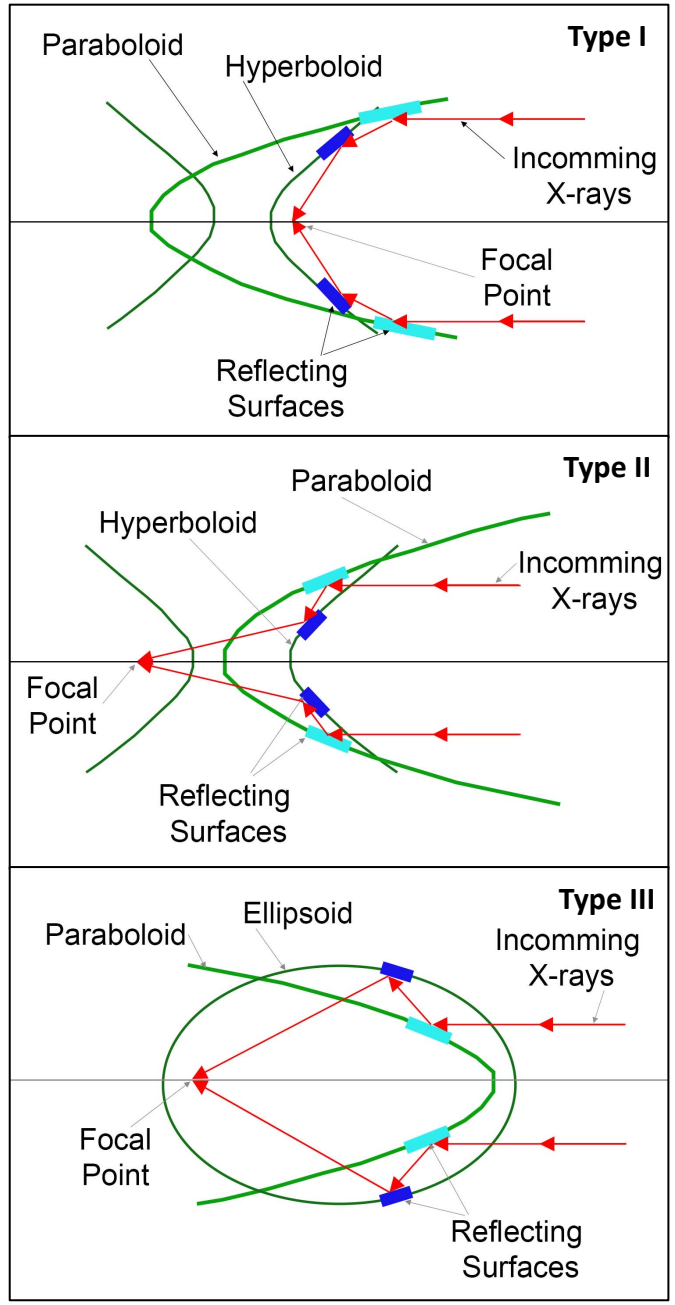
Wolter Telescopes

- In 1952, Hans Wolter showed reflection off two elements; a paraboloid followed by a hyperboloid, almost satisfies Abbé sine condition and mostly eliminates coma aberration for incident rays (optimal focal plane is not flat).

- Three types:
  - **Type I**: Preferentially sort in astronomical applications due to its simplicity and nesting ability.
  - **Type II**: Can achieve higher magnification for comparable aperture size and grazing angles. However, primarily used as a narrow-field imager due to blurring of off-axis images.
  - **Type III**: Never used in X-ray Astronomy

- Costly and difficult to fabricate exactly. Conical Wolter-I geometries devised, approximate the P and H surface of the Wolter-I geometry with double cones.
  - Greatly reduces cost and slightly degrades the on-axis sharpness, in exchange for a more artifact free image when the source is off-axis.
  - Suitable for missions with modest resolution but large effective area.

- Wolter-Schwarzschild telescope exactly satisfies the Abbé sine condition and adopted for Einstein probe mirrors.
  - Coma free but strongly affected by spherical aberration.



Credit: NASA's Imagine the Universe

P and H Wolter I mirrors that are coaxial and confocal:

$$r_p^2 = P^2 + 2PZ + \left[\frac{4e^2Pd}{e^2-1}\right] \quad (Paraboloid)$$

$$r_h^2 = e^2(d+Z)^2 - Z^2 \quad (Hyperboloid)$$

Origin at focal plane. Z is the optical axis and r is the radius of surface Z.

Common focus: $Z = \left[-\frac{2e^2d}{e^2-1}\right]$

Z_0 is the focal length, determines scale of optics:

$$\alpha = \frac{1}{4}\arctan\left(\frac{r_0}{Z_0}\right) = \frac{1}{2}\left(\alpha_p^* + \alpha_h^*\right),$$

where r_0 is the surface radius at the intersection and α_p^*, α_h^* are the grazing angles between the P and H surfaces and paraxial ray that strikes at some distance from the intersection.

If $\tan\theta_p^*$ and $\tan\theta_h^*$ are the slopes of the surfaces at the intersection:

$$\alpha_p^* = \theta_p^*, \alpha_h^* = \theta_h^* - 2\theta_p^*, and\ \alpha = \frac{1}{2}\left(\theta_h^* - \theta_p^*\right); \zeta = \frac{\alpha_p^*}{\alpha_h^*}$$

Original parameters ***e,d,*** **and** ***P*** can be determined as:

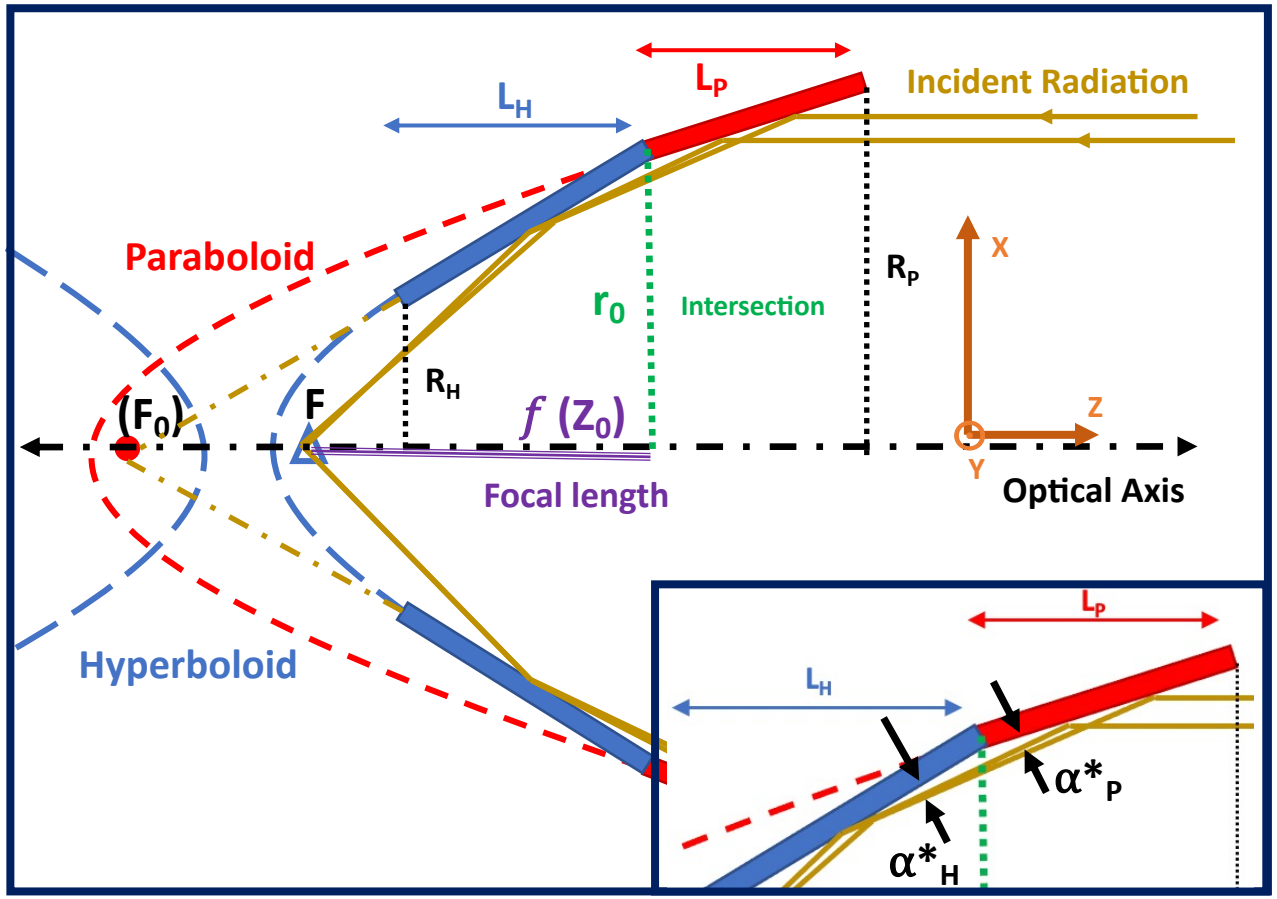
$$(a)\ \theta_p^* = \left[\frac{2\zeta}{1+\zeta}\right](\alpha)$$

$$(b)\ \theta_h^* = \left[\frac{2(1+2\zeta)}{1+\zeta}\right](\alpha)$$

$$(c)\ \boldsymbol{P} = Z_0 \tan(4\alpha)\, tan\ \theta_p^*$$

$$(d)\quad \boldsymbol{d} = Z_0 \tan(4\alpha)\tan(4^{\alpha} - \pi_h^*)$$

$$(e)\quad \boldsymbol{e} = \cos(4\alpha)\left[1 + \tan(4\alpha)\tan(\theta_h^*)\right]$$



L_P and L_H are the paraboloid (P) and hyperboloid (H) lengths, respectively. Leave L_P to be a free parameter. Constrain L_H to be just long enough to that paraxial rays striking the front of the P mirror, also strike the H mirror. Equation for L_H:

$$\frac{L_H}{L_P} = \frac{P}{ed + (e-1)L_P} \approx \frac{\zeta}{1 + \left(\frac{\zeta L_P}{Z_0}\right)}$$

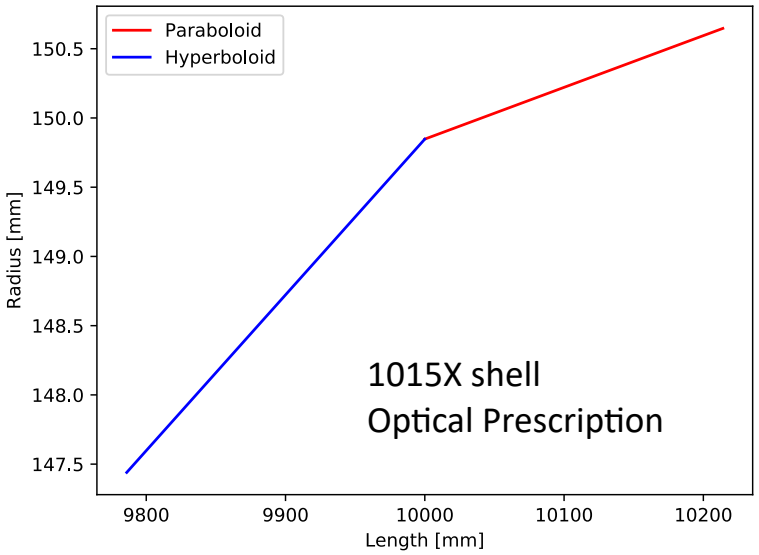
Thus, geometrical properties of a given telescope & source determined by 4 free-design parameters (Z_0, α, ζ, L_p) & angle θ between the rays & optical axis.

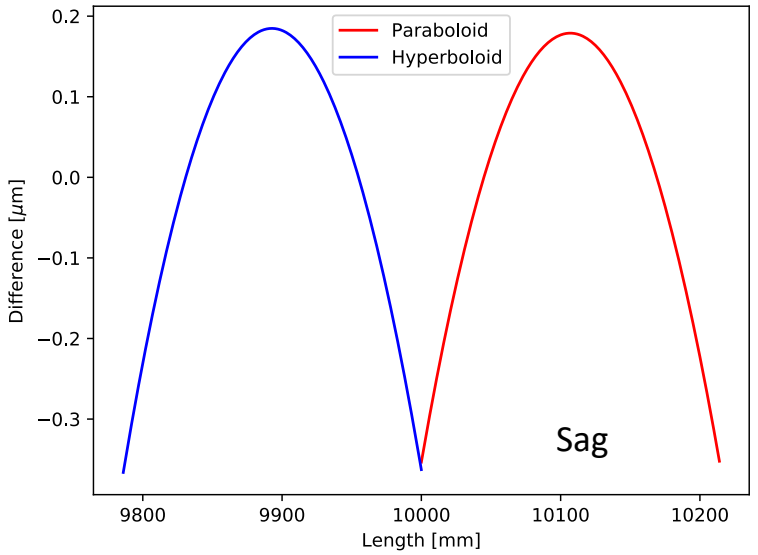
Giaconni et al., (1969) Space Science Reviews, Volume 9, Issue 1, pp.3-57. doi: 10.1007/BF00187578

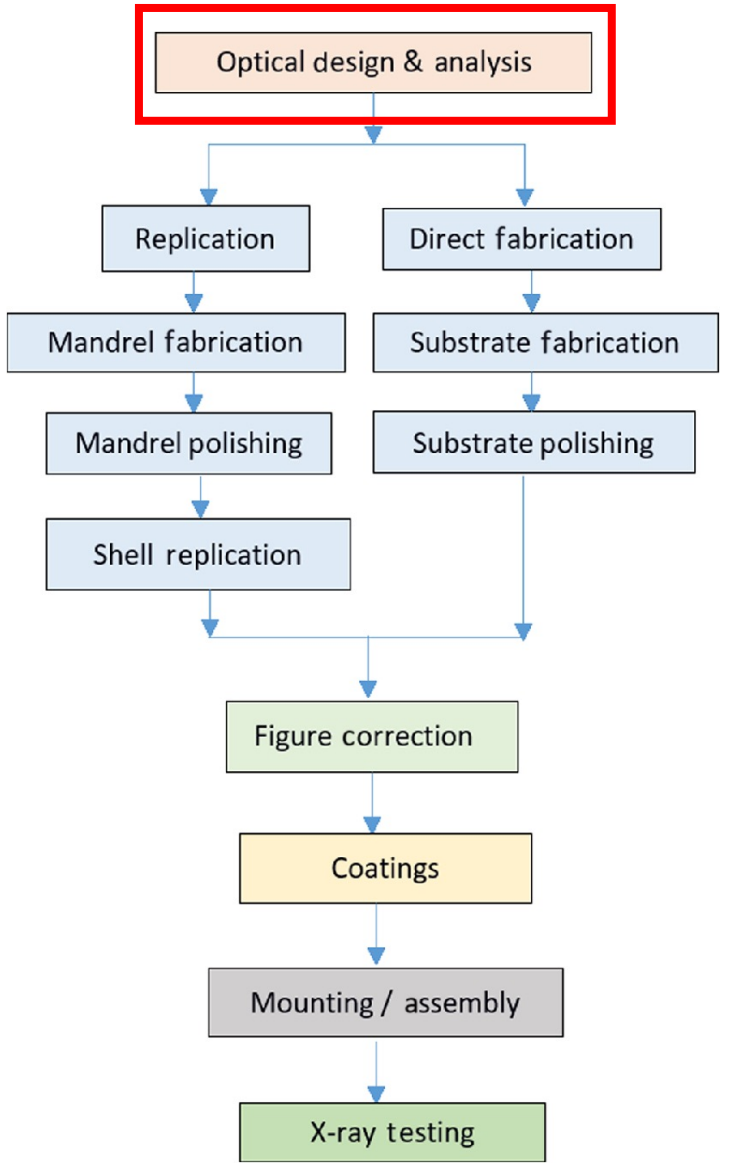
L. P. VanSpeybroeck and R. C. Chase, Appl. Opt. 11, 440-445 (1972), doi: https://doi.org/10.1364/AO.11.000440

Wolter Telescopes – Mirror Fabrication

- Optical Design:
  - Diameter, focal length, segment length, thickness, etc
  - Analytical and Monte-Carlo ray-tracing to characterize on- and off-axis effective area, FoV, angular resolution, stray light analysis, etc.
  - Coatings: Single or Multi-layers
  - Finite Element Analysis (FEA): Mechanical and thermal.

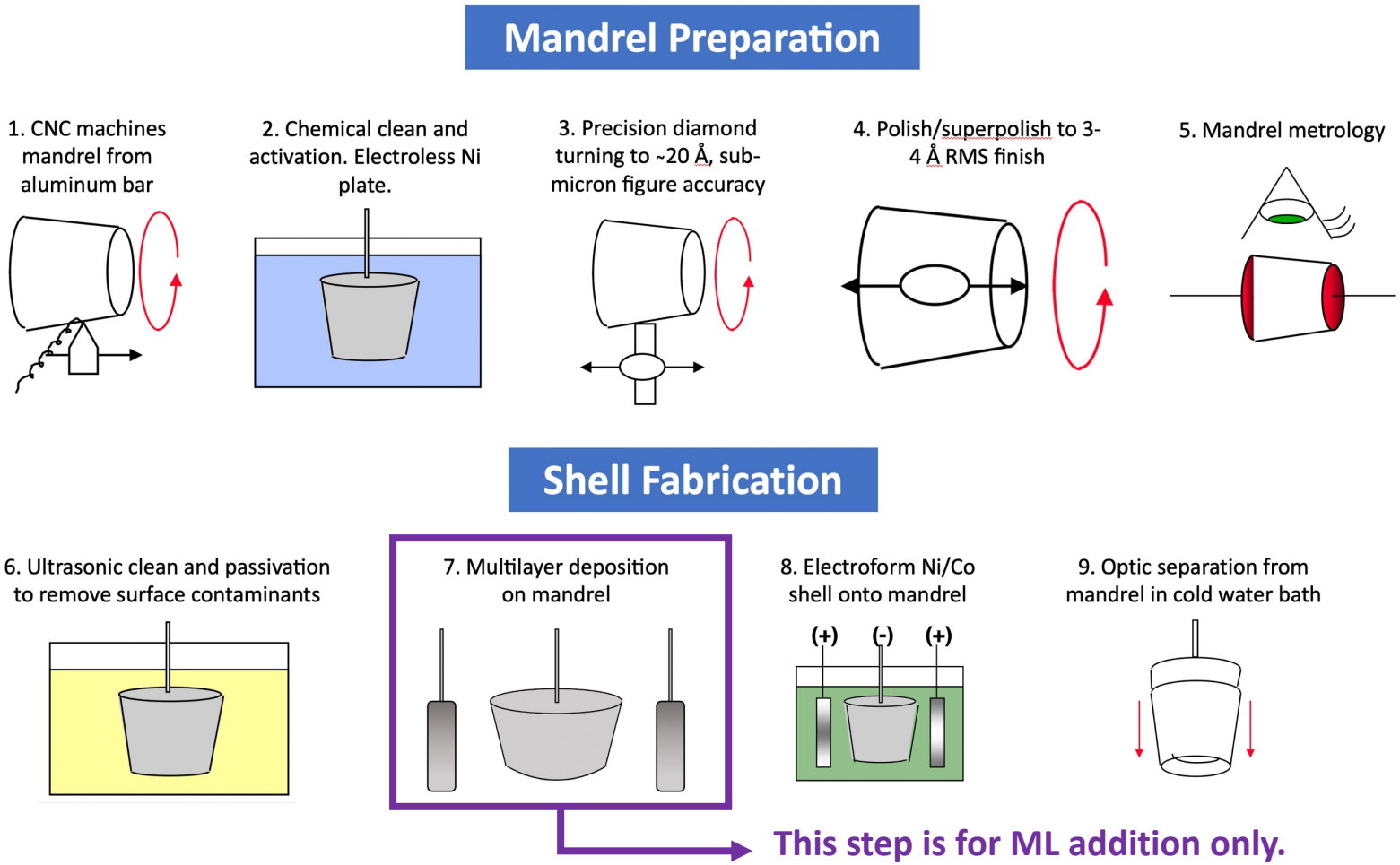


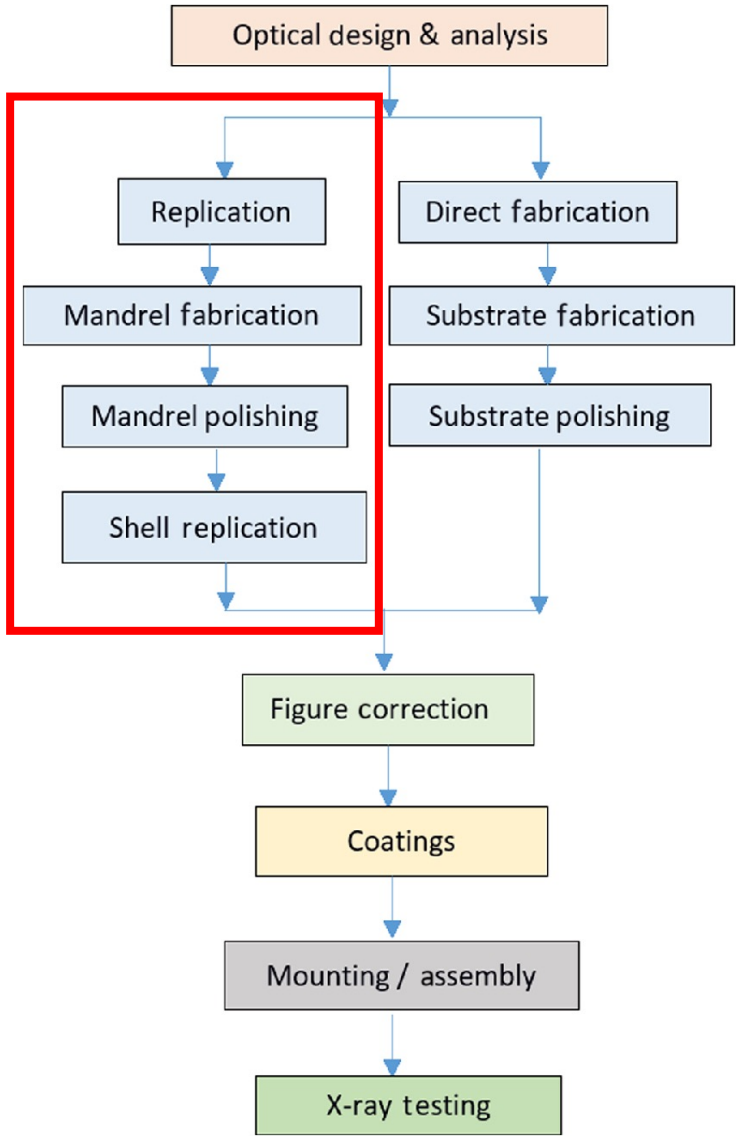




Wolter Telescopes – Mirror Fabrication

- Electroformed Nickel Replication:



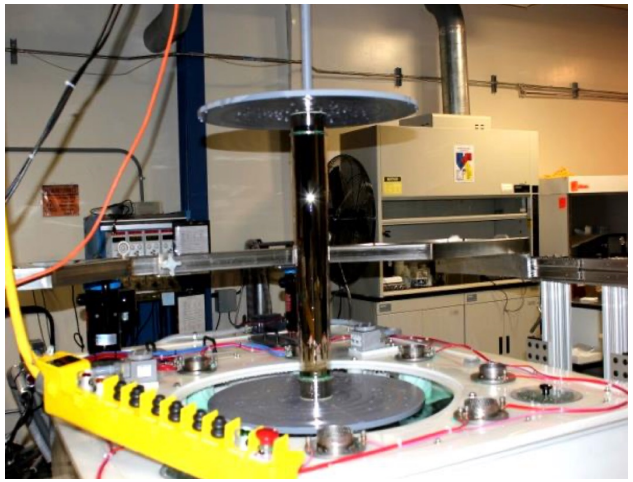


Adapted from: Kilaru, K, https://wwwastro.msfc.nasa.gov/lynx/docs/meetings/TIM01/Xray_Optics_at_MSFC.pdf

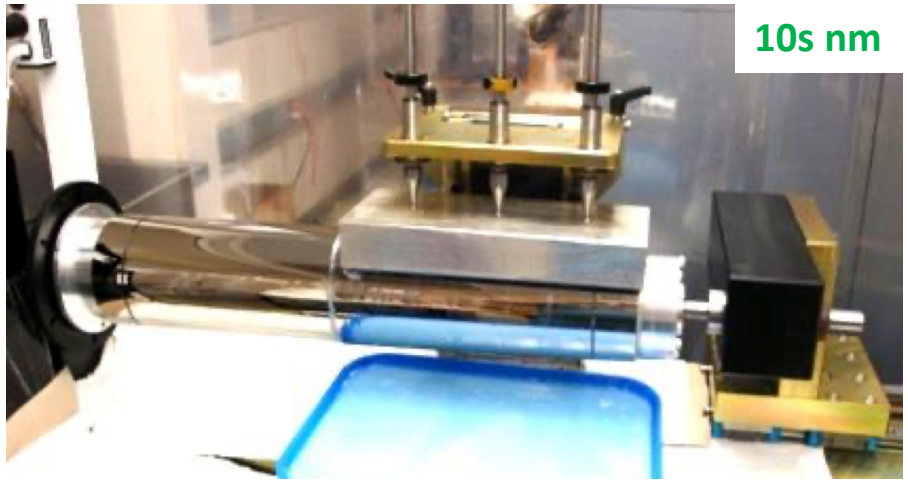
Wolter Telescopes – Mirror Fabrication



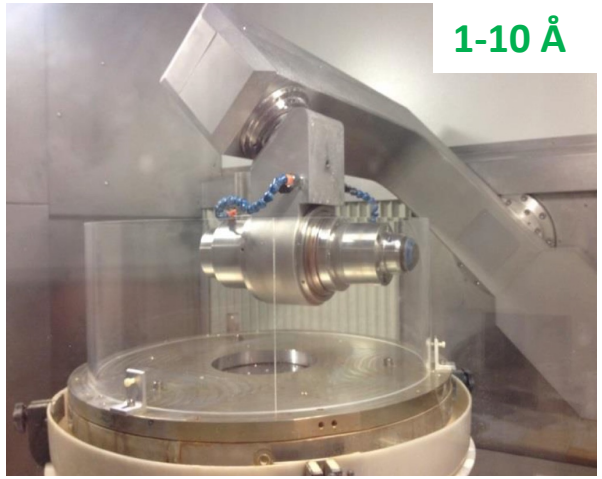
Diamond turning mandrel



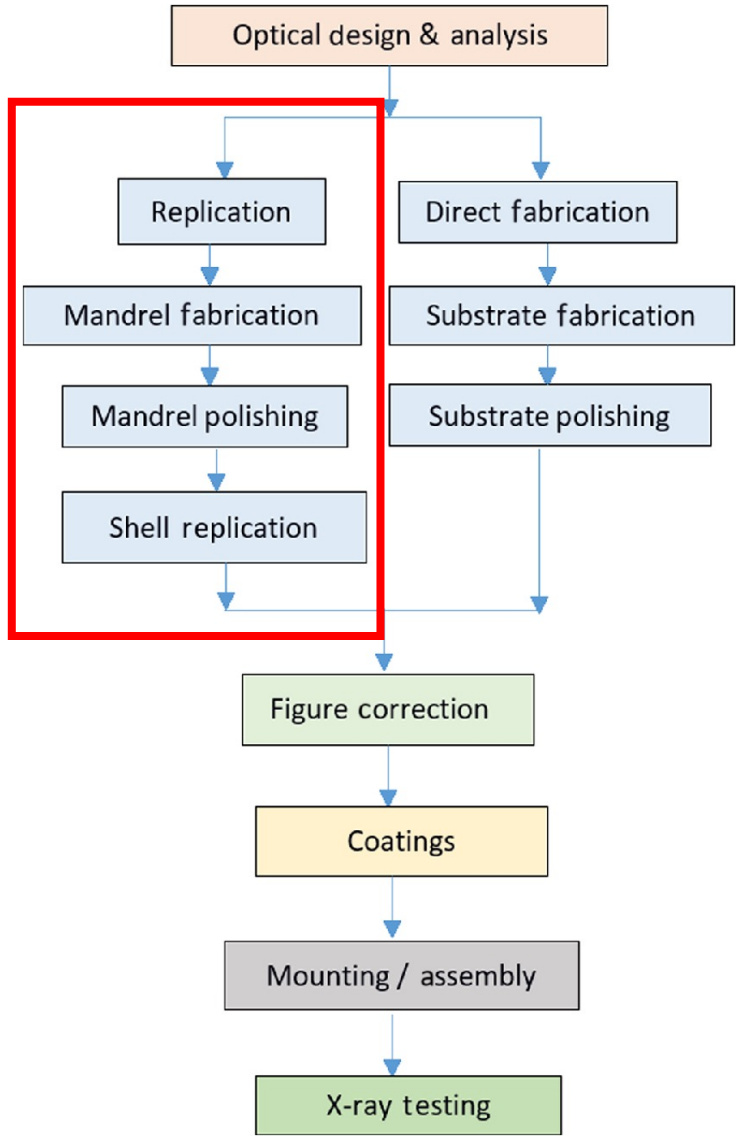
Plating mandrel



Lap-polishing mandrel

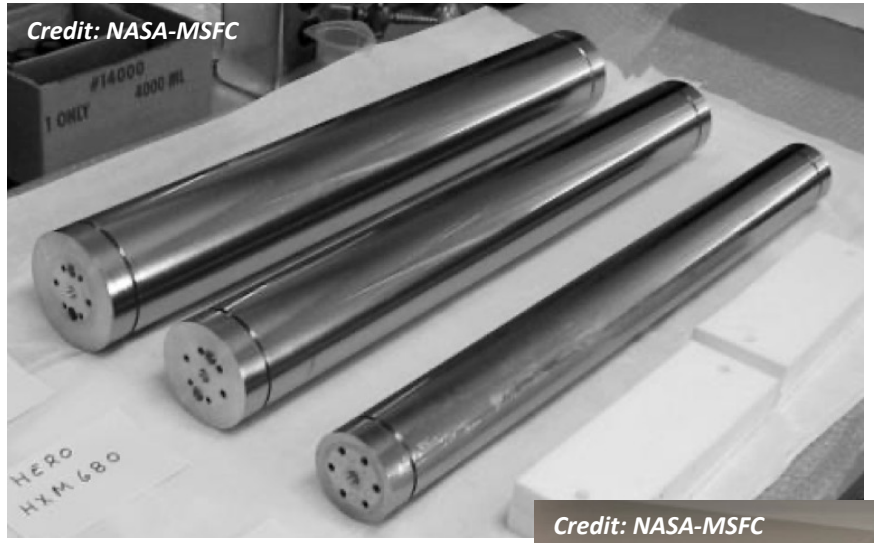


Zeeko Polishing



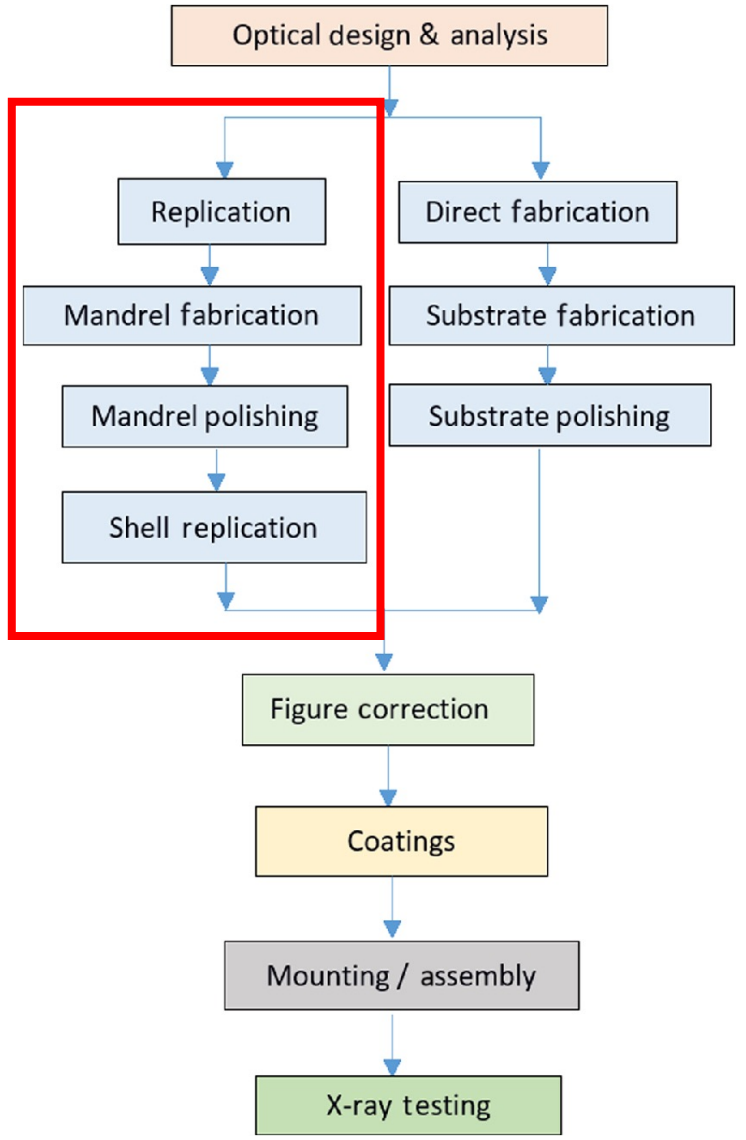
Credit: Kilaru, K, https://wwwastro.msfc.nasa.gov/lynx/docs/meetings/TIM01/Xray_Optics_at_MSFC.pdf

Wolter Telescopes – Mirror Fabrication



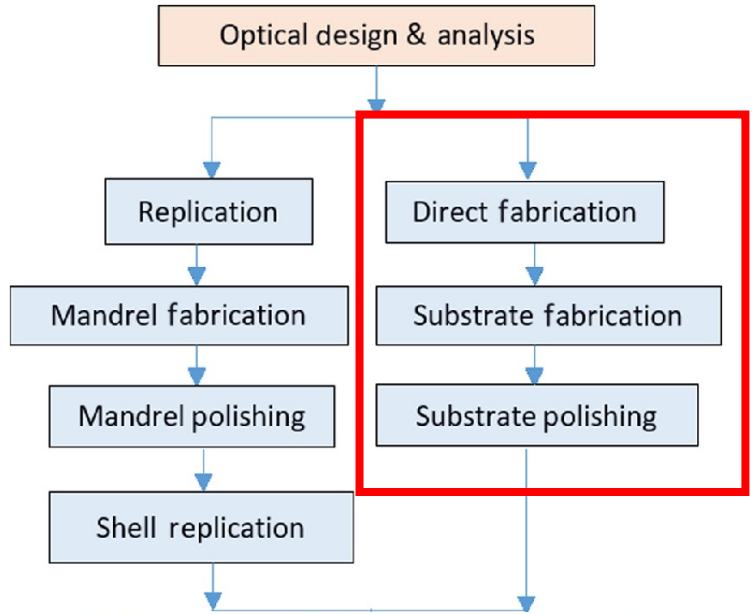


Arrangement of mandrels and shells (ℓ=600 mm) for HERO balloon payload.



Wolter Telescopes – Mirror Fabrication

- Direct Mirror Fabrication:
  - Surface profile with correct optical prescription ground and polished directly into a full shell substrate.
  - Mirrors are thicker, need to be stiffer/resilient.



Chandra direct shell fabrication. Left: Single raw blank prior to grinding and polishing. **Center**: Polished element. **Right**: Coated element prior to insertion into fixture.



All image credit: NASA/CXC/SAO

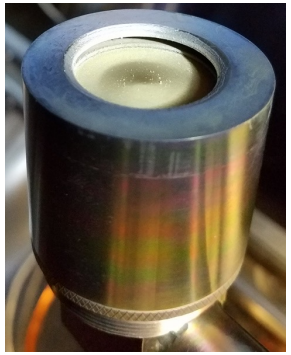


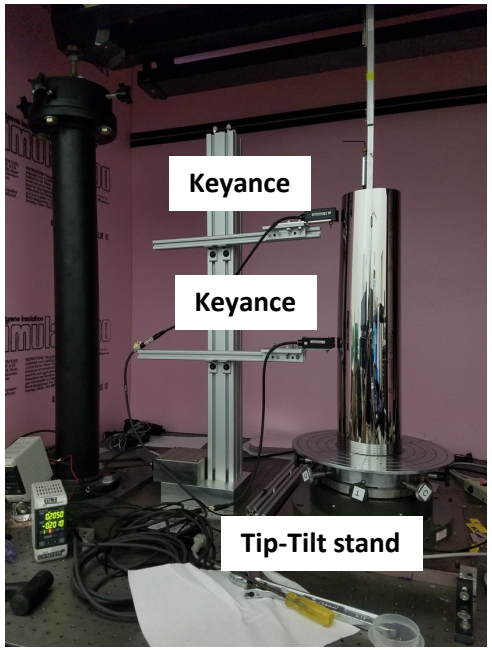
One of the Chandra paraboloid mirrors during rough grinding

Wolter Telescopes – Mirror Fabrication

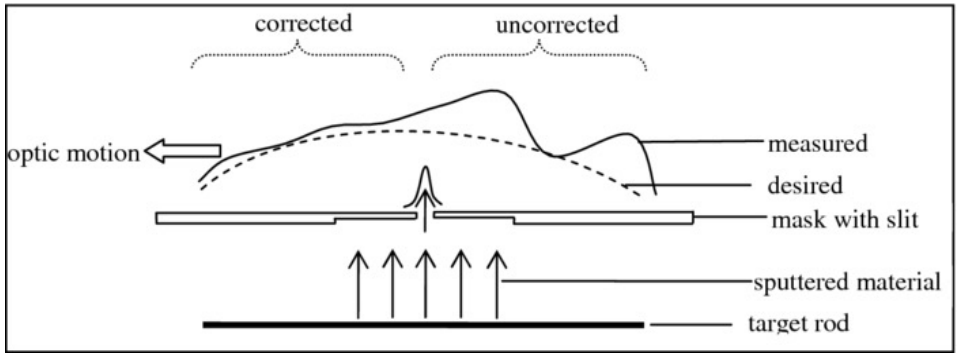
Differential Deposition Chamber



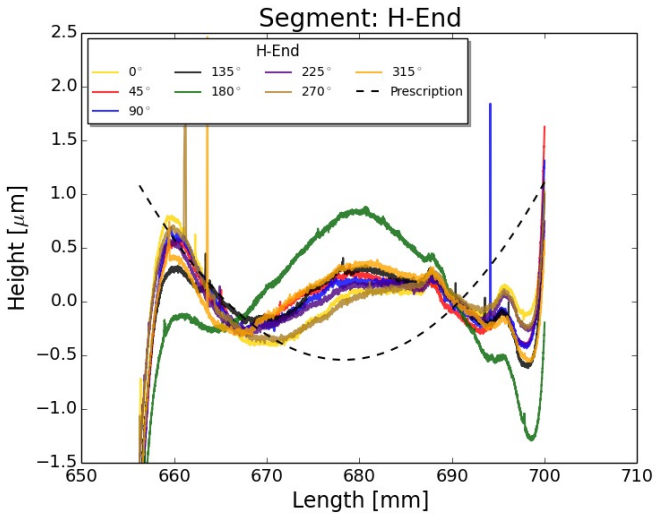


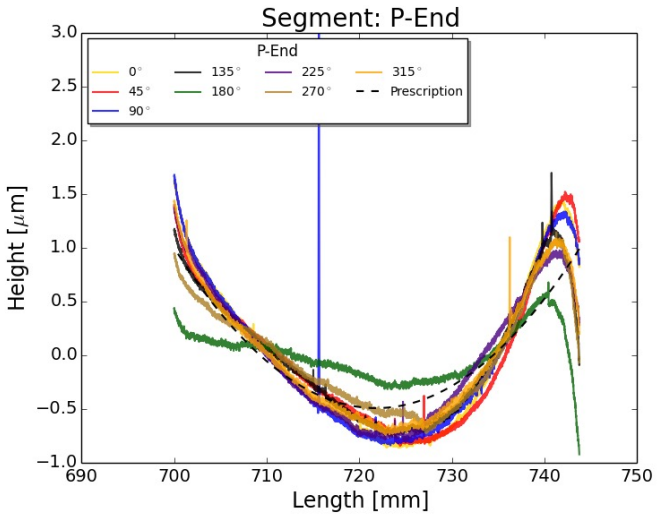


VLTP Metrology test stand with 1015X shell

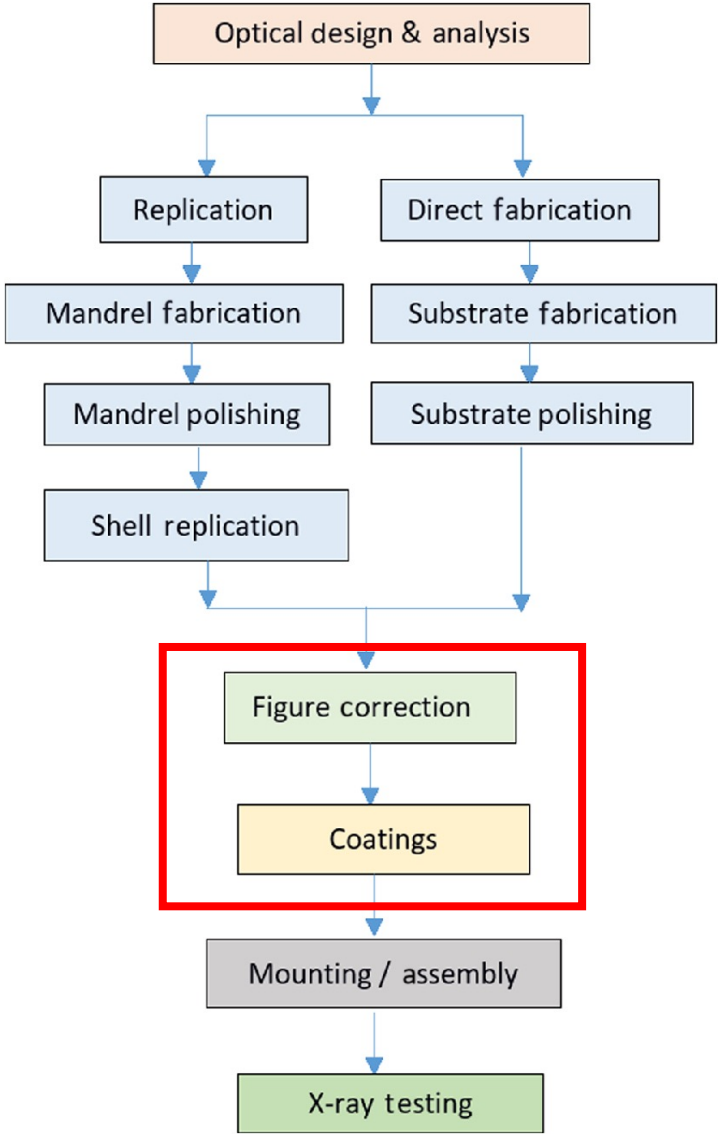


Kilaru et al. Optical Engineering, 50(10), 106501 (2011). https://doi.org/10.1117/1.3631851



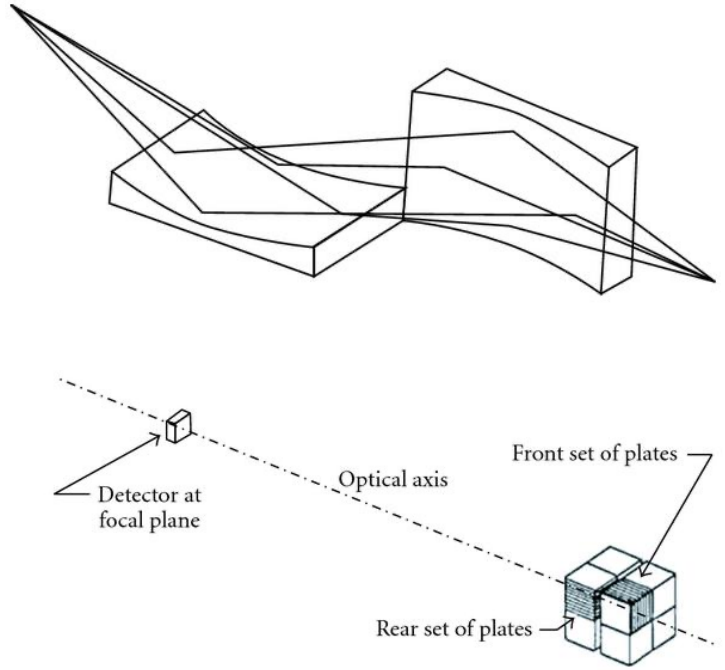


Metrology Measurements of MIXO shell



Kirkpatrick-Baez Optics

- 2-D image by Kirkpatrick-Baez in 1948 **[1]**
- Easy to assemble, modular, can be bent to improve curvature
- Can nest, but this introduces aberrations
- Requires longer focal length / telescope
- 1-D KBO successfully flown in rocket tests **[2]**
- Van Speybroeck **[3]** designed several telescope configurations which would have good applications in astronomical observations such as high-sensitivity surveys, photometry and spectroscopy due to large effective area.
- Increasing spacing between plates maximizes effective area over FoV.
- Spurious images present but can be eliminated with collimators/baffles.



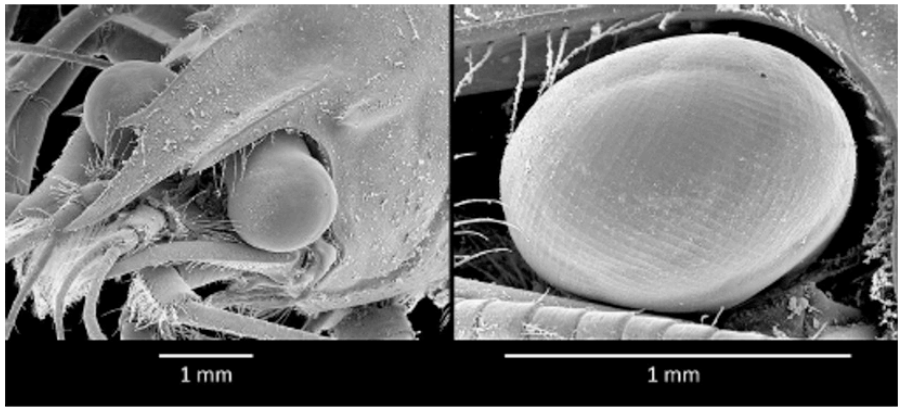
The KB optics design studied for HEAO-A **[4]**.

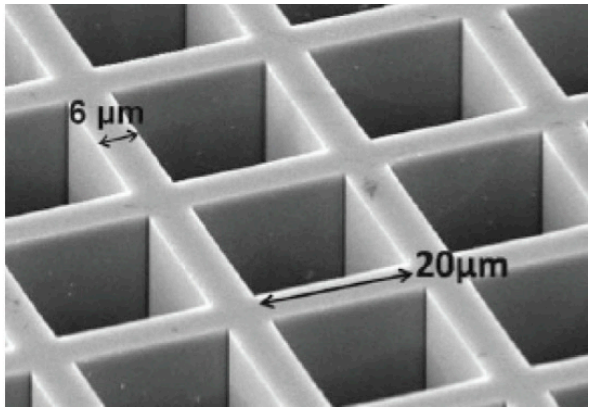
1. P. Kirkpatrick and A. V. Baez, “Formation of optical images by X-rays,” *Journal of the Optical Society of America*, vol. 38, no. 9, pp. 766–773, 1948.
2. P. Gorenstein, B. Harris, H. Gursky, and R. Giacconi, “A rocket payload using focusing X-ray optics for the observations of soft cosmic X-rays,” *Nuclear Instruments and Methods*, vol. 91, pp. 451–459, 1971.
3. L. P. Van Speybroeck, R. C. Chase, and T. F. Zehnpfennig, “Orthogonal mirror telescopes for X-ray astronomy,” *Applied Optics*, vol. 10, p. 537, 1971.
4. J. W. Kast, “Scanning kirkpatrick-baez x-ray telescope to maximize effective area and eliminate spurious images; design,” *Applied Optics*, vol. 14, no. 2, pp. 537–545, 1975.

Lobster-Eye Optics

- Lobster-eye optics based off a lobster eye, naturally developed for high, efficient light collection in dark, deep-ocean environments.
  - Square channels roughly 20x20x60 microns in size with reflecting walls.
  - Image is formed by corner reflections from adjacent channel walls.
  - Lobster eye resembles a spherical mirror. Although a spherical mirror produces a virtual image while a Lobster eye produces a real image.
  - Lobster eyes use naturally organic, multilayer coatings perfectly suited to work in visible light. – **How do we adapt this for X-rays?**

- Two configurations:
  - Schmidt (1975)
  - Angel(1979)





Credits: Courtesy of J. Camp: https://www.nasa.gov/feature/goddard/2017/proposed-nasa-mission-employs-lobster-eye-optics-to-locate-source-of-cosmic-ripples

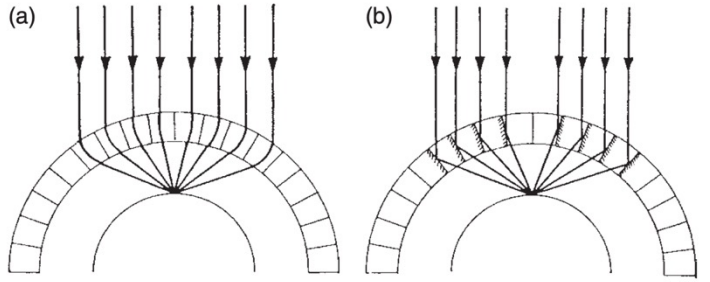
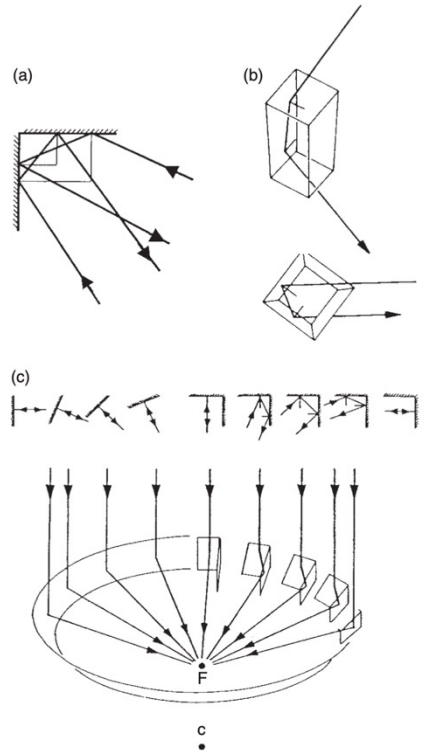


Fig. 8.14 Comparison of ray paths in a refracting (a) and reflecting (b) superposition eye. Both redirect the rays as required by Fig. 8.3.

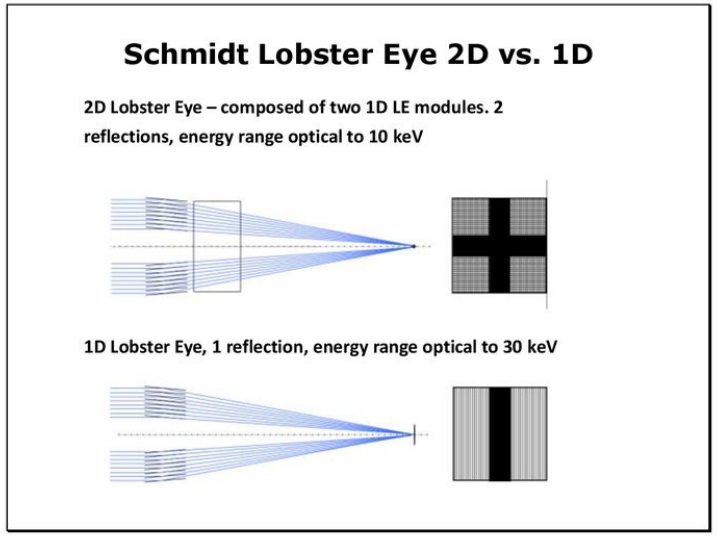


Land and Nilsson, Animal Eyes, Chapter 8, OABS, 2002 : http://www.softouch.on.ca/kb/data/Animal%20Eyes.pdf

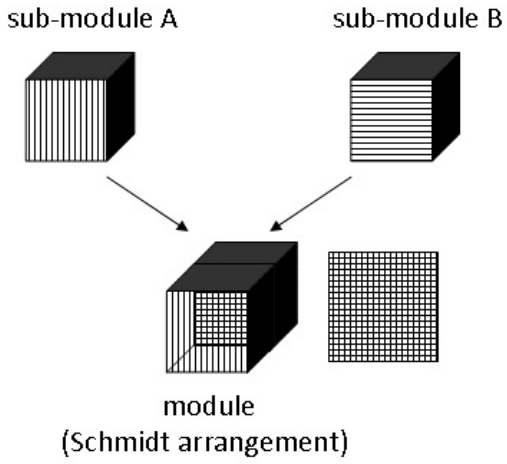
Fig. 8.15 (a) The principle of the corner reflector. Whatever the angle of incidence, incoming rays are reflected through two right angles, and so emerge parallel to their original path. (b) In the mirror box of a shrimp, the incident and reflected rays are not in the same horizontal plane, but viewed along the axis of the structure (*below*) the corner reflector behaviour is evident. (c) Ray paths for rays that are not in the central plane of the eye (unlike Fig. 8.14b). The mirror boxes act as 'corner reflectors' in which rays reflected from two sides emerge in the same plane as the incident rays to reach a focus at *F*. This is the condition for obtaining a clear image over a wide angular field. See text for further explanation. *C* is the eye's centre of curvature.

Schmidt Lobster-eye Optics:

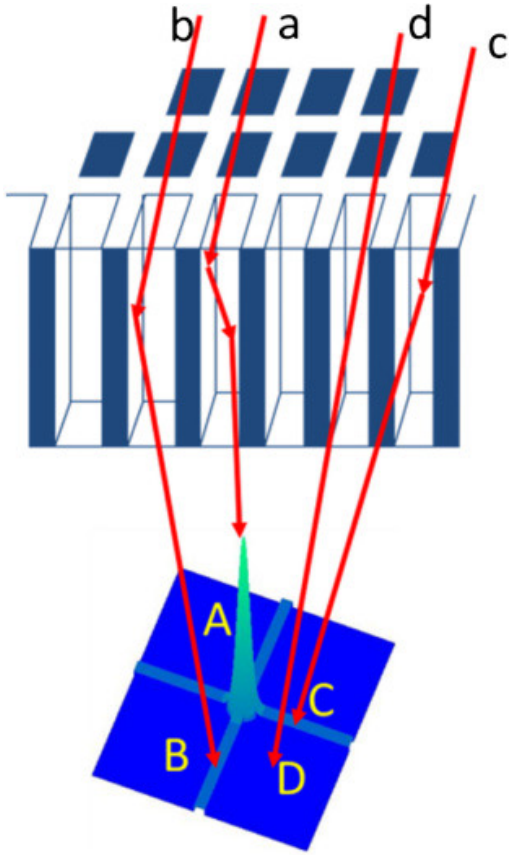
- 1-D Schmidt LE optics:
  - Very wide FoV (half sphere)
  - Flat reflectors, arranged uniformly in radial pattern around cylinder perimeter
  - Finite image size (not perfect), 1/10th degree or better.
- 2-D Schmidt LE optics:
  - Orthogonal stacks of reflectors in sequence (two); double-focusing.
  - FoV of up to 1000 deg^2 at moderate angular resolution (several arcmins)



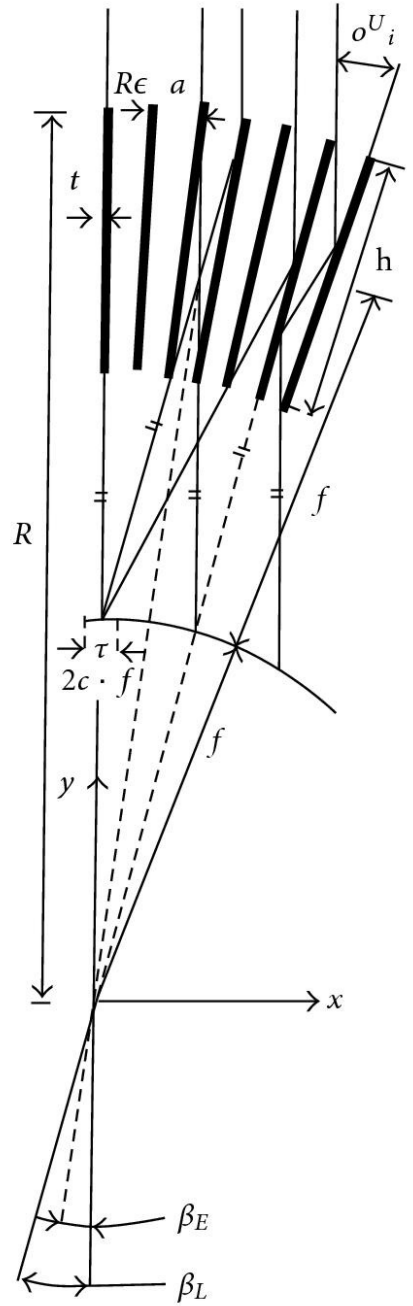
Hudec, R., et al. Proc. SPIE 9510, 95100A (2015); https://doi.org/10.1117/12.2177792



Pina, L. et al. (2019); DOI:10.1117/12.2543412



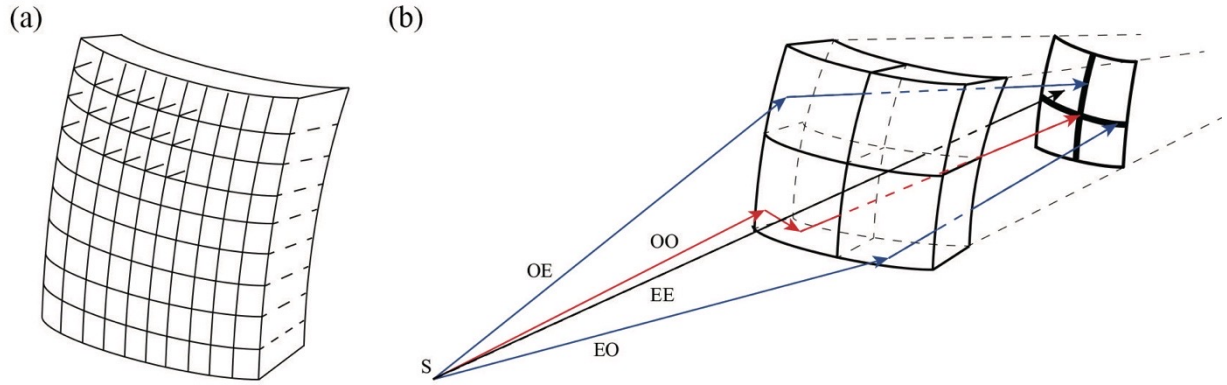
Luning, Su, et al. Appl. Opt. 56, 6267-6271 (2017)



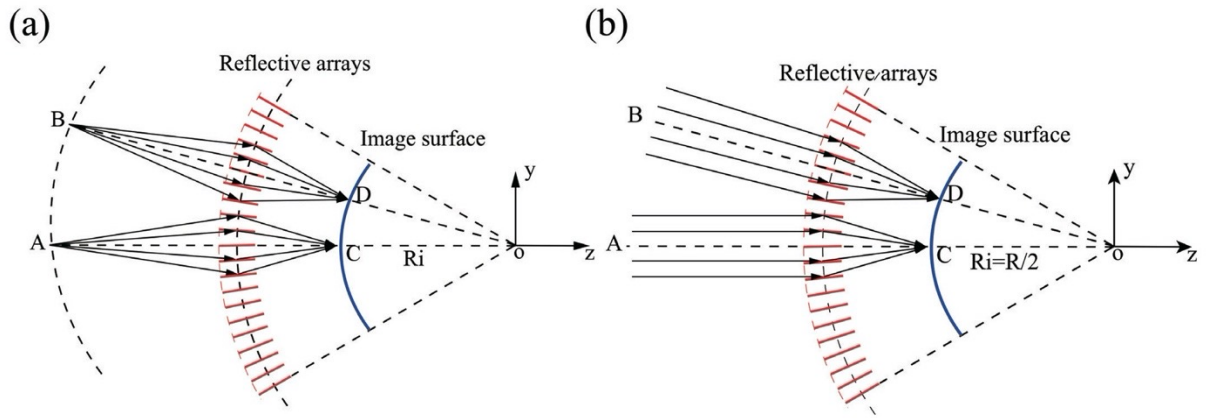
Hudec, R., X-Ray Optics and Instrumentation, 139148, 2010. https://doi.org/10.1155/2010/139148

Angel Lobster-eye Optics:

- Square micropore optics tiled into a sphere to emulate a Lobster-eye.
- Common configuration sought for X-ray instrumentation given its high sensitivity, excellent spectral line resolution, reasonable FoV (several degrees sq.) and spatial resolution over 0.2 to 5 keV.



(a) Angel-type lobster-eye optic with the imaging principle (b).



1-D diagram for multiple point-light sources at finite (a) and infinite (b) object distances in Lobster Eye Optics.

Peng et al., Optical Express, 26, 12, 2018, 15138

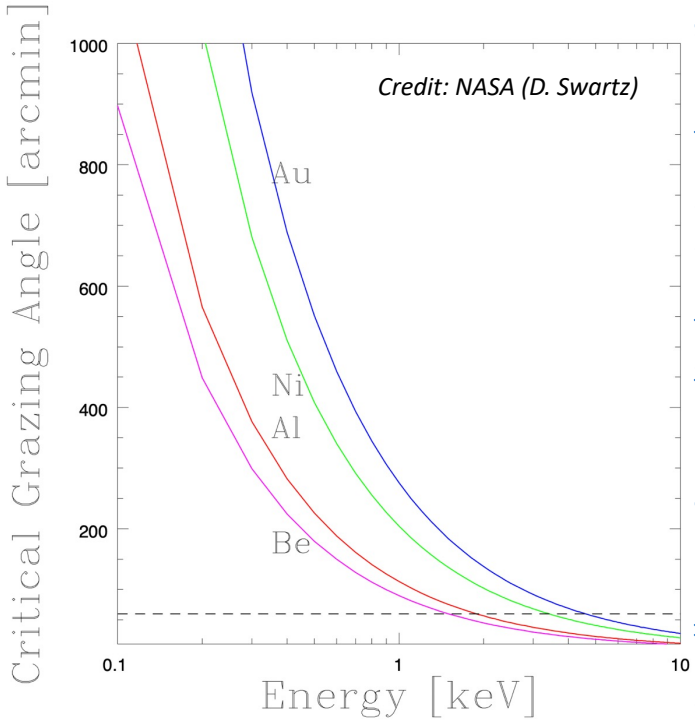
Multi-layers

- Reflectivity for non-multilayer (ML) coatings are high up to the critical angle ($\boldsymbol{\theta_c}$).

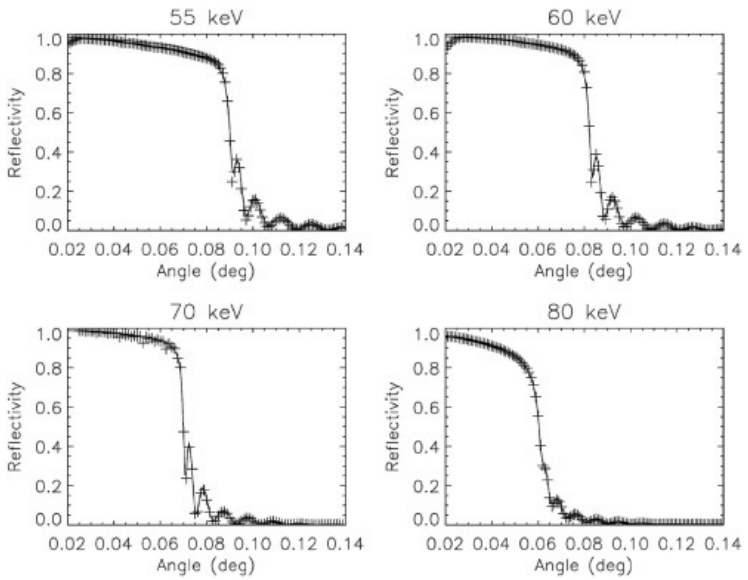
- $\boldsymbol{\theta_c} \sim 10^{-2}\sqrt{2\rho}$ /E.
  - **E** = photon energy in keV
  - ρ = density of reflecting material in g/cm^3

- $\boldsymbol{\theta_c}$ decreases with increasing energy.
  - **θ_c ~ 0.04° for Plexiglas at 35 keV**
  - **θ_c ~ 0.10° for Plexiglas at 17.4 keV (Mo-Kα)**
  - **θ_c ~ 0.55° for Plexiglas at 8.4 keV (W-Lα)**

Critical grazing angle as a function of energy for popular X-ray telescope coatings and optic mirrors



https://heasarc.gsfc.nasa.gov/docs/xrayschool-2003/opt03.pdf



Reflectivity measurements of Iridium (thickness = 30 nm), at various energies as a function of graze angle.

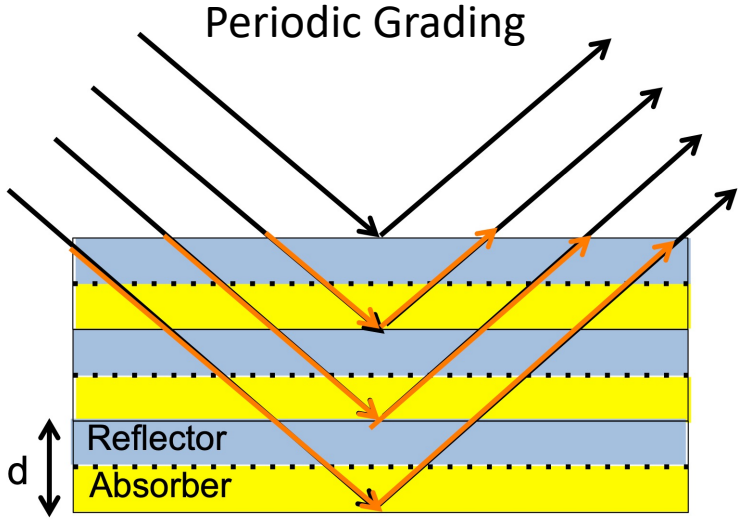
S. Romaine et al., Applied Optics, 46, 2, 185-189,2007.

Multi-layers

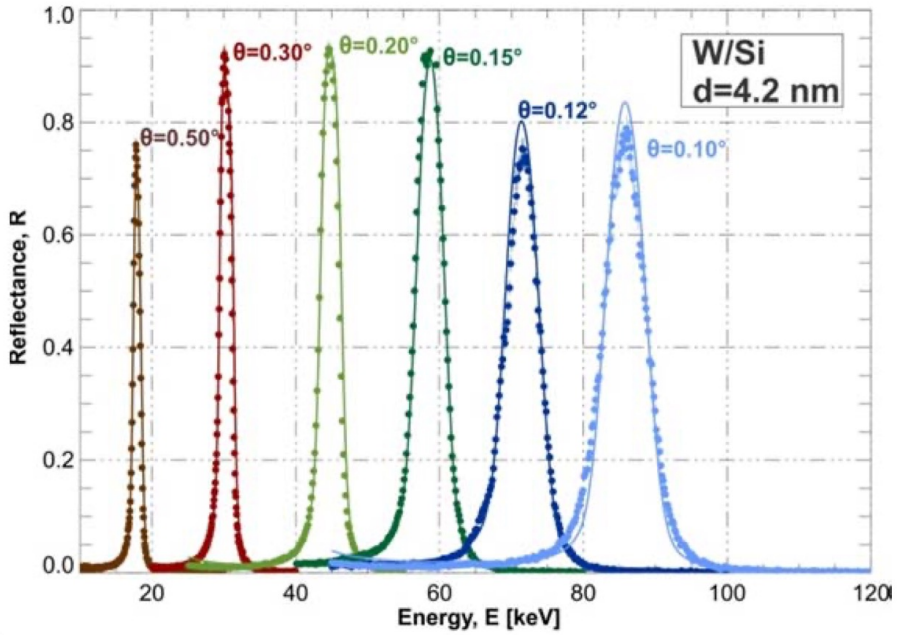
- Extend energy range using ML coatings using Bragg's law:

$$m\lambda = \sim 2dsin\theta$$

- ML coatings with depth-graded d-spacings:
  - By varying the bilayer thickness through the stack, a range of energies for a single incident angle can be realized.
  - Width of energy can be extended but lose reflectivity; **Broader energy response means lower overall reflectivity.**

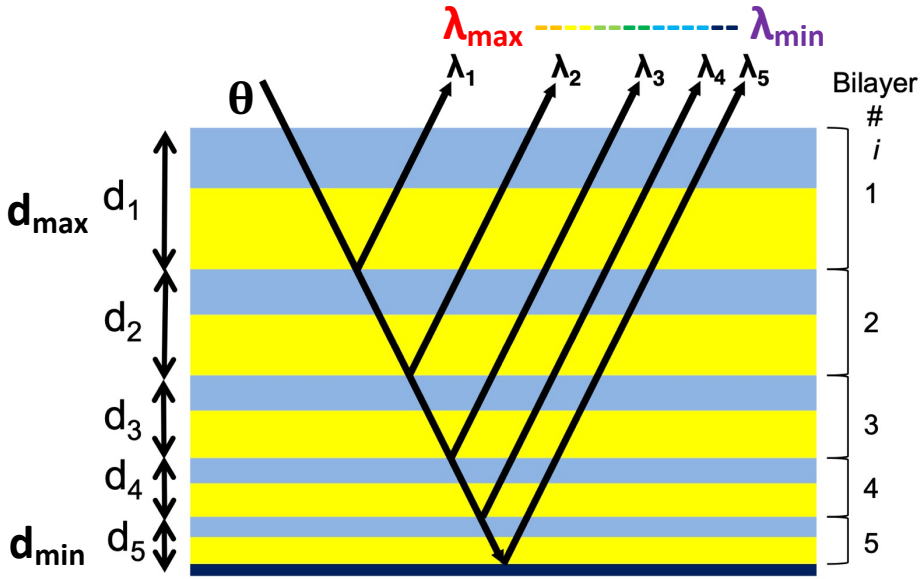


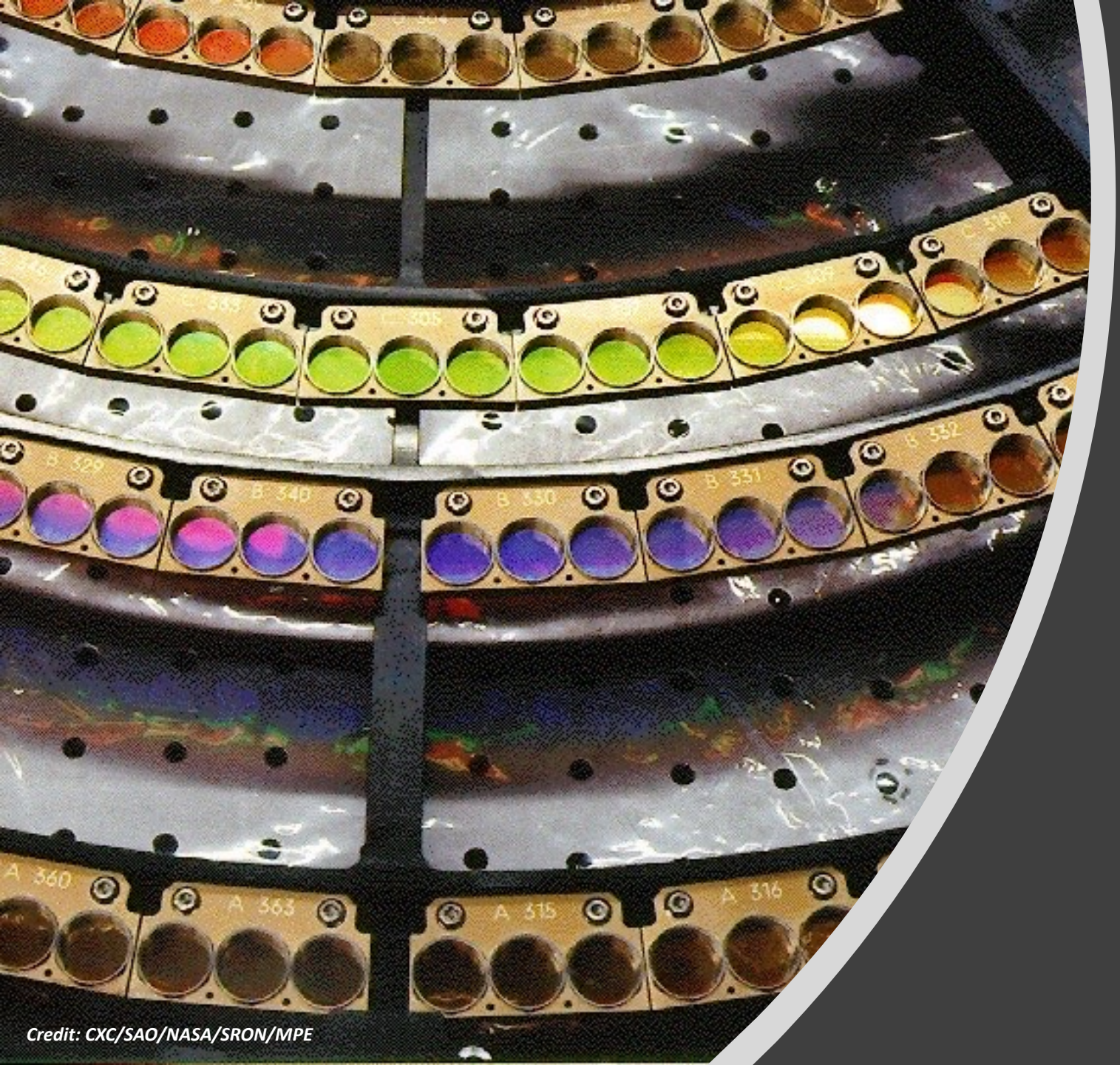
D. Windt et al.: http://www.rxollc.com/windt/papers/2015_SPIE_9603-42.pdf



Reflectance of a periodic W/Si multilayer having a period d=4.2 nm, measured at graze angles in the range θ=0.1° to θ=0.5°.

Non-periodic (depth) Grading





Credit: CXC/SAO/NASA/SRON/MPE

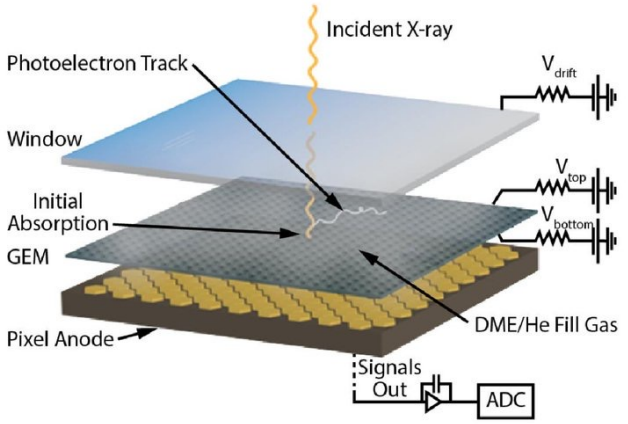
2. Detectors and Gratings

Left: Chandra LETG

Detectors for X-ray Astronomy

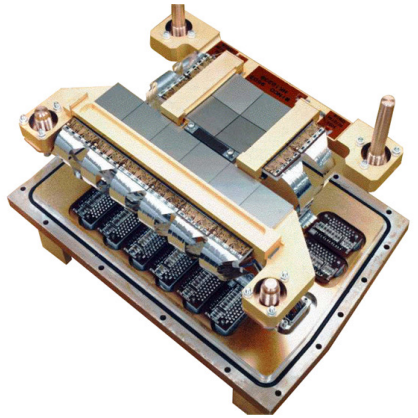
- Usually designed/configured for a particularly energy band using technology at the time (limiting).
- Examples:
  - Proportional counter (gaseous ionization detector/GPD - i.e. EXOSAT, Ariel, IXPE, etc.)
  - Scintillation detector (**uncommon** – Vela, KONUS, older missions).
  - Solid-state detector (CdTe/CdZnTe/SDD)
  - Charge-Coupled Detector (CCD) / Active-pixel sensor (Complementary metal–oxide–semiconductor /CMOS) – **Popular**
  - Microcalorimeters (single-counting mode).
    - Transition-Edge Sensors (TES) **(super-conducting, state-of-the-art).**

Credit: NASA



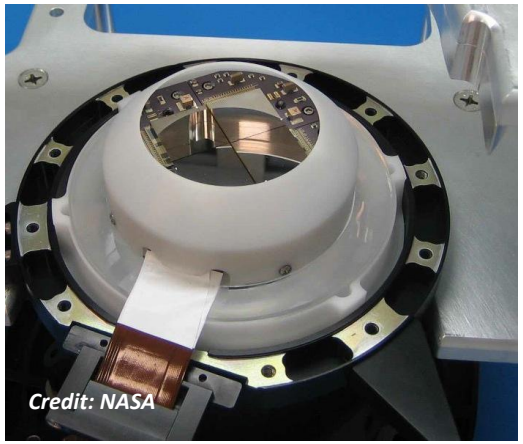
IXPE Gas Pixel Detector[1]

Credit: CXC NASA/SAO



Chandra ACIS

(Advanced CCD Imaging Spectrometer)



NuSTAR CdZnTe detector



Suzaku CCDs (XIS)

https://heasarc.gsfc.nasa.gov/docs/suzaku/gallery/instruments/xis.html

[1]Carmelo Sgrò, Proc. SPIE 10397 (2017); https://doi.org/10.1117/12.2273922

CCD (and other ionization detectors)

- X-ray photon is absorbed, creates primary photoelectron and secondary electrons which are amplified/multiplied.
- Total charge (Q) proportional to photon energy (not true for optical CCDs).
- Statistical fluctuation on Q due to Poisson/Shot noise.
  - Variance, Material (Si), dark noise, pair-creation energy, etc.

- Drawbacks:
  - Usually the limiting factor in energy resolution
  - Slow readout (loss of information) -> classical CCDs.
  - Deadtime -> Saturation (blooming) and pulse pile-up (reduces dynamic range)
  - High background (temp. dependent).

Gratings

- **Transmission or Reflection?**
- **You want to be able to distinguish/resolve the energies of key elements in astrophysical X-ray sources**

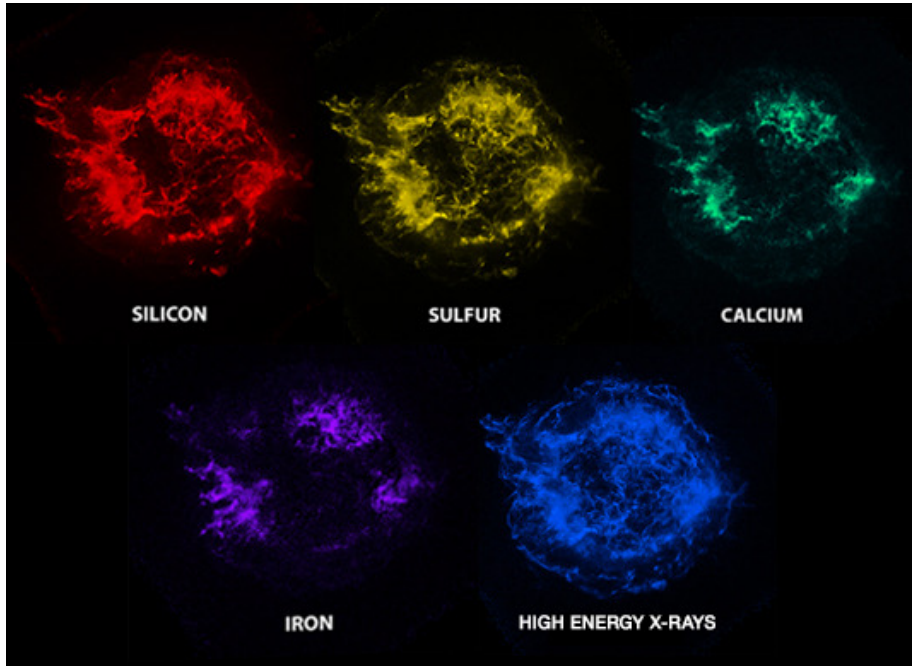
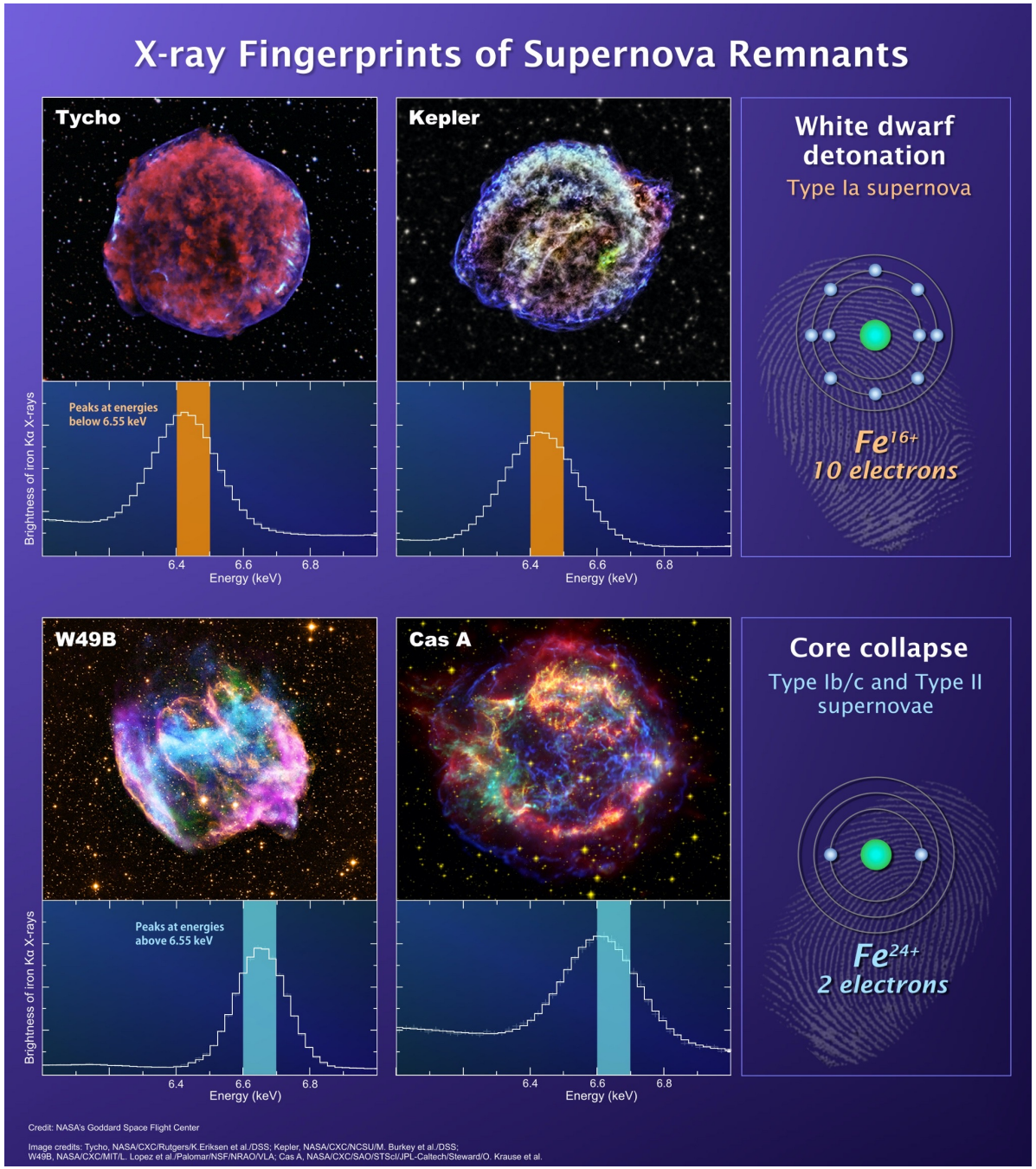
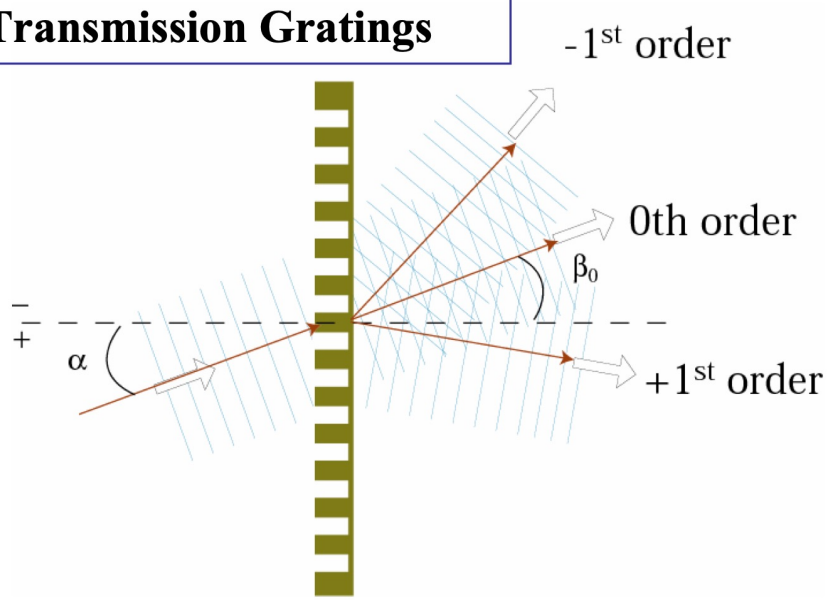


Image Credit: NASA/CXC/SAO



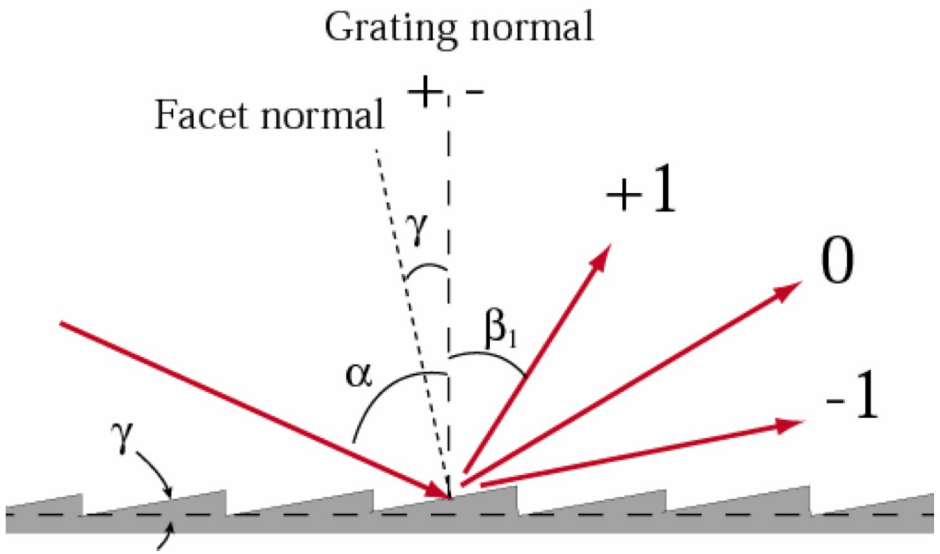
Diffraction Gratings for X-ray Spectroscopy

Transmission Gratings



- Relaxed alignment & surface flatness tolerance
- Low diffraction efficiency (absorption, etc.)

Blazed Reflection Gratings



- High diffraction efficiency
- Requires precise alignment, flat & smooth surface

Grating with thinner bars generally has a higher diffraction efficiency "bump" at shorter wavelengths (higher energies).

Lower blaze angle gratings will have the highest reflectivity at shorter wavelengths.

Image credit: Ralf K. Heilmann, et al., (2009) https://pcos.gsfc.nasa.gov/studies/rfi/Heilmann-Ralf-RFINNH11ZDA018L.pdf (White Paper).

X-ray Gratings

Transmission Grating

- Dispersion Equation (Constructive interference):

$$d \sin\theta = m\lambda$$

- Increase the diffraction grating distance for increase in wavelength.

- Take differential to find resolution:

$$d \cos\theta \Delta\theta = m\Delta\lambda$$

- Resolving power:

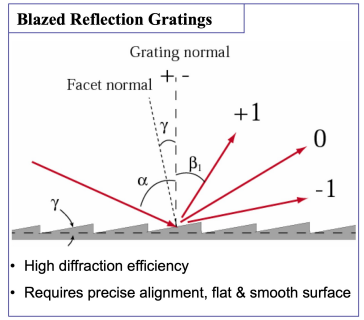
$$\frac{\tan\theta}{\Delta\theta} = \frac{\lambda}{\Delta\lambda} \approx \frac{\theta}{\Delta\theta} \qquad (\theta \; usually \; small)$$

- High resolving power: small $\Delta\theta$ and/or large θ

Reflection Grating

Dispersion Equation:

$$\cos\beta = \cos\alpha + \frac{m\lambda}{d}$$



Credit: Heilmann+ (2009)

Spectral resolution:

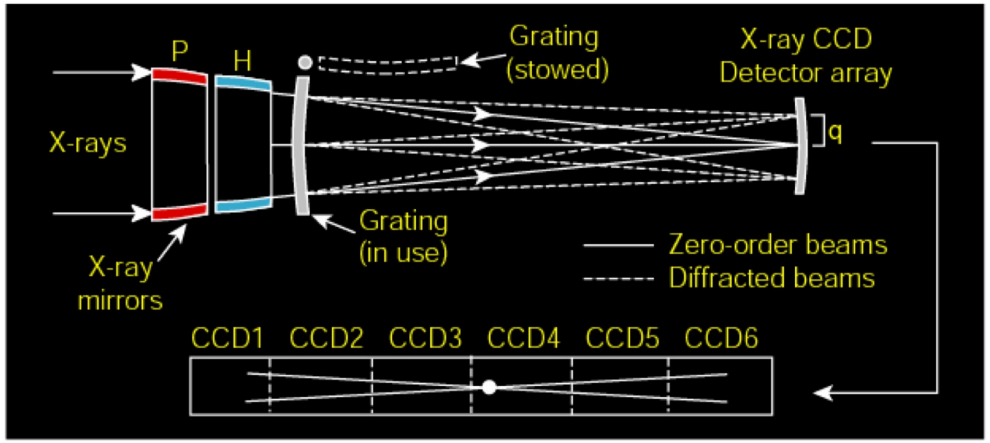
$$\Delta\lambda = \left(\frac{d}{m}\right) \sin\alpha \Delta\alpha$$

Telescope blur ($\Delta\alpha$): suppressed by large dispersion.

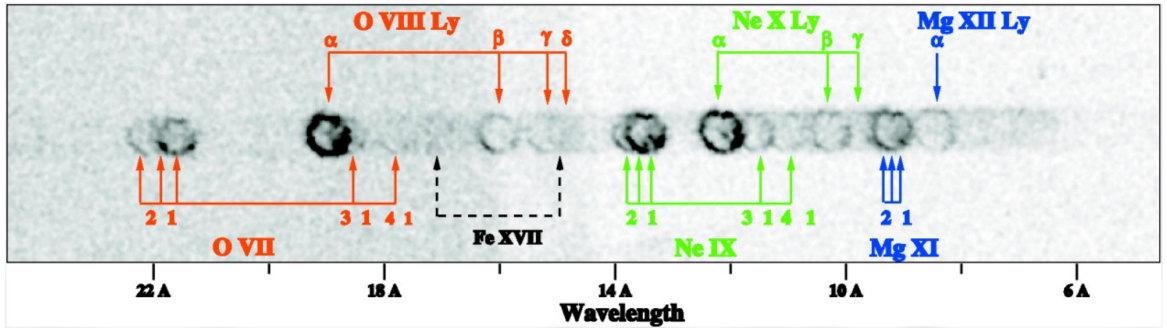
Large dispersion due to small incidence angle; offsets telescope blur; have to align gratings to high angular tolerance.

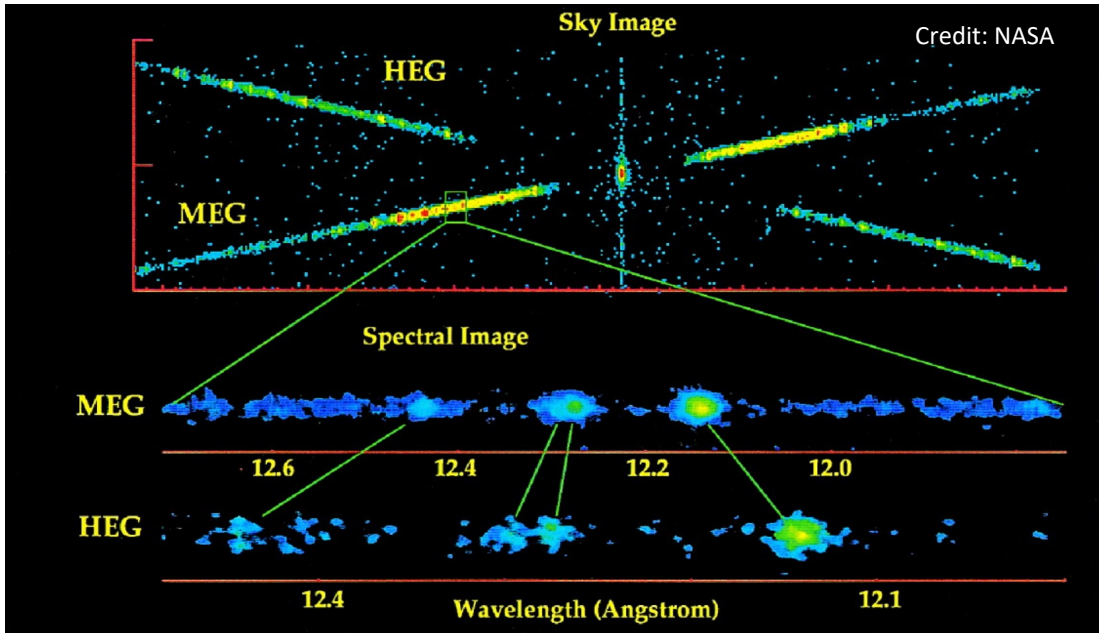
Diffraction Gratings for X-ray Spectroscopy

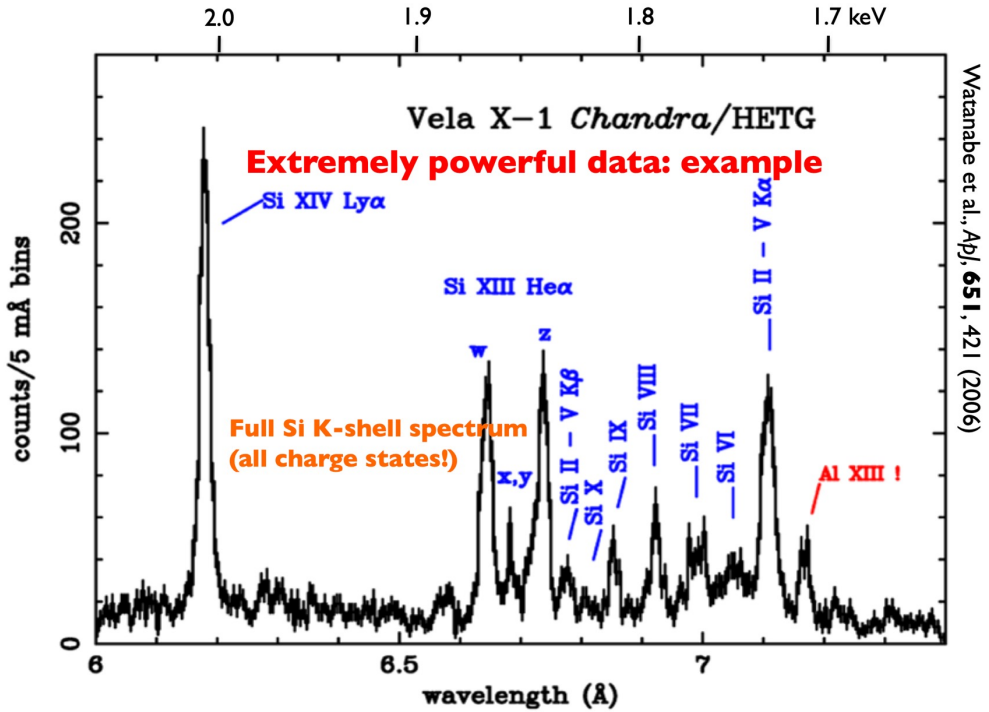
Canizares, C., et al. . Publications of the Astronomical Society of the Pacific (117), 836 (2005), 1144



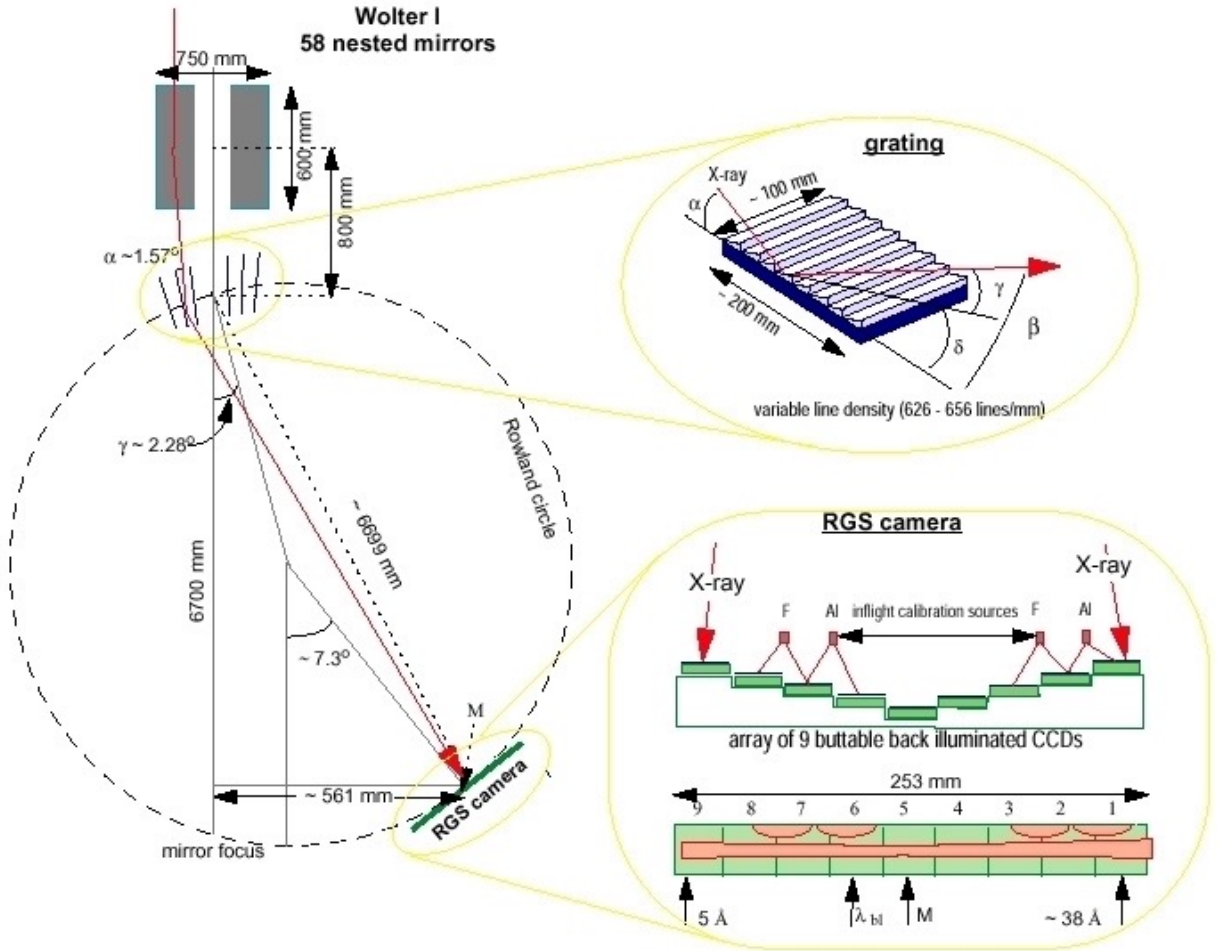
Flanagan et al., 2004, *ApJ*, **605**, 230







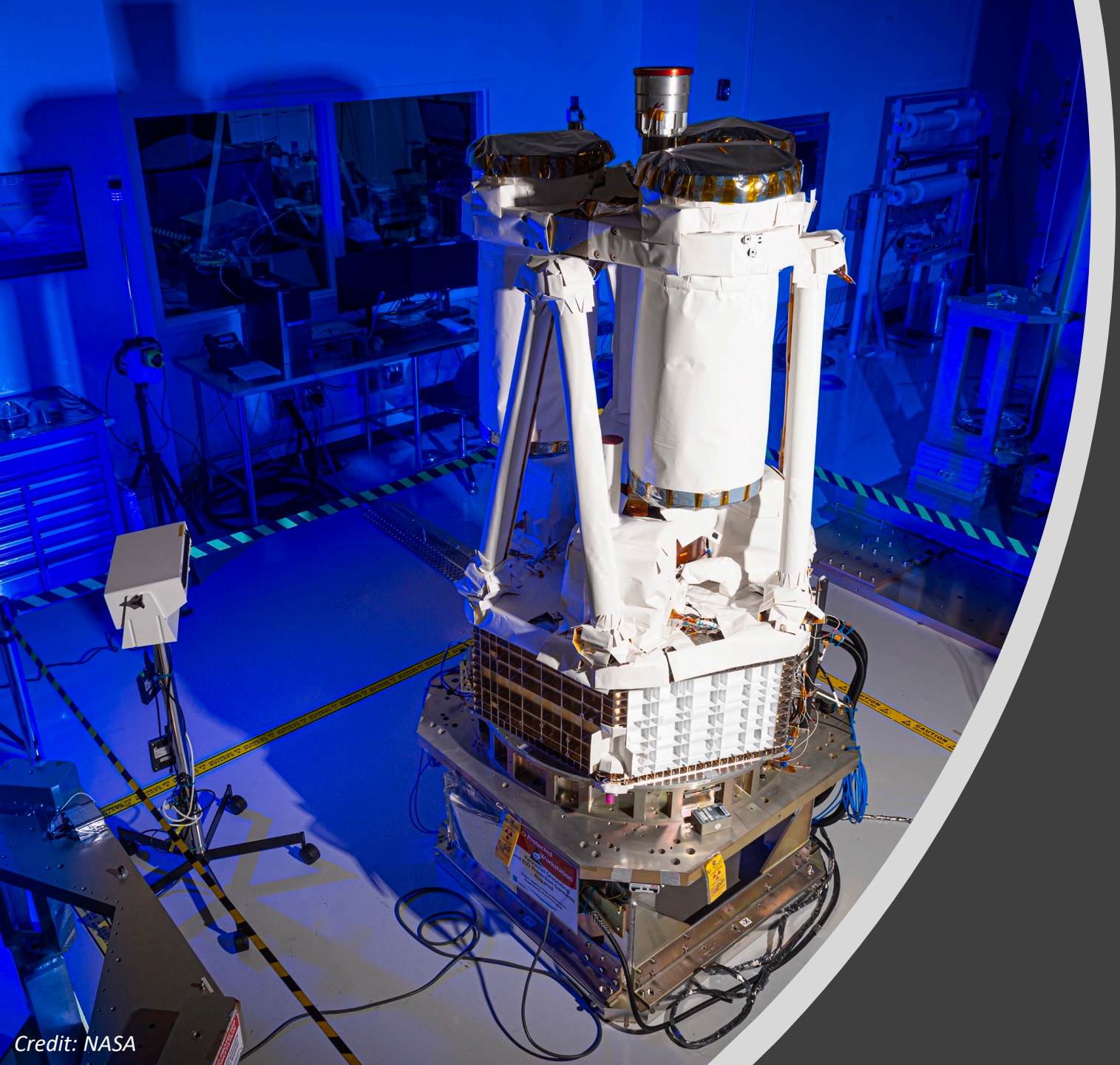
Diffraction Gratings for X-ray Spectroscopy
XMM-Newton



Schematic layout of the RGS (from Brinkman et al. 1998)

- Launched in 10th December 1999.
- 3x 58 nested ENR* Wolter-I optics; confocal and coaxial. Au coated (2000 Å)
- Grazing angle 30’ due to interest at 7 keV.
- f = 7500 m, mirror dia. = 700 mm
- Baffles for straylight / single reflection rejection (47%)

*Electroformed Ni Replicated



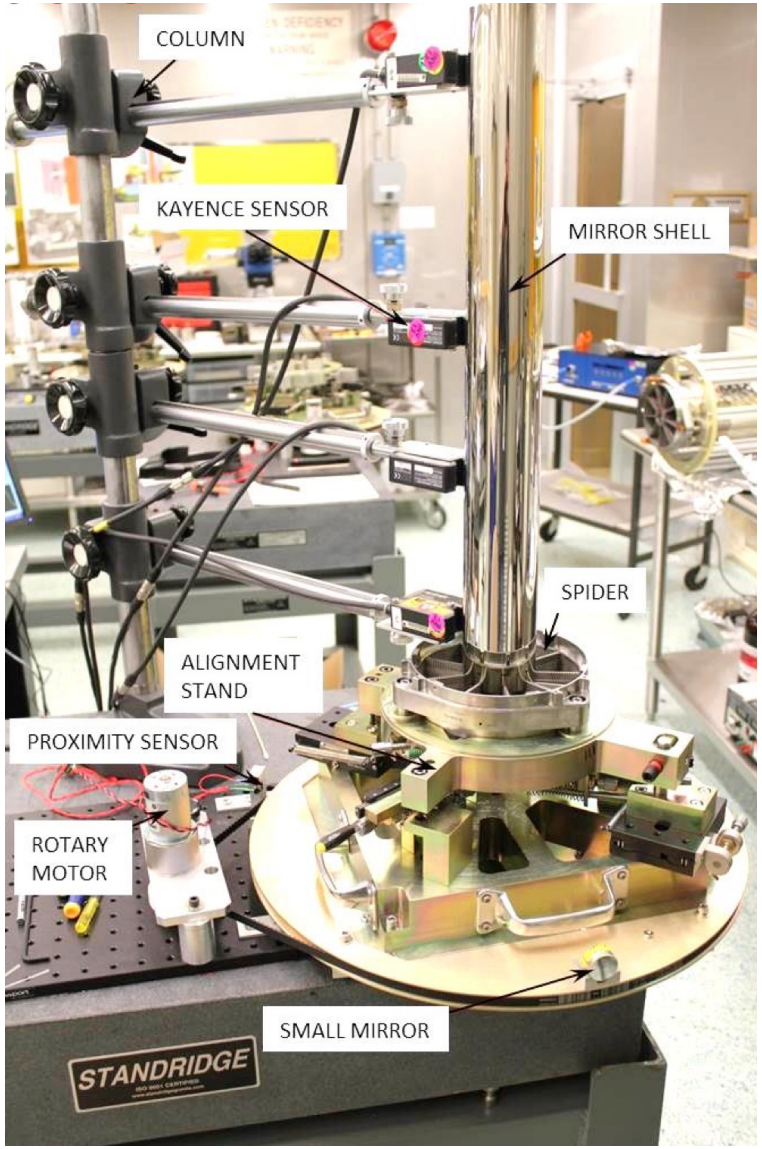
Credit: NASA

3. Assembly and Calibration

Integration of IXPE at Ball, NASA

Assembly and Calibration

- Nest carefully into the spider, and glue using clips instead of epoxy due to shrinkage and distortions
- Make sure each shell is co-aligned/axial and confocal
- Vibration and environment (thermal) testing (Shake and Bake).



Mikhail Gubarev et.al; Proc. SPIE 7360, EUV and X-Ray Optics: Synergy between Laboratory and Space, 73600A (April 30, 2009); https://doi:10.1117/12.823848 .

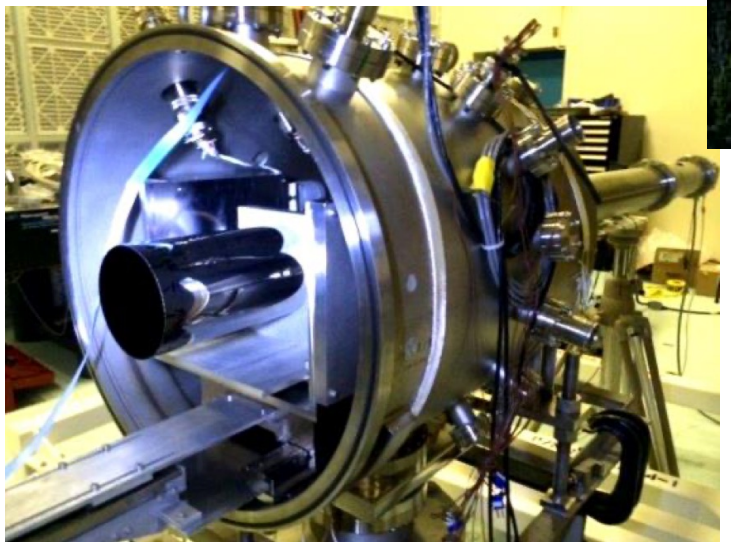
X-ray Testing

- **Straylight Test Facility (SLTF)**
  - 100 m vacuum tube (10^{-7} torr)
  - Clean room
  - Accommodate 1m mirrors

- **X-ray and Cryogenic Facility (XRCF)**
  - World's largest optically clean cryogenic and X –ray test facility.
  - 520 m X-ray guide tube, instrument chamber, clean rooms.
  - Smaller cryogenic test chambers for smaller instruments.
- Use suite of X-ray sources within dynamic range of telescope.
- Check for straylight "optical noise".









Credit: Kilaru, K, https://wwwastro.msfc.nasa.gov/lynx/docs/meetings/TIM01/Xray_Optics_at_MSFC.pdf *All images: NASA*

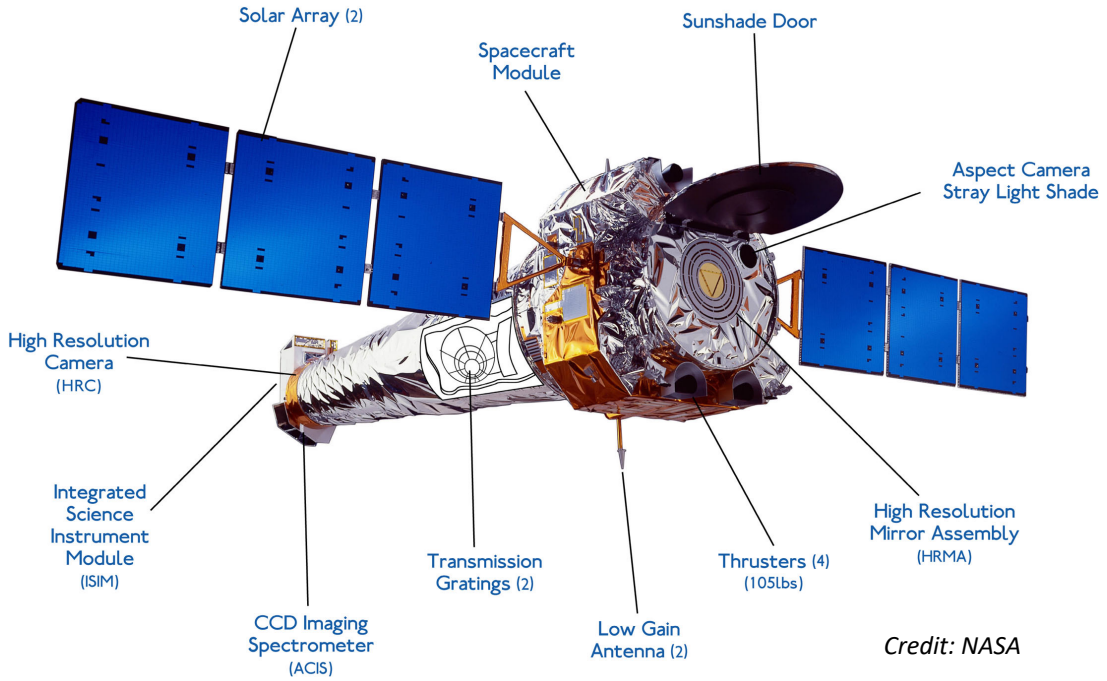


Chandra X-Ray Observatory

Credit: NASA

Chandra X-ray Observatory

- One of NASA's four "Great Observatories", named after Subrahmanyan Chandraeskhar (Nobel Laureate).
- Launched on July 23rd 1999.
- 10,000 lbs telescope in Highly Eccentric Orbit (65 hours) around Earth
- Planned mission duration of 5 years (currently 22 years).



Credit: NASA



Telescope Mirror:

Diameter: 1200 mm (1.2 m)
Focal Length: 10000 mm (10 m)
Collecting Area: 0.04 m^2
Energy Band: 0.1-10 keV
Resolution: 0.5 arcseconds

Instruments:

Advanced CCD Imaging Spectrometer (**ACIS**)
High Resolution Camera (**HRC**)
High Energy Transmission Grating (**HETG**)
Low Energy Transmission Grating (**LETG**)

Chandra: High Res. Mirror Assembly

- Chandra consists of 4 directly-fabricated, nested Wolter-I mirror pairs.
- Mirror substrate is 2-cm thick Zerodor Schott glass (slumped glass)
- Reflective surface is 33 nm iridium with a chromium binding layer

Mirrors in the Mirror Module Assembly



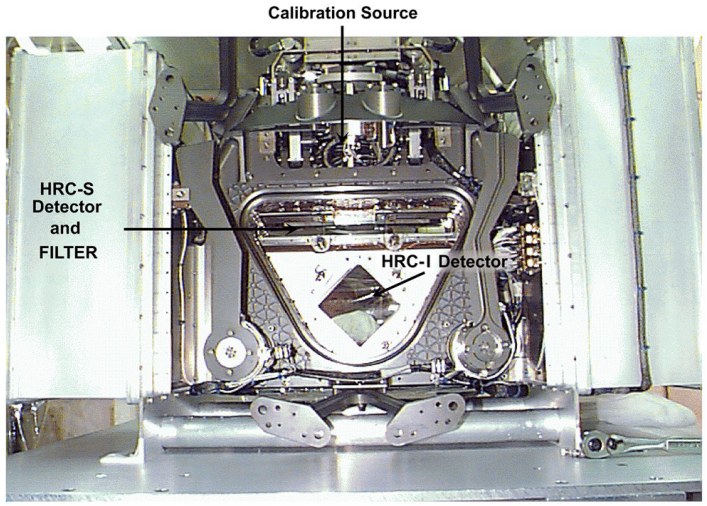
Weisskopf, https://arxiv.org/pdf/1110.4020.pdf

Credit: CXC/SAO/NASA

Optics	Wolter Type-I
Mirror coatings	Iridium
Mirror outer diameters (1, 3, 4, 6)	1.23, 0.99, 0.87, 0.65 m
Mirror lengths	84 cm
Unobscured clear aperture	1145 cm^2
Focal length	10.066 m
Plate scale	48.8 µm/arcsec
PSF FWHM (with detector)	0.5 arcsec
Ghost-free field of view	30 arcmin diameter
Effective Area:	
@ 0.25 keV	800 cm^2
@ 5.0 keV	400 cm^2
@ 8.0 keV	100 cm^2
Read more in the HRMA chapter of the Proposer's Observatory Guide	

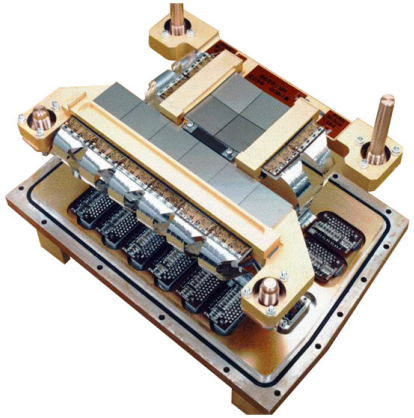
Chandra: Detectors

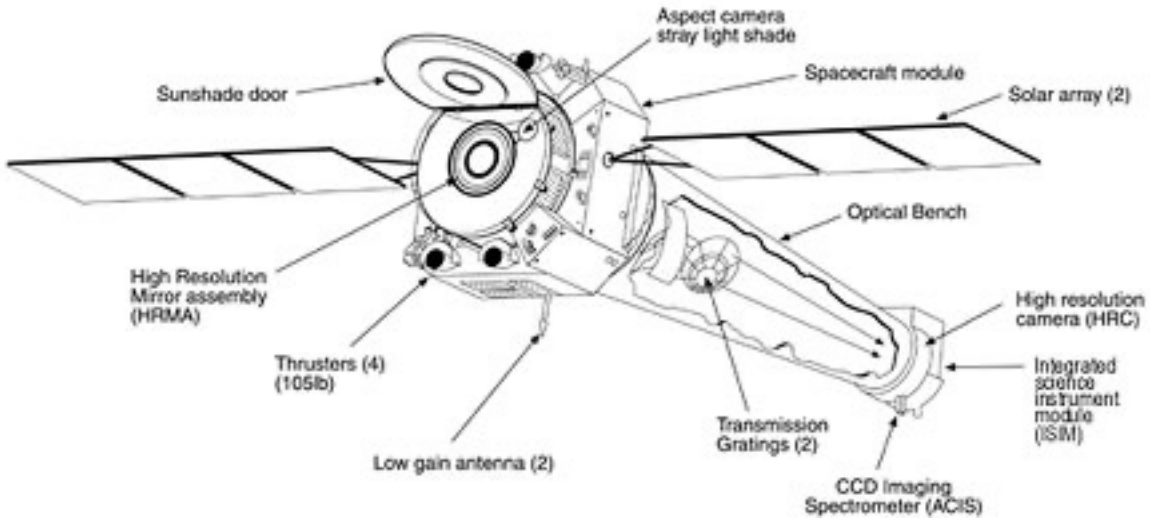
- **Two focal plane instruments:**
  - **High Resolution Camera (HRC)**
    - Two Micro-channel Plates; 10 cm^2 cluster of 69 million PbO_2 glass tubes (d=10 µm, 1.2 mm long), wire grid gives X-ray position.
    - FoV of 30 x 30 arcminutes.
    - lower background, anti-coincidence shield
    - Energy range: 0.06-10 keV
    - 16 µs time resolution in timing mode.
    - Useful for faint sources and imaging hot matter in exploding stars.
  - **Advanced CCD Imaging Spectrometer (ACIS)**
    - CCD array (FoV=16.9 x 16.9 arcminutes)
    - Simultaneous imaging and spectroscopy
    - Time-tagged photons -> 1 arcsecond imaging
    - Energy range: 0.08-10 keV
    - Instrument of choice for studying temperature variations in X-ray sources.



Looking into the HRC Vacuum Housing

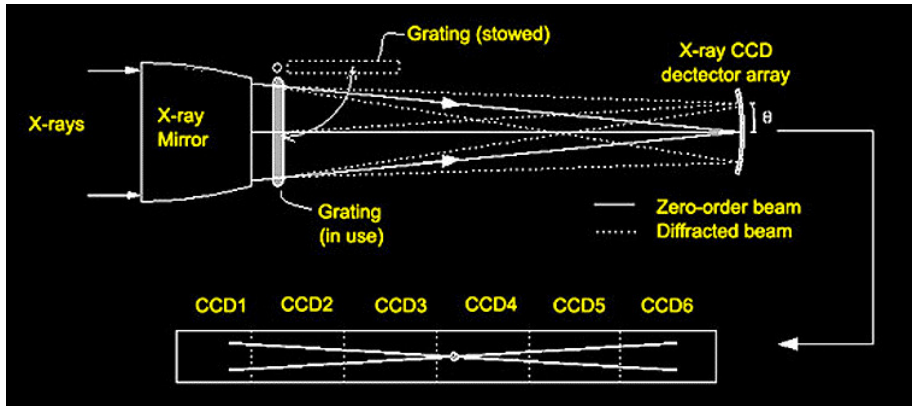
Chandra ACIS





All Image Credits: CXC/SAO/NASA

Chandra: Gratings

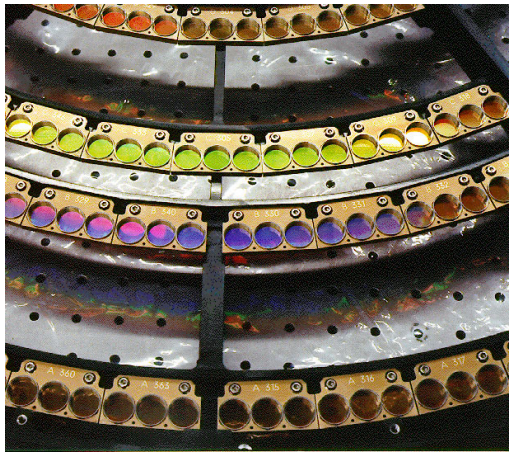


- **Low-Energy Transmission Grating (LETG)**
  - Freestanding gold grating of wires and bars with a spacing/period of 1 µm.
  - Energy Range = 0.08-2 keV
  - Dispersion = 1.15 Å/mm
  - Resolving power >1000 (50-160 Å)
  - Spectral resolution = 0.05 Å

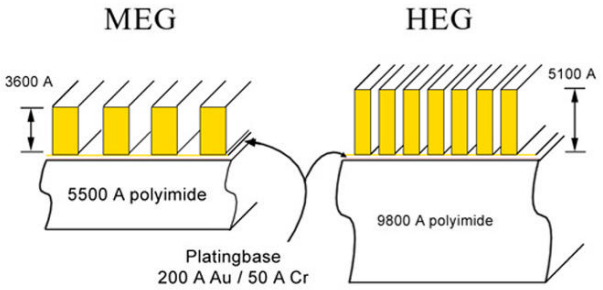
- **High-Energy Transmission Grating (HETG)**
  - Two inner rings are high-energy gratings (HEG), outer two rings are medium-energy gratings (MEG).
  - 336 gold grating facets. Grating period of 2000 and 4000 Å for the HEG and MEGs.
  - Energy Range
    - HEG = 0.8-10 keV
    - MEG = 0.4-5 keV
  - Resolving Power
    - HEG: 1000 @ 1 keV
    - MEG: 600 @ 0.83 keV



HETGS Instrument

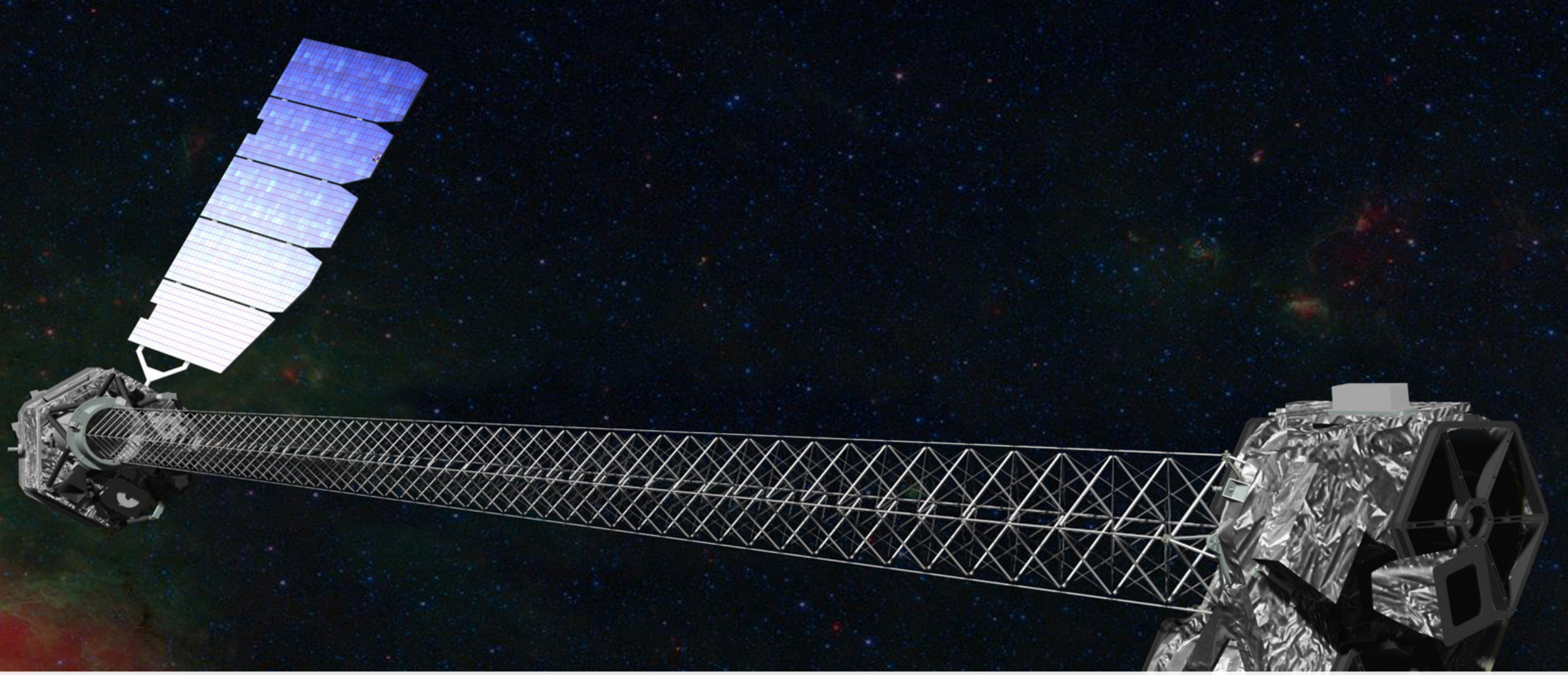


LETGS Instrument



NB: HEG and MEG are tilted at some angle to give “X” across CCD.

All Image Credits: CXC/SAO/NASA/MIT

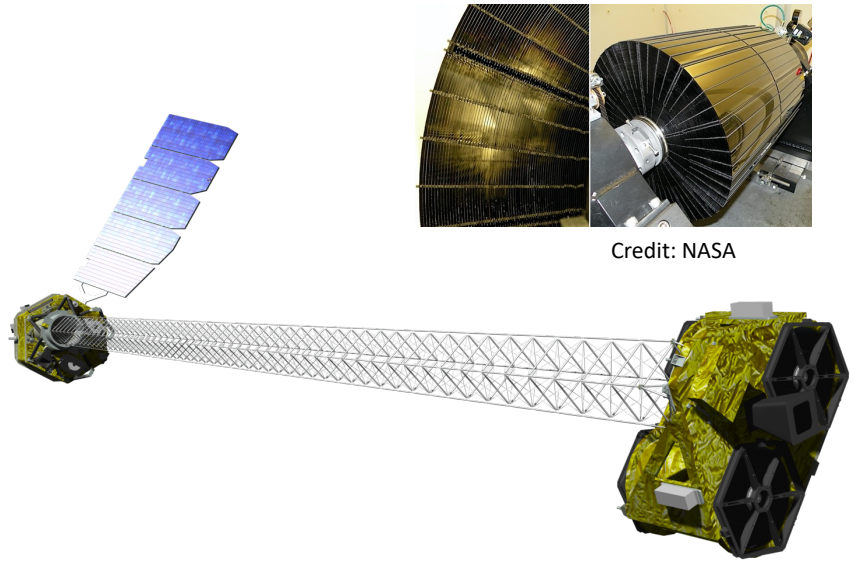


NuSTAR (Nuclear Spectroscopic Telescope Array)

Credit: NASA

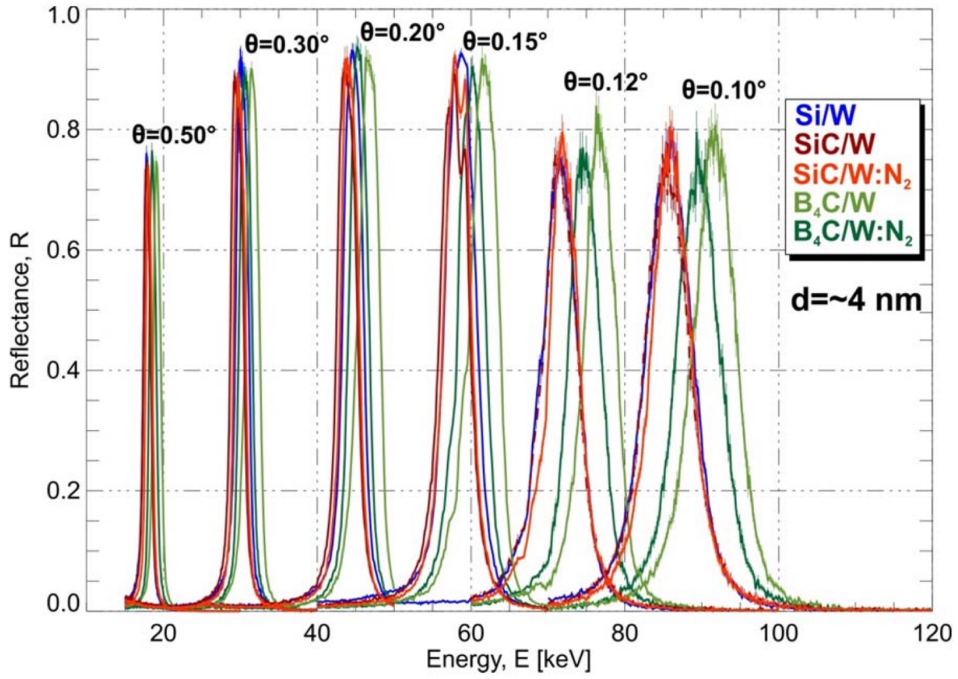
Multi-layers: NuSTAR Coatings

- NuSTAR is a space telescope with 130 X-ray mirrors (4680 segments) each with 291 bilayers of W/Si or Pt/SiC in a depth-graded configuration on slumped glass 210 µm thick, which gives an energy range of 3-79 keV (Pt K-edge).

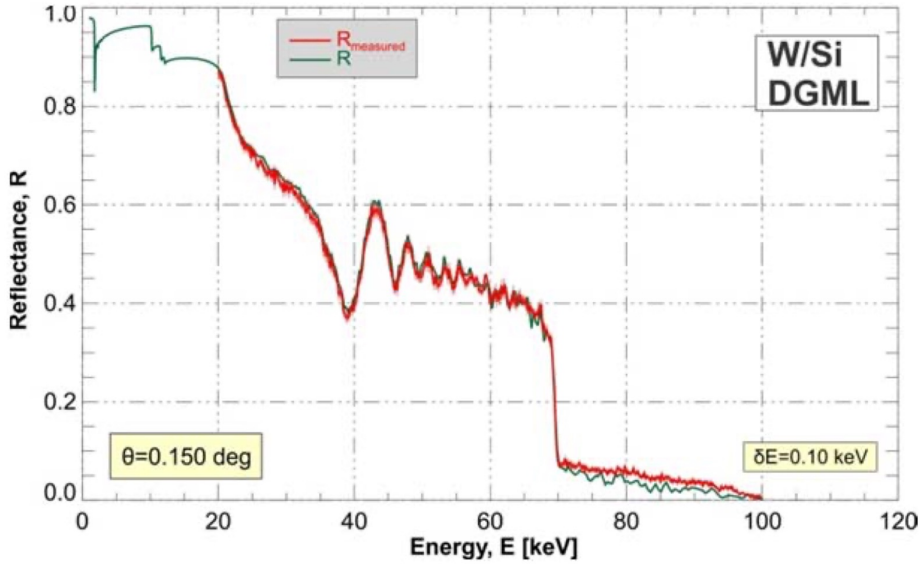


Credit: NASA

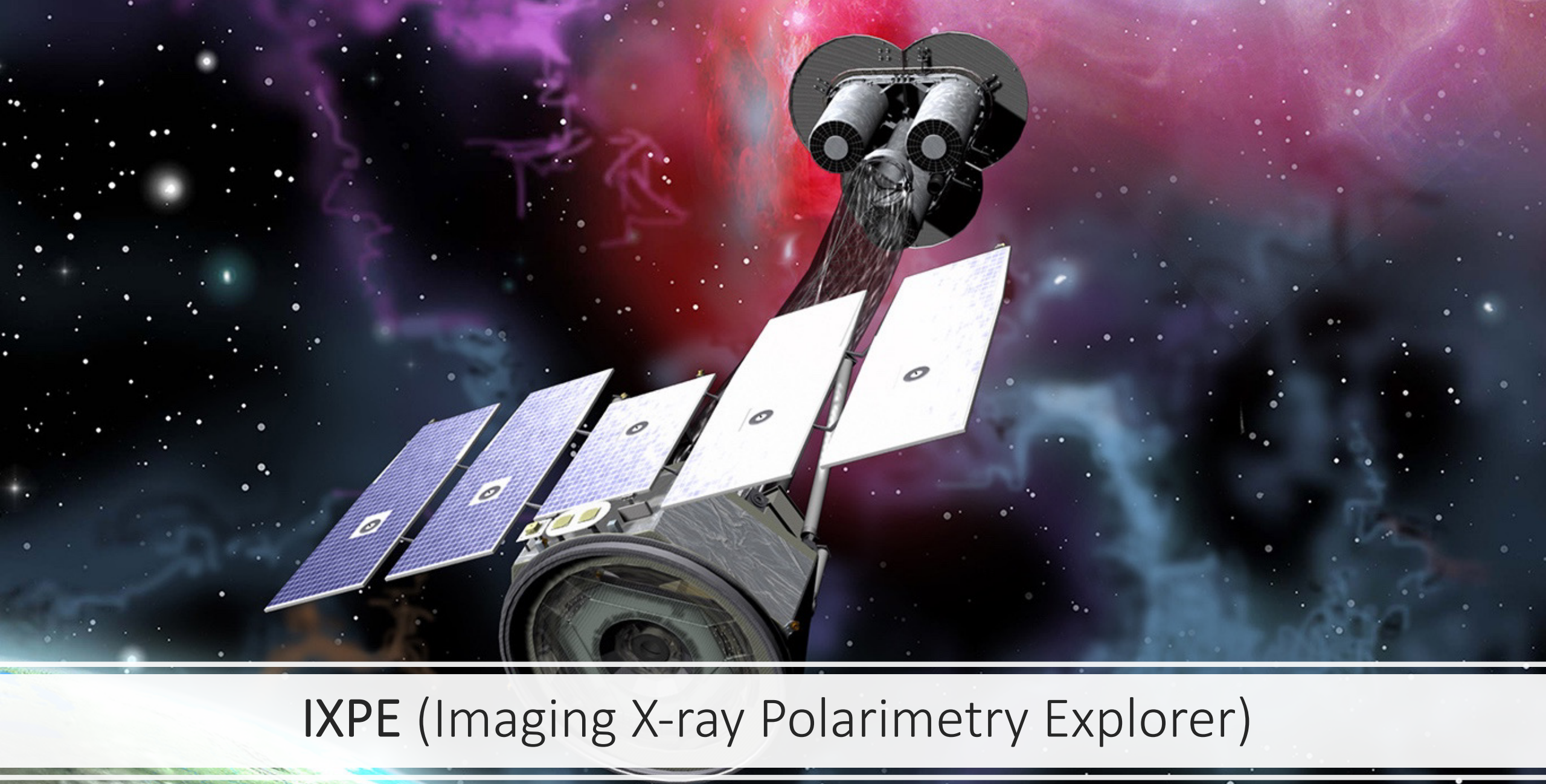
D. Windt et al.: http://www.rxollc.com/windt/papers/2015_SPIE_9603-42.pdf



D. Windt et al.: http://www.rxollc.com/windt/papers/2015_SPIE_9603-42.pdf



Measured reflectance of a depth-graded W/Si multilayer, and a fit to the measured data.



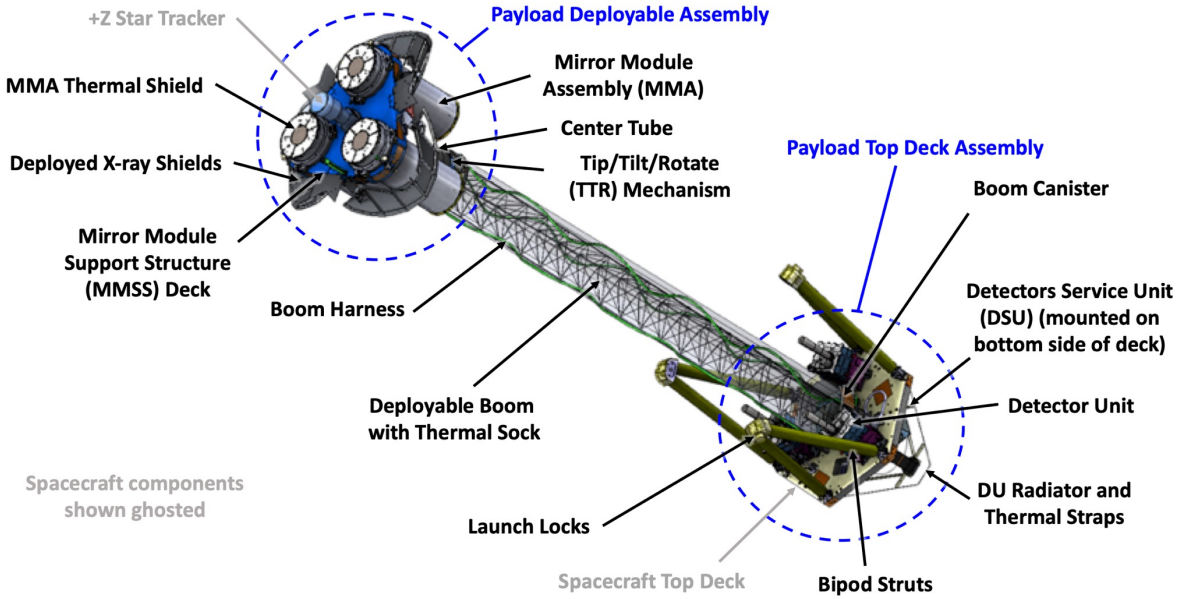
IXPE (Imaging X-ray Polarimetry Explorer)

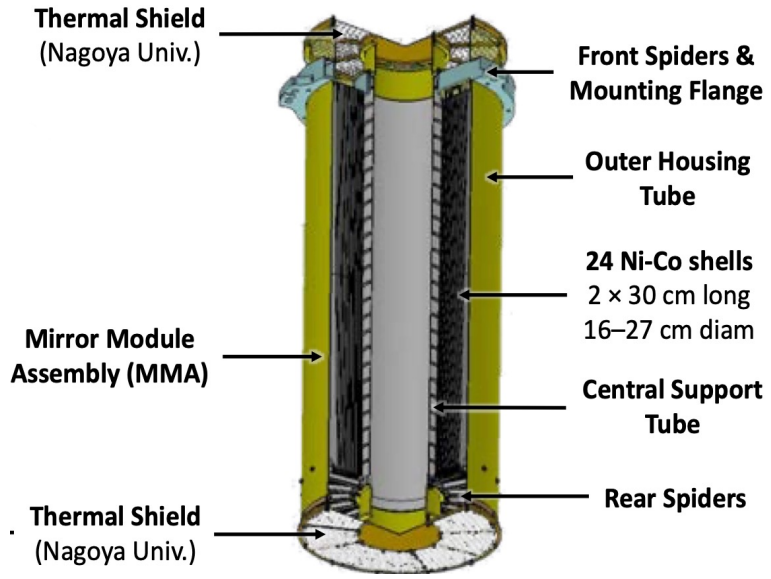
Credit: NASA

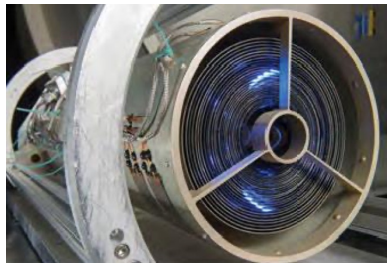
O'Dell, SPIE, 2019 https://ixpe.msfc.nasa.gov/for_scientists/papers/2019SPIE11118-30_Odell.pdf

IXPE

- Launch late 2021 / early 2022.
- 3 telescopes of 24 NiCo alloy Wolter-I optics
  - 2x30 cm long, 16-27 cm diameter
  - Total collecting area: >700cm^2 at 3 keV
- f = 4 m, Energy range (2-8 keV)
- PSF <30 arcsec, time accuracy = 100 µs
- Objectives:
  - >100x improvement in polarization sensitivity over OSO-8 (launched 70s).
  - Simultaneous spectral, spatial and temporal measurements
  - Geometry and emission mechanism in AGN
  - Magnetic field configuration / magnitude in Magnetars
  - Mechanism for X-ray production in pulsars.
  - Particle acceleration in PWNe.



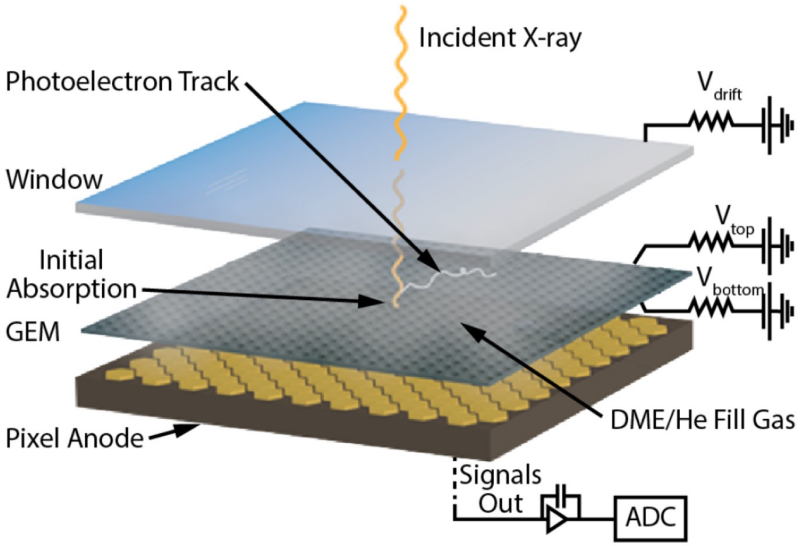




O'Dell, SPIE, 2019 https://ixpe.msfc.nasa.gov/for_scientists/papers/2019SPIE11118-30_Odell.pdf
https://ixpe.msfc.nasa.gov/for_scientists/presentations/Muleri_IXPE_Catiadas.pdf

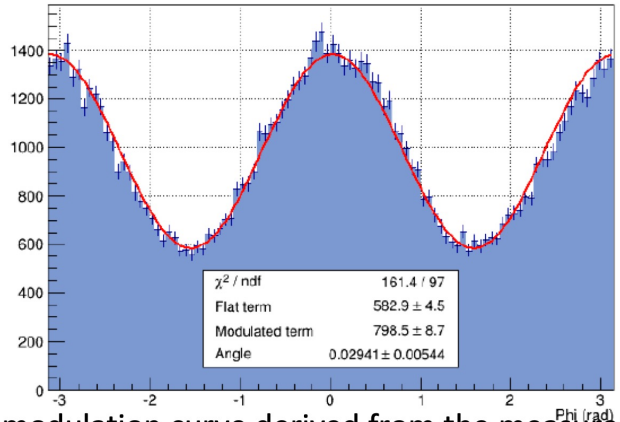
Credit: https://ixpe.msfc.nasa.gov/for_scientists/presentations/Muleri_IXPE_Catiadas.pdf
https://ixpe.msfc.nasa.gov/for_scientists/papers/2017spie_0829_sgro.pdf

IXPE

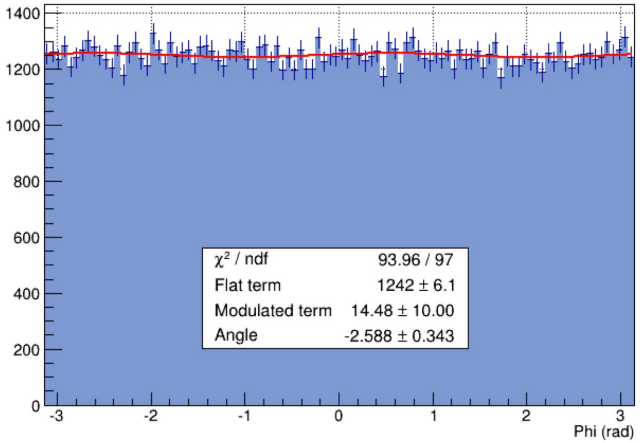


Gas is dimethyl ether (DME) at 0.8 atm.

50 µm pitch,
15 mm^2 active area,
50 µm Be window.



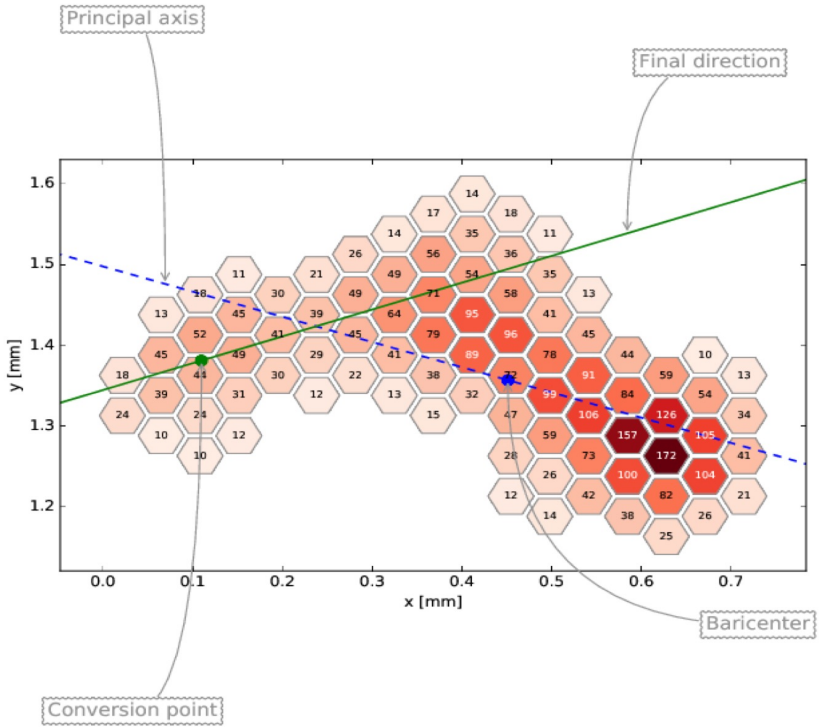
Real modulation curve derived from the measurement of the emission direction of the photoelectron.



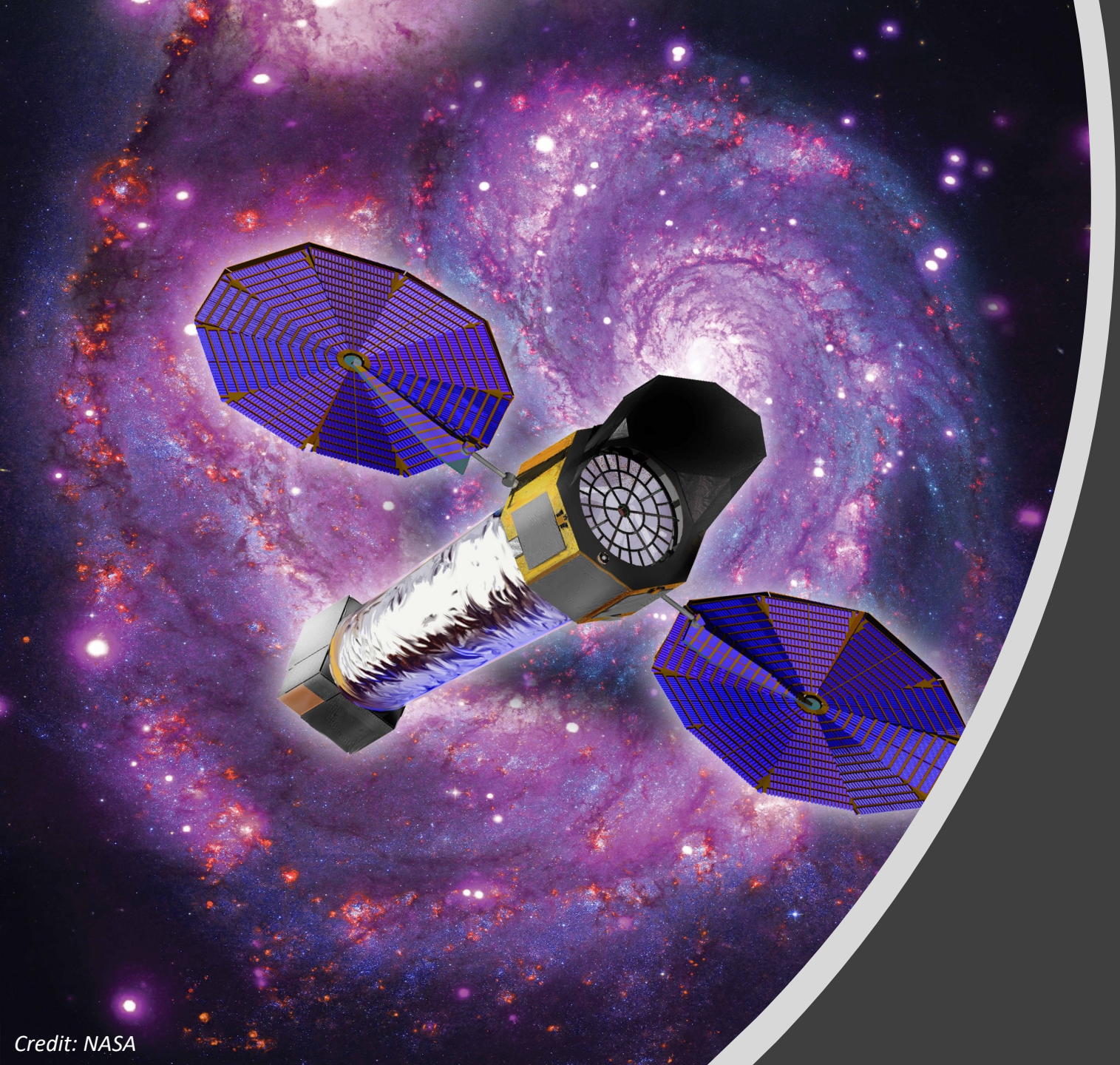
Bellazzini et al. 2012

Residual modulation for unpolarized photons.

Photoelectron track of a 5.9 keV photon as seen by the GPD. Color scale (and numbers) of each pixel show the collected charge. Reconstruction algorithm shows the **principal axis of the charge distribution**, and the **emission direction**. The reconstructed absorption point is also shown.



Modulation factor	20% (70%) at 2 (8) keV
Residual modulation	<0.5%
Spatial resolution	90μm at 5.9 keV
Energy resolution	<20% at 5.9 keV
Timing resolution	$\sim 10mus$



Future Instrumentation

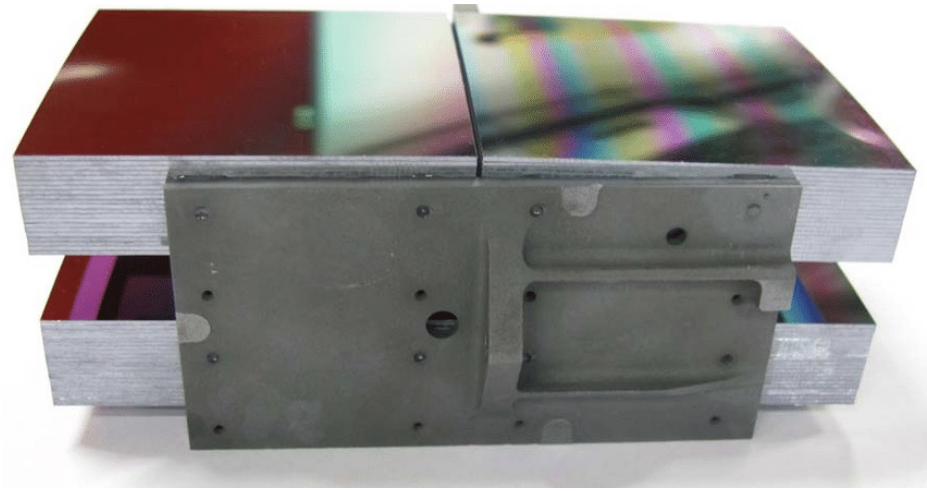
Credit: NASA

Left: Lynx Mission Concept

Future Instrumentation

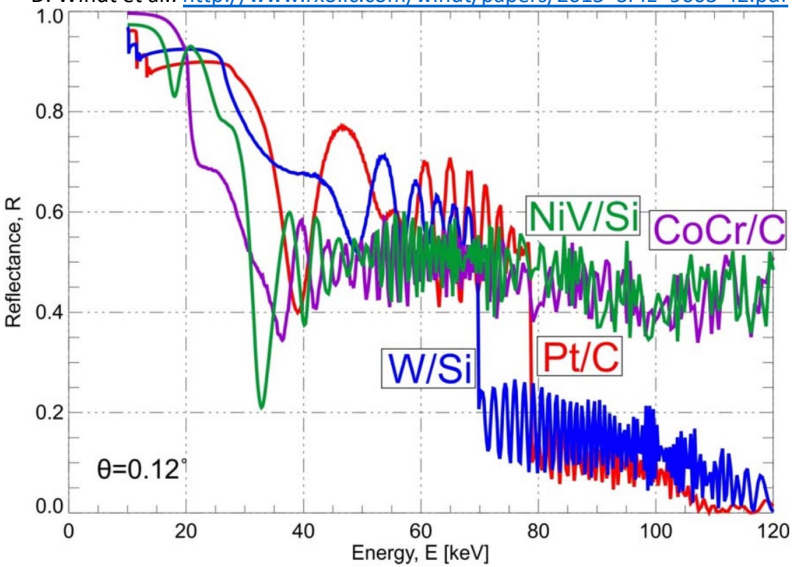
- Future instrumentation **needs** to be:
  - ***More sensitive***
    - Higher collection area
    - Higher effective area
    - Orbits have less background
  - ***Cover more sky***
    - Larger FoV (Earth blocks about half the sky in LEO).
  - ***Miniaturized and lighter***
    - Payloads must fit into CubeSat configurations (i.e. optics much have short focal length)
    - Cheaper (less fuel)
  - ***Higher localization accuracy***
    - Sub-arcsecond position resolution
  - ***Higher Timing and Spectral resolutions/ranges***
    - Sub-keV (Spectral), Sub-μs (temporal)
    - Broader spectral range.
  - ***More robust***
    - I.e. If outside Earth's magnetosphere, we expect much higher radiation doses
  - ***Other***
    - If slewing telescope, how fast?
    - Data rates, how is the data beamed down, how fast for follow-up?
    - Autonomy?
    - Many more…

M.Bavdaz et al., (2012), SPIE, 8443:29, DOI:10.1117/12.926111



Two ATHENA Si Pore Optic H and P mirror elements in module

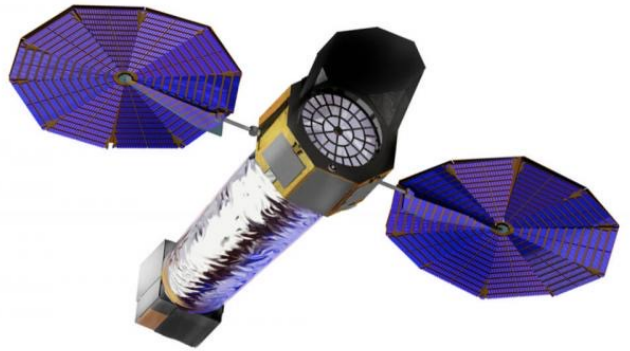
D. Windt et al.: http://www.rxollc.com/windt/papers/2015_SPIE_9603-42.pdf



New high-energy multi-layer coatings

Future Instrumentation

- Future instrumentation **needs** to be:
  - ***More sensitive***
    - Higher collection area
    - Higher effective area
    - Orbits have less background
  - ***Cover more sky***
    - Larger FoV (Earth blocks about half the sky in LEO).
  - ***Miniaturized and lighter***
    - Payloads must fit into CubeSat configurations (i.e. optics much have short focal length)
    - Cheaper (less fuel)
  - ***Higher localization accuracy***
    - Sub-arcsecond position resolution
  - ***Higher Timing and Spectral resolutions/ranges***
    - Sub-keV (Spectral), Sub-μs (temporal)
    - Broader spectral range.
  - ***More robust***
    - I.e. If outside Earth's magnetosphere, we expect much higher radiation doses
  - ***Other***
    - If slewing telescope, how fast?
    - Data rates, how is the data beamed down, how fast for follow-up?
    - Autonomy?
    - Many more…





Gaskin et al., J. Astron. Telesc. Instrum. Syst. 5(2) 021001 (29 May 2019) https://doi.org/10.1117/1.JATIS.5.2.021001

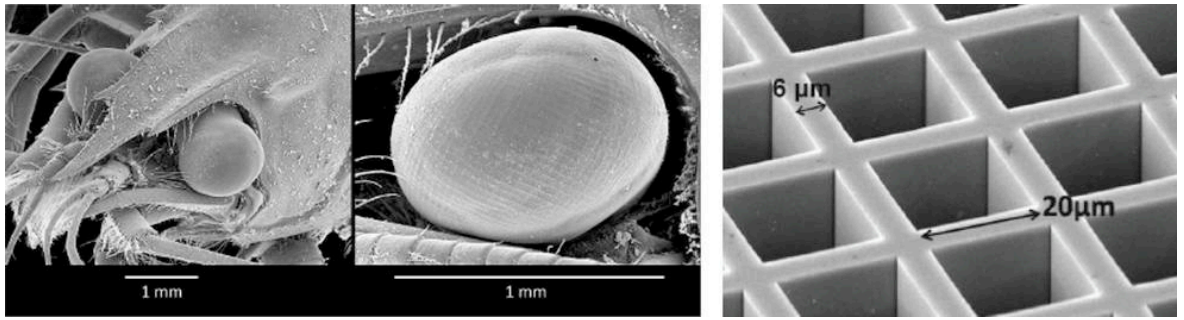
Back to Basics

- It is extremely difficult to design the “perfect” optic which satisfies all these criteria with current instrumentation.

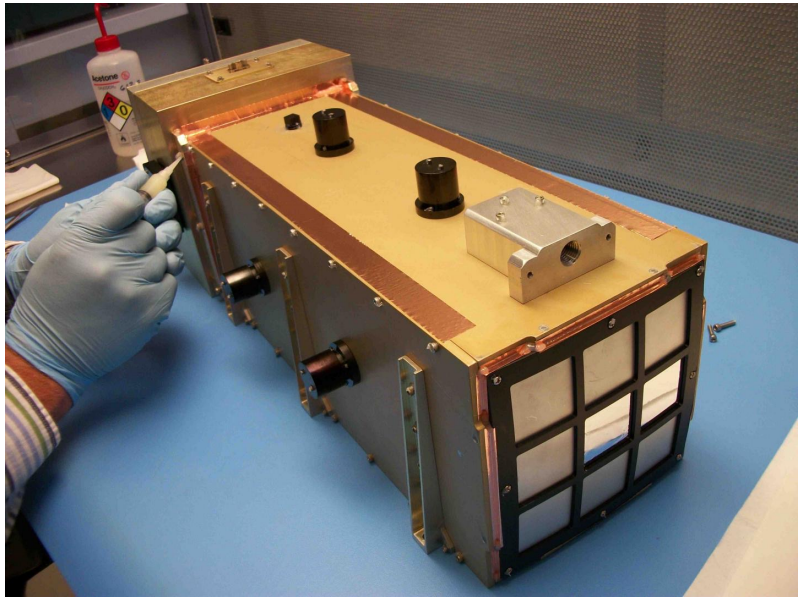
- *Nature still much better than we are at making optics*
  - Eyes (i.e. human eyes) are still much better than current optics in terms of their sensitivity of a large field of view at different wavelengths.

- Revisit older methods with current technology
  - High TRL methods with low TRL technology (i.e. KB foils).

- New Methods/Technology



Credit: NASA GSFC (Jordan Camp)

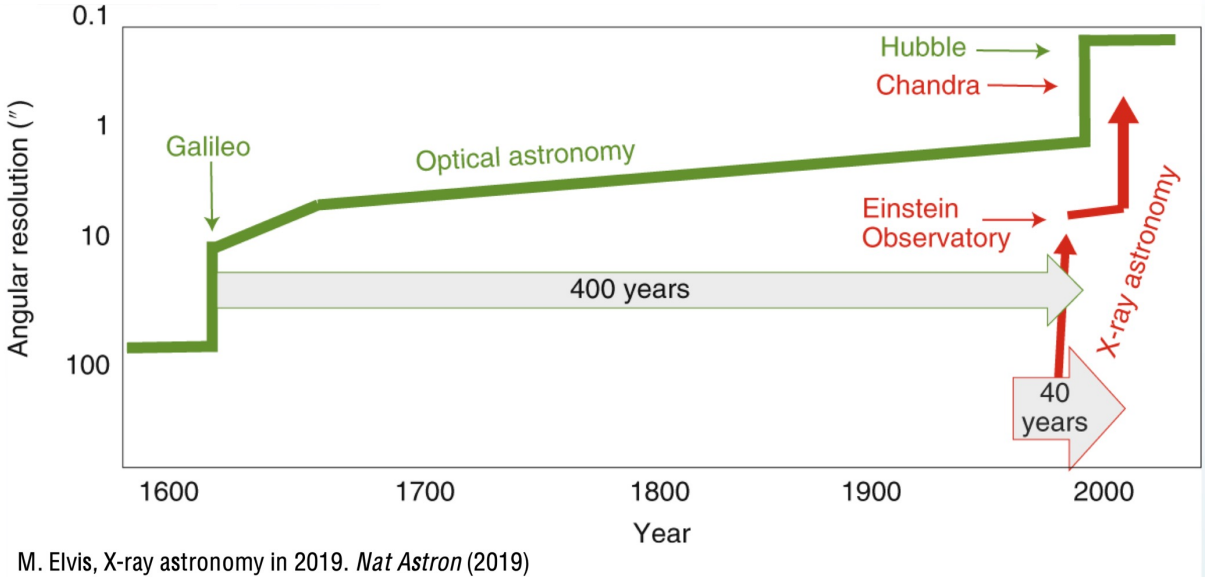


Credit: NASA GSFC

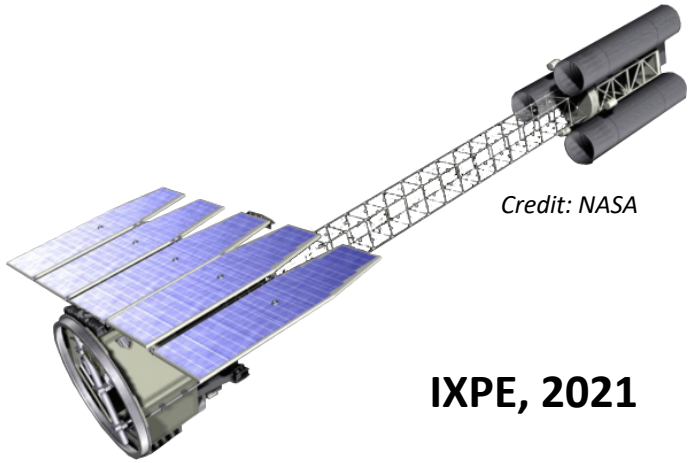
Concluding thoughts…

- Last 50 years have seen huge advances in X-ray Astronomy.
- Currently: Active pursuit to improve and advance optic development
  - i.e. new Wolter-I coating, Si-Pore optics, hybrids, improving replication steps, interferometers, formation-flying, etc.
  - Sub-arcsecond resolution, broader energy range, high grating resolving power, etc.
- Many exciting upcoming missions.

X-ray Astronomy is very young!



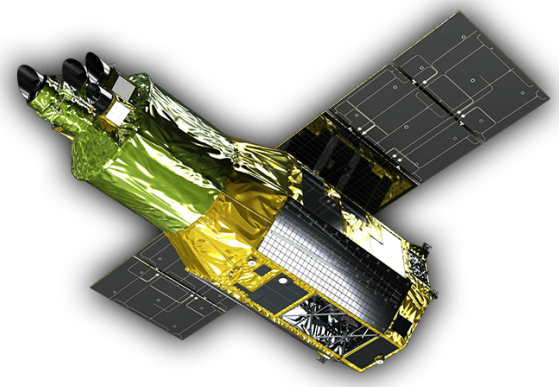
M. Elvis, X-ray astronomy in 2019. *Nat Astron* (2019)



Credit: NASA

IXPE, 2021

XRISM, 2022



Credit: https://heasarc.gsfc.nasa.gov/docs/xrism/about/XRISM_White_Paper.pdf

EXTRAS

Optical Defects

- Wolter-I telescope is a *focusing telescope (i.e. convex lens)* and is thus subject to optical imperfections that include:
  - Vignetting or off-axis effective area
  - Aberrations:
    - Monochromatic:
      - Coma
      - Defocus
      - Astigmatism
      - Field curvature
      - Image distortion
    - Chromatic:
      - Axial
      - Lateral

- Biggest contributors are vignetting, spherical comatic aberrations and field curvature.



Hubble Images of M100. Optical Aberration due to a mirror flaw taken with WPC-1 (bottom) resulted in the installation of corrective optics (WPC-2).

Spherical Aberration and Coma

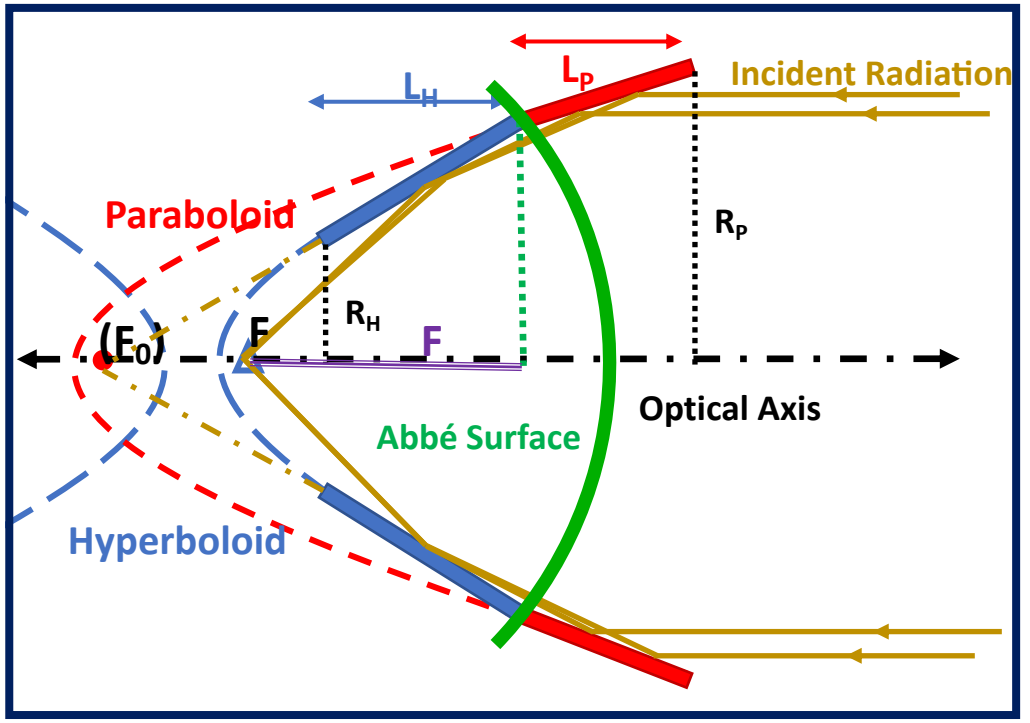
- Abbé surface intersects a “separation surface” between the two different focusing mirrors.

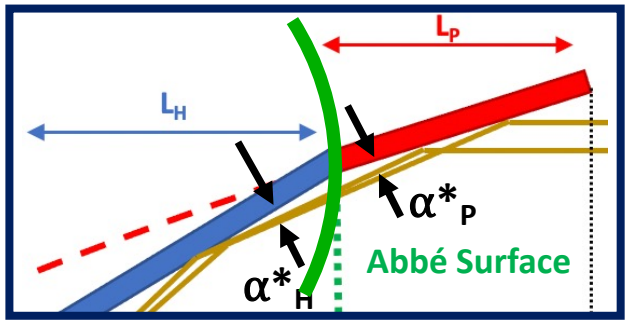
- Optimal focal plane not flat, will introduce a blur in the PSF:

$$\sigma_{rms} = 0.2\frac{tan^2\gamma}{tan\theta}\left(\frac{L}{F}\right) + 4\tan\gamma tan^2\theta$$

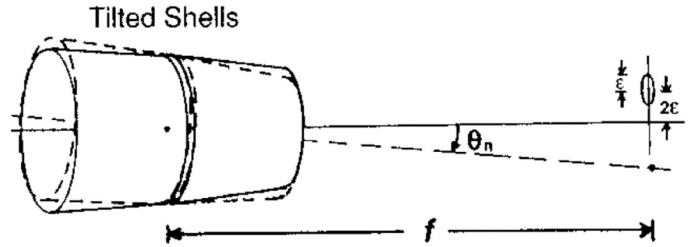
σ_{rms} = RMS blur circle, θ = incidence angle, γ = off-axis angle, L = mirror height, F = focal length.

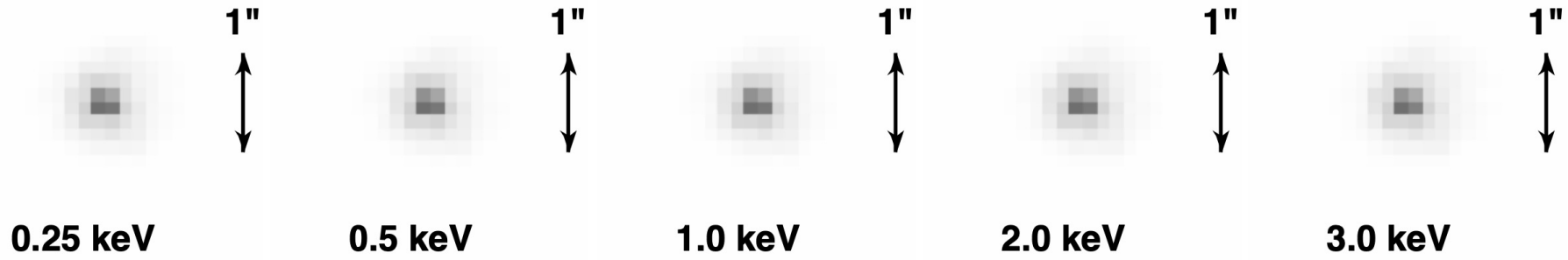
$$\delta_{flat} \propto r^2 \frac{L}{F^2}\frac{1}{tan^2\theta}$$



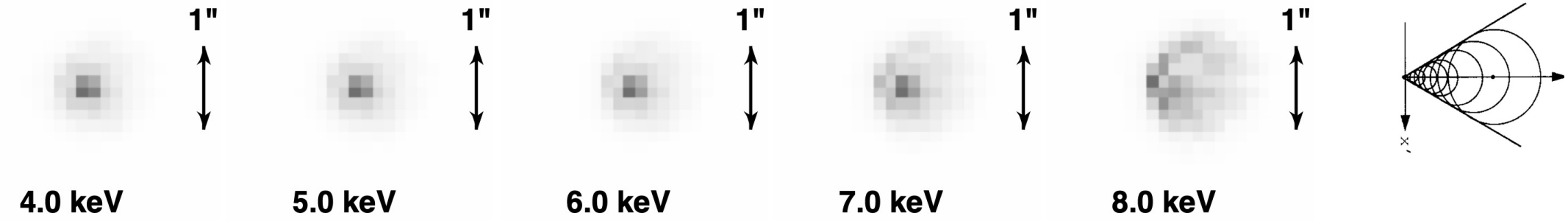


P. Thrasher, MSc, "X-ray Focusing Optics", Uni. of Arizona 2016





Coma illustration



Credit: CXC/SAO/NASA

Figure 7: Change in the on-axis PSF with energy, at HRC-I resolution (from simulations).

MP6 (smallest diameter), has some tilt in the mirror system which produces on-axis coma at higher energy.

Vignetting

- Less photons entering the telescope reach the focal plane with increasing off-axis angle (especially hard photons)

- The vignetting of the X-ray telescopes (i.e. XMM-Newton), is reflected by the decline of the telescopes effective area as a function of off-axis angle.

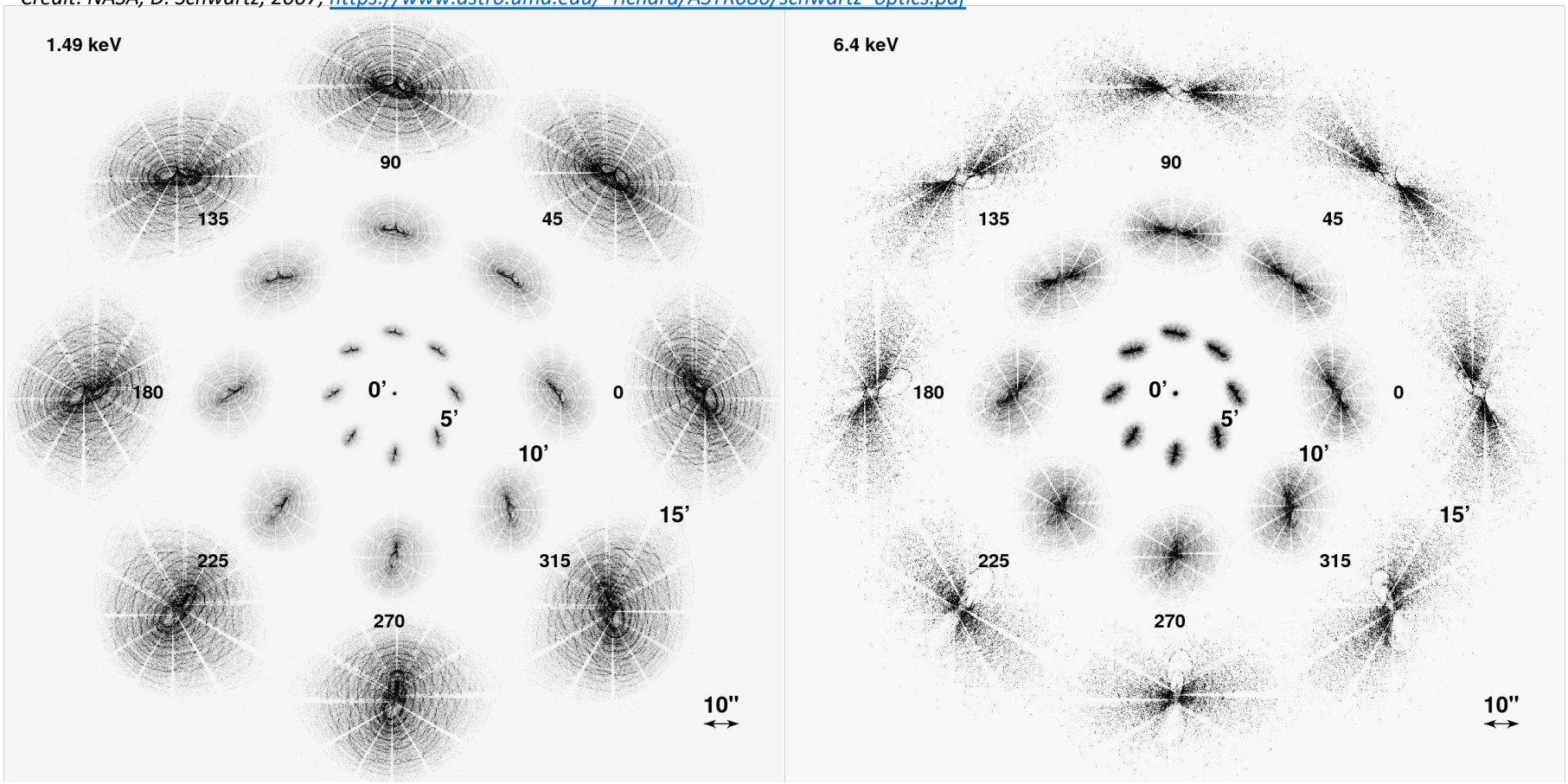
- Reflectivity and vignetting cause the geometric area to be reduced to a smaller effective area.

Effective Area:

$$A_{effective}(E,\theta,x,y) = A_{geometric} \times R(E) \times V(E,\vartheta) \times QE(E,x,y)$$

$A_{effective}(E,\theta,x,y)$ is the effective area (response files)
$A_{geometric}$ is the geometric area (telescope cross-section)
$R(E)$ is the fraction of photons reflected by the mirror as a function of energy (E)
$V(E,\vartheta)$ is the fraction of lost photons off-axis relative to the optical axis (ϑ) and energy of incoming photon (E).
$QE(E,x,y)$ is the fraction of registered photons in the CCD (and filters). Function of energy and position.

Credit: NASA, D. Schwartz, 2007; https://www.astro.umd.edu/~richard/ASTR680/schwartz_optics.pdf



Dominating off-axis aberration is field curvature over astigmatism (rays propagate in two perpendicular planes and have two different foci) and distortion (latter not zero).

Assembly Optical Errors

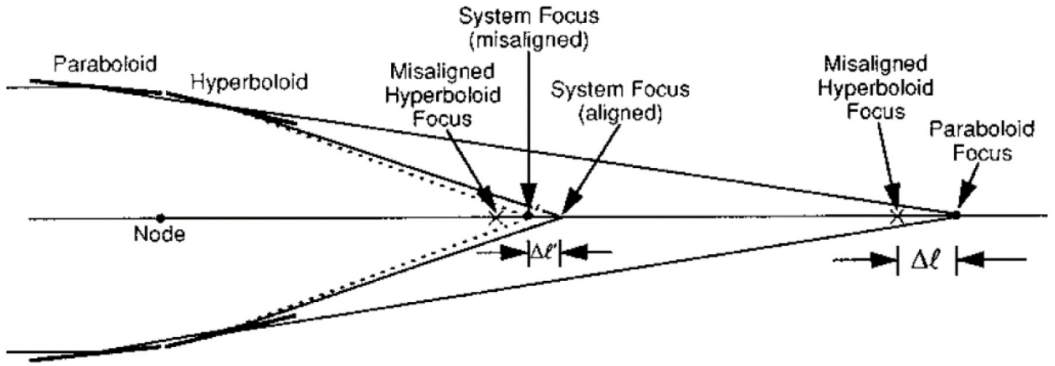
- Misalignment along the optical axis is characterized by:

$$Angular\ RMS\ Img.Dia. = \frac{\Delta \mathrm{l}_{\mathrm{rms}}}{16f}\sqrt{\frac{1}{f^2 A_T}\sum_{n=1}^{N} D_n^2 A_n}$$

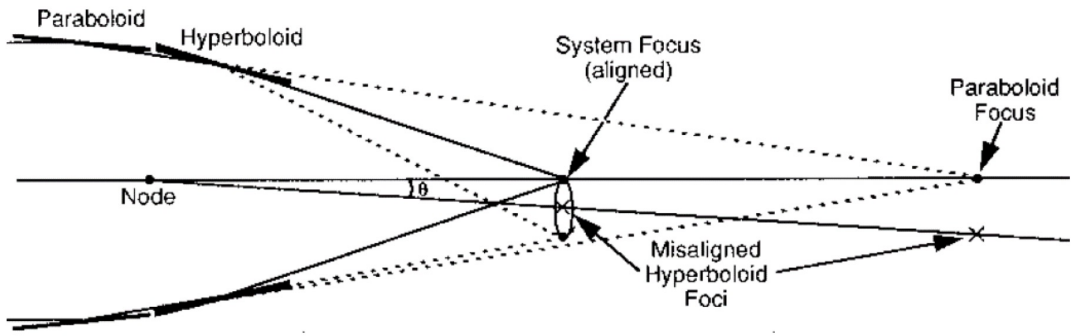
- Where there is a rms axial separation between each of the N mirror shells. The total collecting area of the the telescope (A_T) with each shell (A_n) contributing to that area with outer diameter D_n.
- Angular misalignment between mirror pairs:

$$Angular\ RMS\ Img.Dia. = 2\sqrt{2}\theta_{rms}$$

- Angular misalignment much bigger effect than axial.



Axial misalignment in a Wolter-I telescope



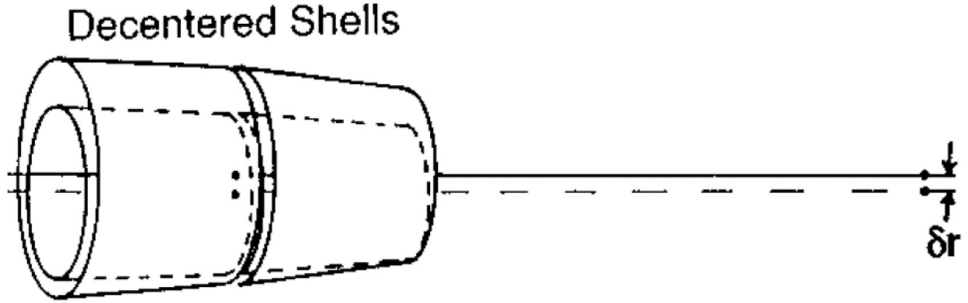
Angular misalignment in a Wolter-I telescope

P. Thrasher, MSc, "X-ray Focusing Optics", Uni. of Arizona 2016

Assembly Optical Errors

- Decentered shells will increase the spatial spot size by amount of decenter.

$$Angular\ RMS\ Img.Dia. = \frac{2\delta_{rms}}{f}$$

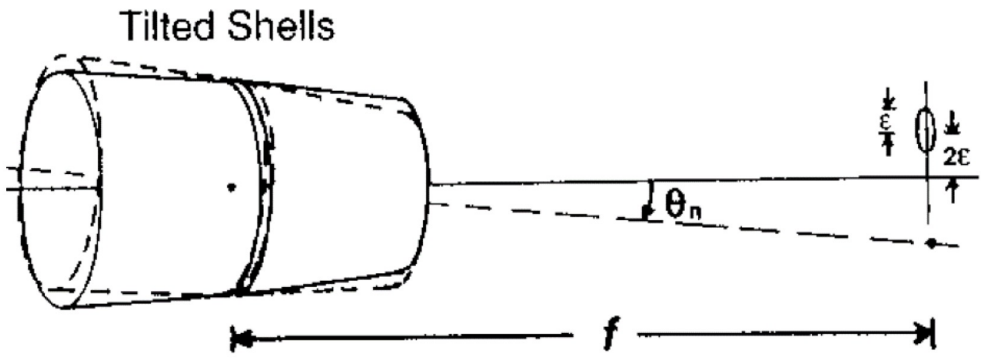


Decentered mirror pair in a Wolter-I telescope

- Angular misalignment between mirror pairs:

$$Angular\ RMS\ Img.Dia. = 2\sqrt{\frac{1}{A_T}\sum_{n=1}^{N} A_n 5(4\alpha_n\theta_n)^2}$$

Where α_n is the incident angle of a ray on the n^{th} shell.



Tilted mirror pair in a Wolter-I telescope

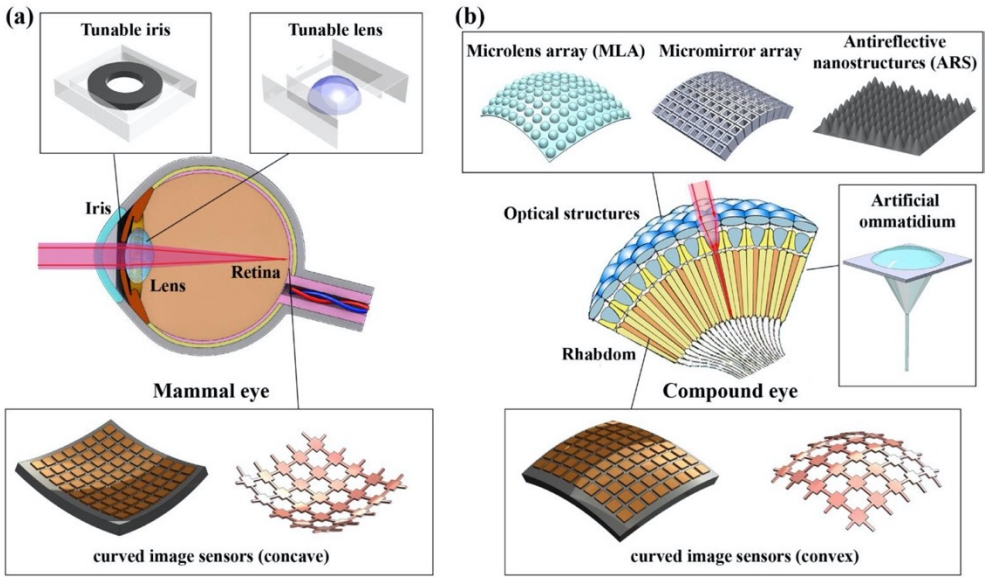
P. Thrasher, MSc, "X-ray Focusing Optics", Uni. of Arizona 2016

Bio-adaptive optics

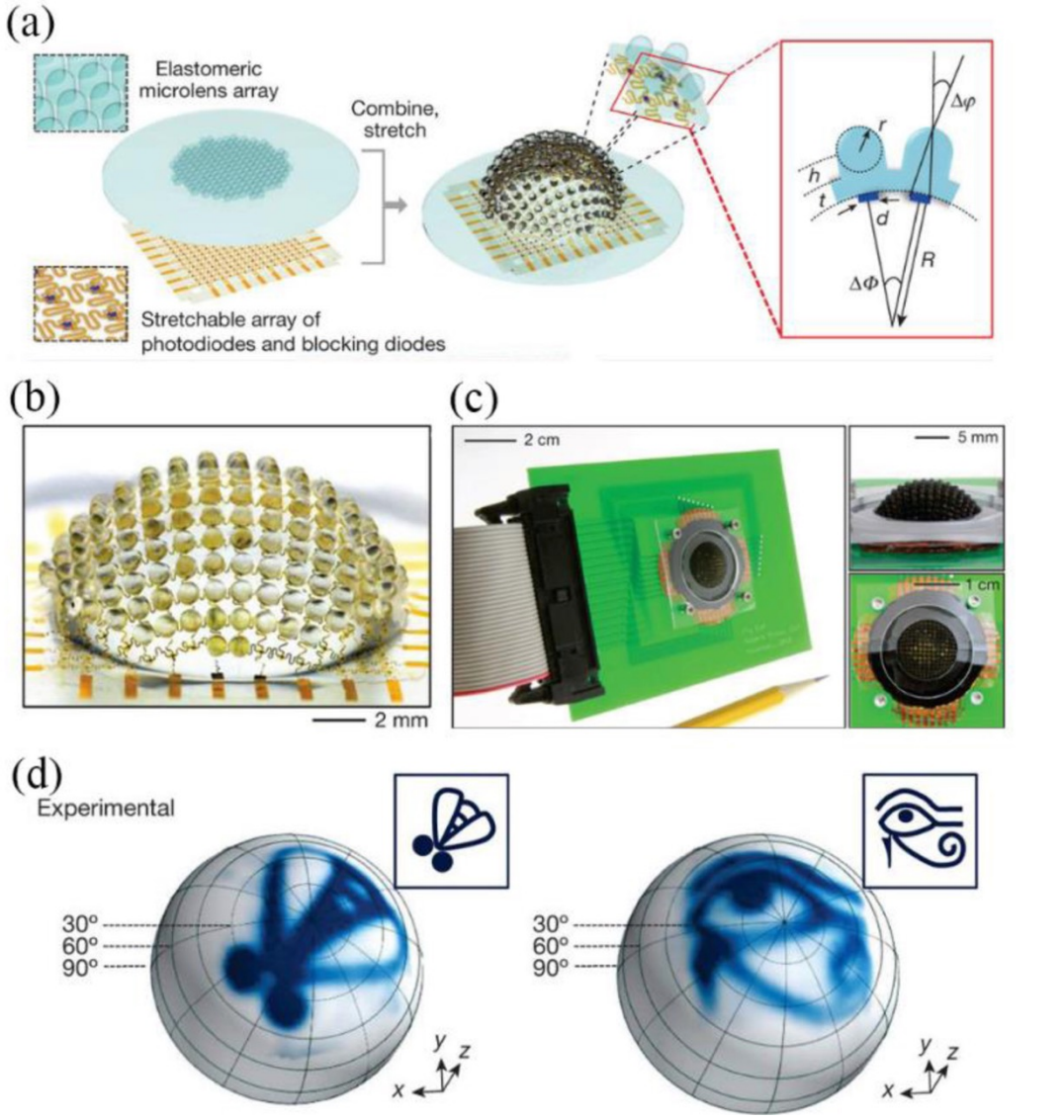
Look at biological eyes and try to take a different approach to developing optics (i.e. using tunable lenses composed of hydrogel actuators and water). Use of microlenses for sub-orbital, CubseSat configurations?

Can this be scaled up our applications? Can this be augmented to address our needs?

Issues: Outgassing? How robust are the liquids? How to get them up. Mechanically feasible?



Jae-Jun Kim et al 2020 Rep. Prog. Phys. ***83*** *047101*

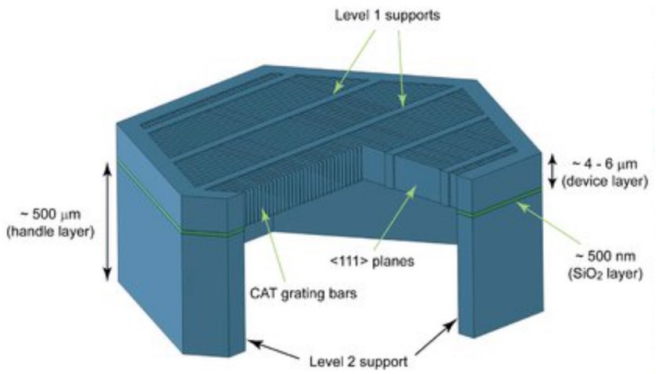


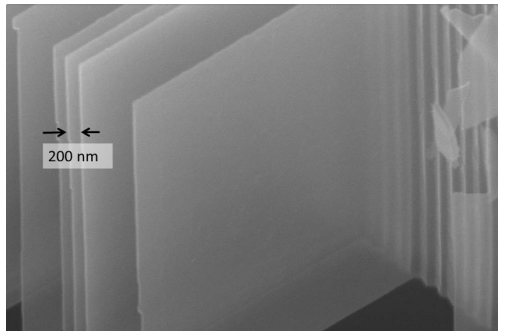
Song, Y., Xie, Y., Malyarchuk, V. *et al.* Digital cameras with designs inspired by the arthropod eye. *Nature* **497,** 95–99 (2013). https://doi.org/10.1038/nature12083

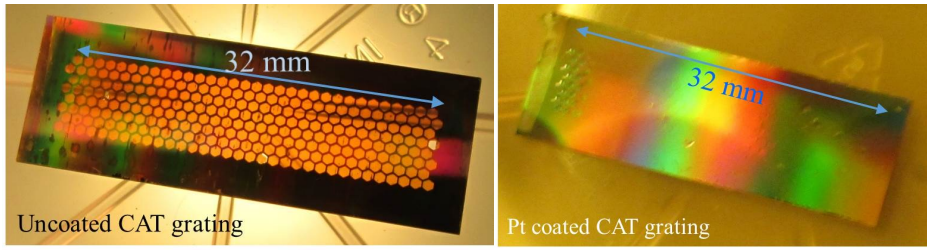
R. Hamilton Shepard, "Towards an optimized Gabor Superlens," Proc. SPIE 9293, International Optical Design Conference 2014, 92930G https://doi.org/10.1117/12.2073294

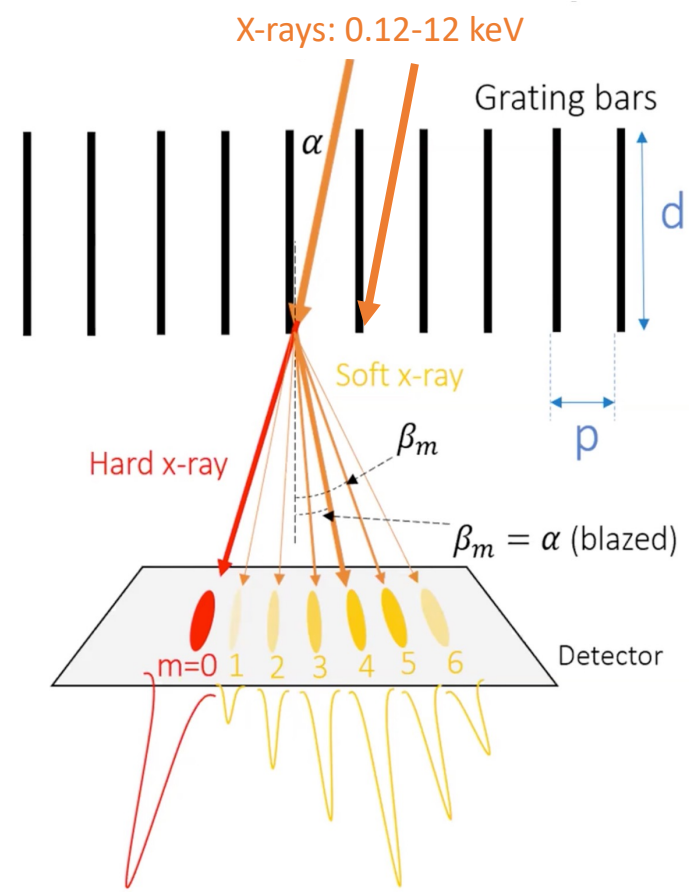
Critical-Angle Transmission (CAT) gratings

- Hybrid between a blazed reflection grating and transmission grating.
- Working parameters:
  - Grating period, **p** =200 nm,
  - Grating depth, **d** = 4 µm,
  - Grating bar thickness = 40 nm,
  - Sidewall roughness = < 1 nm.
- Boosts diffraction efficiency (~32% @ 0.48 keV):
  - Incident X-rays mostly reflected below critical angle for total external reflection
  - Free-standing. No absorption by support structure/membrane.
  - Majority of X-rays directed into the negative non-zero diffraction orders via blazing.









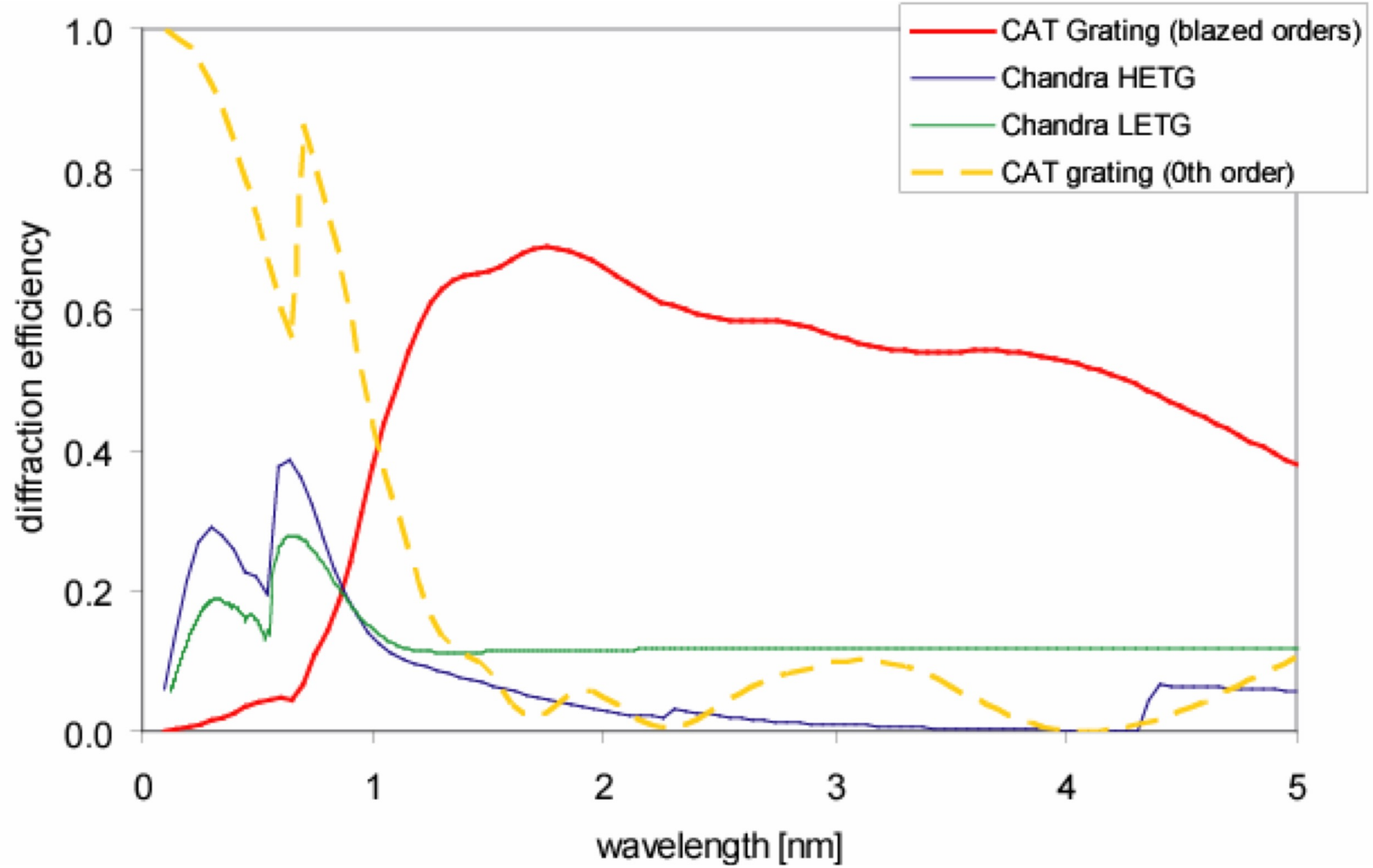
Grating Equation: $\frac{m\lambda}{p} = sin\alpha - sin\beta_m$

m = diffraction order
α = Incident angle
β_m = diffracted angle

Constructive Interference when: $PLD = 2psin(\theta) = m\lambda$

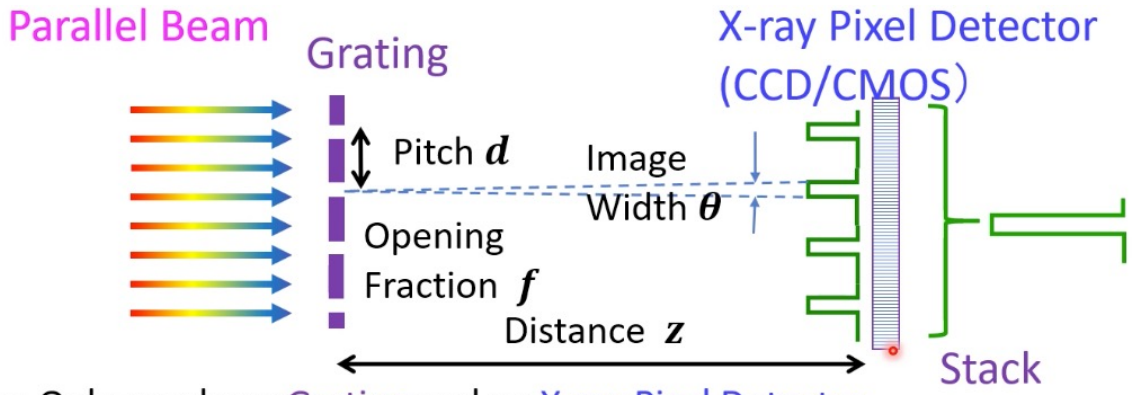
Ralf K. Heilmann, et al., Proc. SPIE 11444, Space Telescopes and Instrumentation 2020: Ultraviolet to Gamma Ray, 114441H (2020);https://doi.org/10.1117/12.2562388

Critical-Angle Transmission (CAT) gratings



Ralf K. Heilmann, et al., Proc. SPIE 11444, Space Telescopes and Instrumentation 2020: Ultraviolet to Gamma Ray, 114441H (2020);https://doi.org/10.1117/12.2562388
Ralf K. Heilmann, et al., (2009) https://space.mit.edu/~ralf/Heilmann-IXO-IWG-Jan09.pdf

MIXIM: Multi-Imaging X-ray Interferometer Method

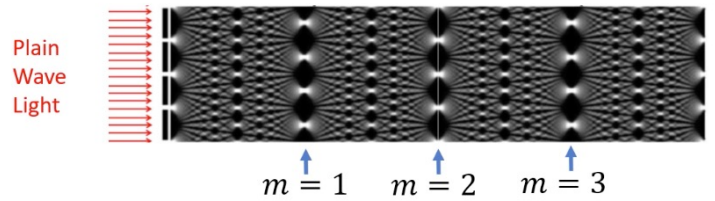


- Only employ a Grating and an X-ray Pixel Detector
- Image profile detected reflects the profile of the X-ray source.
- Stacking the image with a period of d in the analysis, accurate source profile is obtained.
- Image Width $\theta = fd/z = 0.4'' \left(\frac{f}{0.2}\right)\left(\frac{d}{5\mu m}\right)/\left(\frac{z}{50cm}\right)$

Chandra Resolution with a 50 cm sized satellite? Yes, it is possible, but diffraction will blur the image.

Solution? Talbot Effect

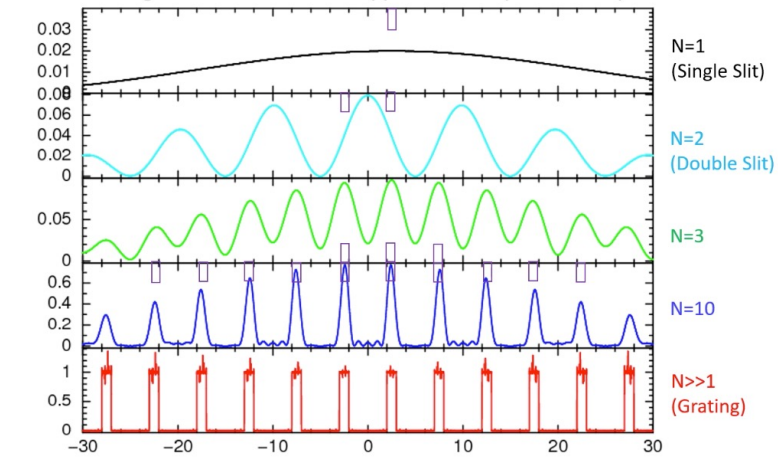
- **Talbot Effect**
  - Parallel Light through a grating makes **Self Image** of the grating at periodic distances. (H.F.Talbot, 1836)
  - Explained with **Diffraction** and **Interference** (Rayleigh, 1881)
  - Hard X-ray Talbot Effect in experiment (P. Cloetens, 1997)
- **Talbot Distance** $z_T = m\frac{d^2}{\lambda}$



Talbot Carpet
Image from
Wen et al. Advances in Optics and Photonics 5, 83–130 (2013)

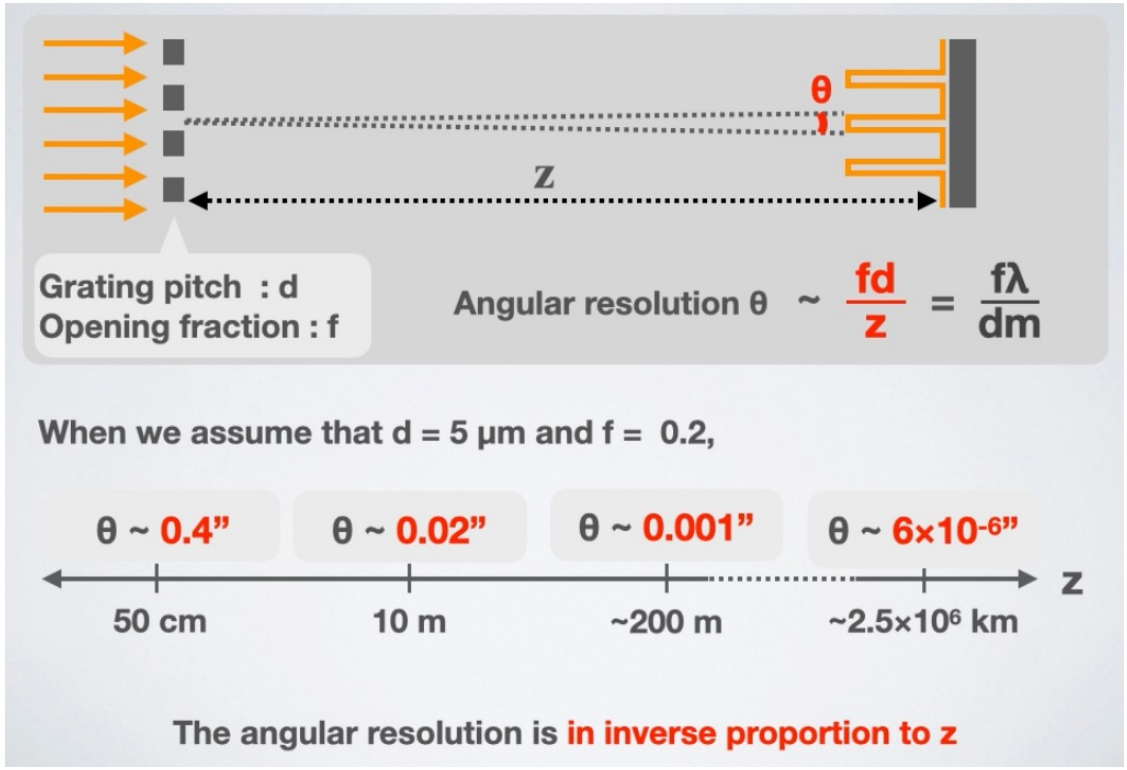
For λ=0.1nm(12keV) X-rays and a d=5μm pitch grating, Talbot distance z_T of m=2 is 50cm

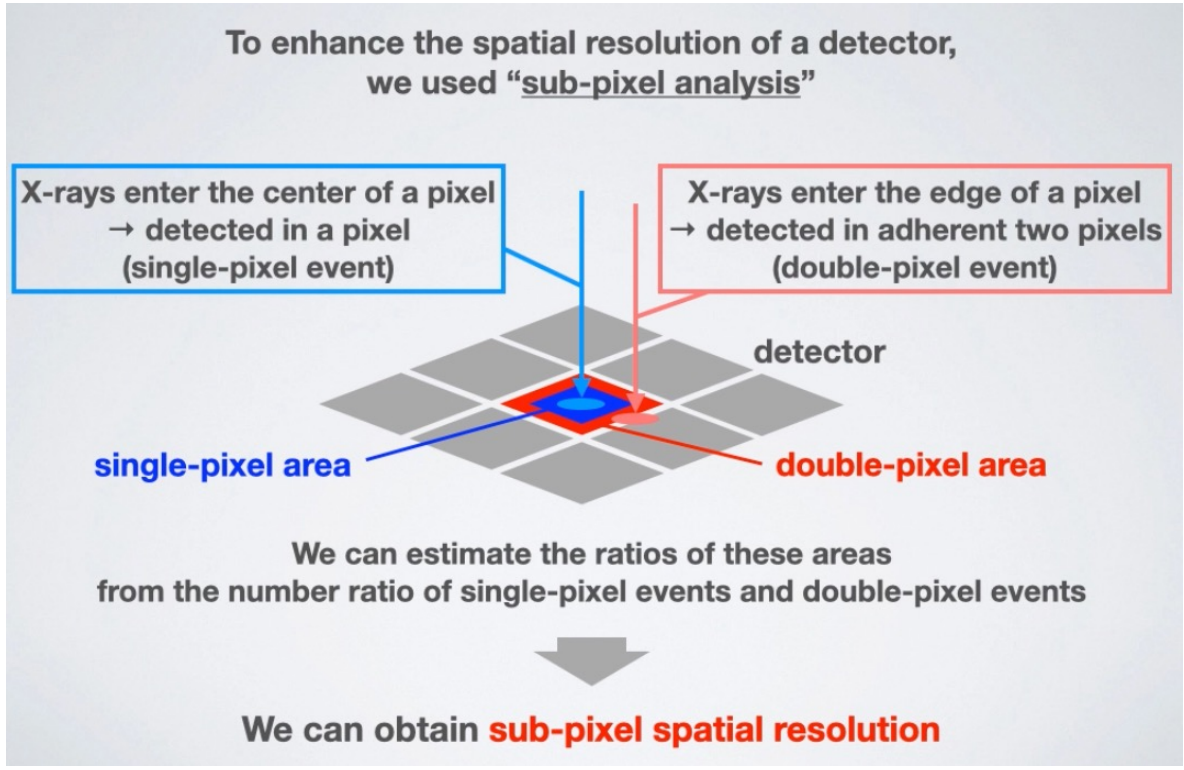
Simulated Image Profile with Fresnel Approximation (not stacked)



Kiyoshi Hayashida, et al., "Sub-arcseconds to micro-arcsecond x-ray imaging with multi image x-ray interferometer method (MIXIM): Concept and scalabe mission plans," Proc. SPIE 11444, Space Telescopes and Instrumentation 2020: Ultraviolet to Gamma Ray, 114441C (13 December 2020);https://doi.org/10.1117/12.2562193

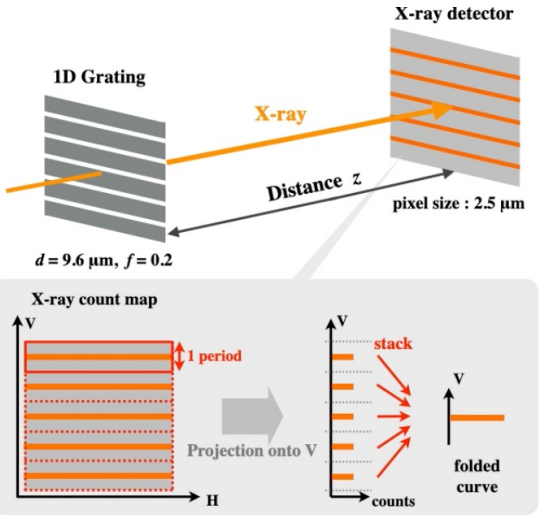
MIXIM: Multi-Imaging X-ray Interferometer Method

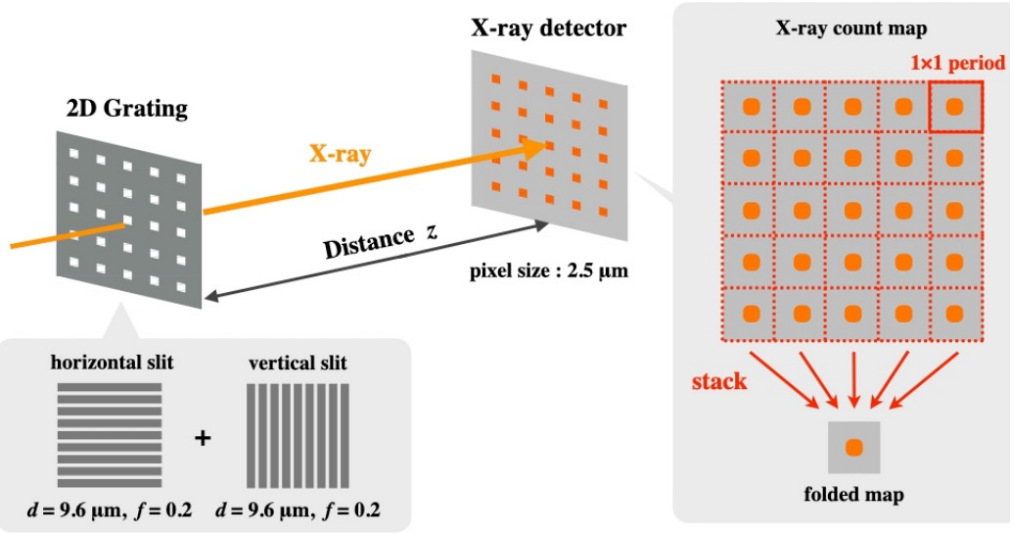


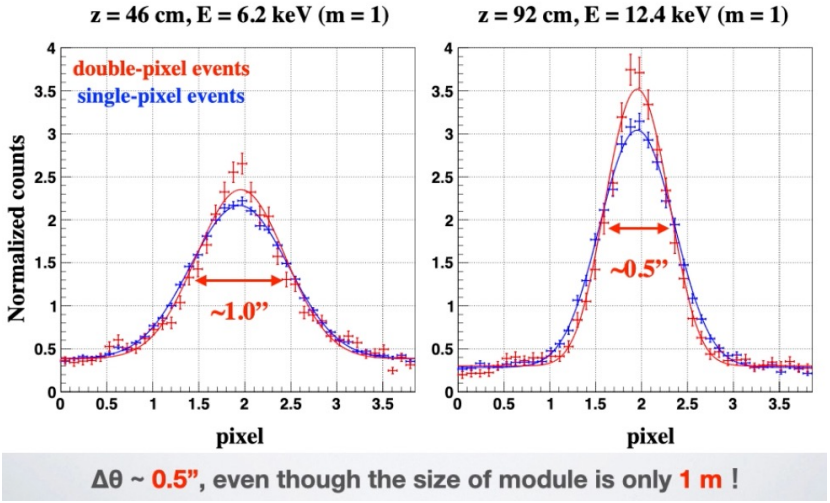


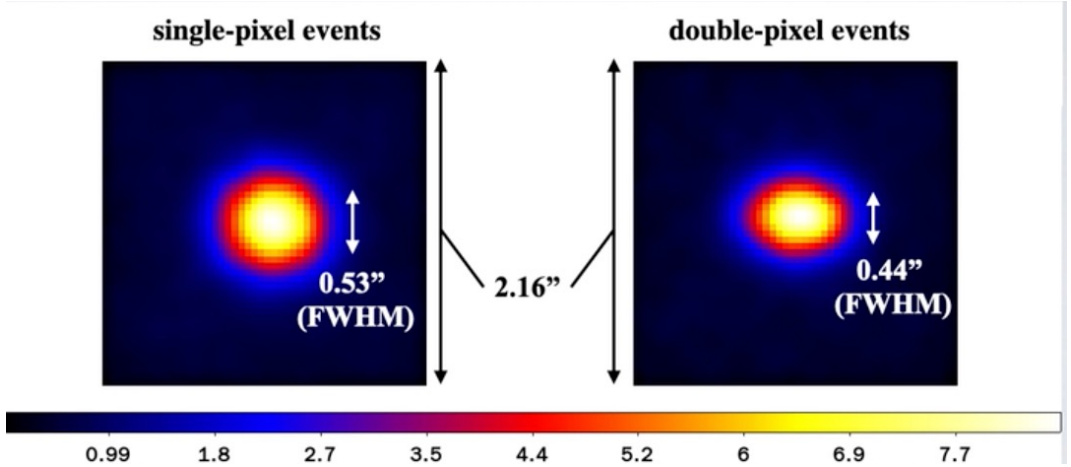
Kiyoshi Hayashida, et al., "Sub-arcseconds to micro-arcsecond x-ray imaging with multi image x-ray interferometer method (MIXIM): Concept and scalabe mission plans," Proc. SPIE 11444, Space Telescopes and Instrumentation 2020: Ultraviolet to Gamma Ray, 114441C (13 December 2020);https://doi.org/10.1117/12.2562193

MIXIM: Multi-Imaging X-ray Interferometer Method









Kiyoshi Hayashida, et al., "Sub-arcseconds to micro-arcsecond x-ray imaging with multi image x-ray interferometer method (MIXIM): Concept and scalabe mission plans," Proc. SPIE 11444, Space Telescopes and Instrumentation 2020: Ultraviolet to Gamma Ray, 114441C (13 December 2020);https://doi.org/10.1117/12.2562193